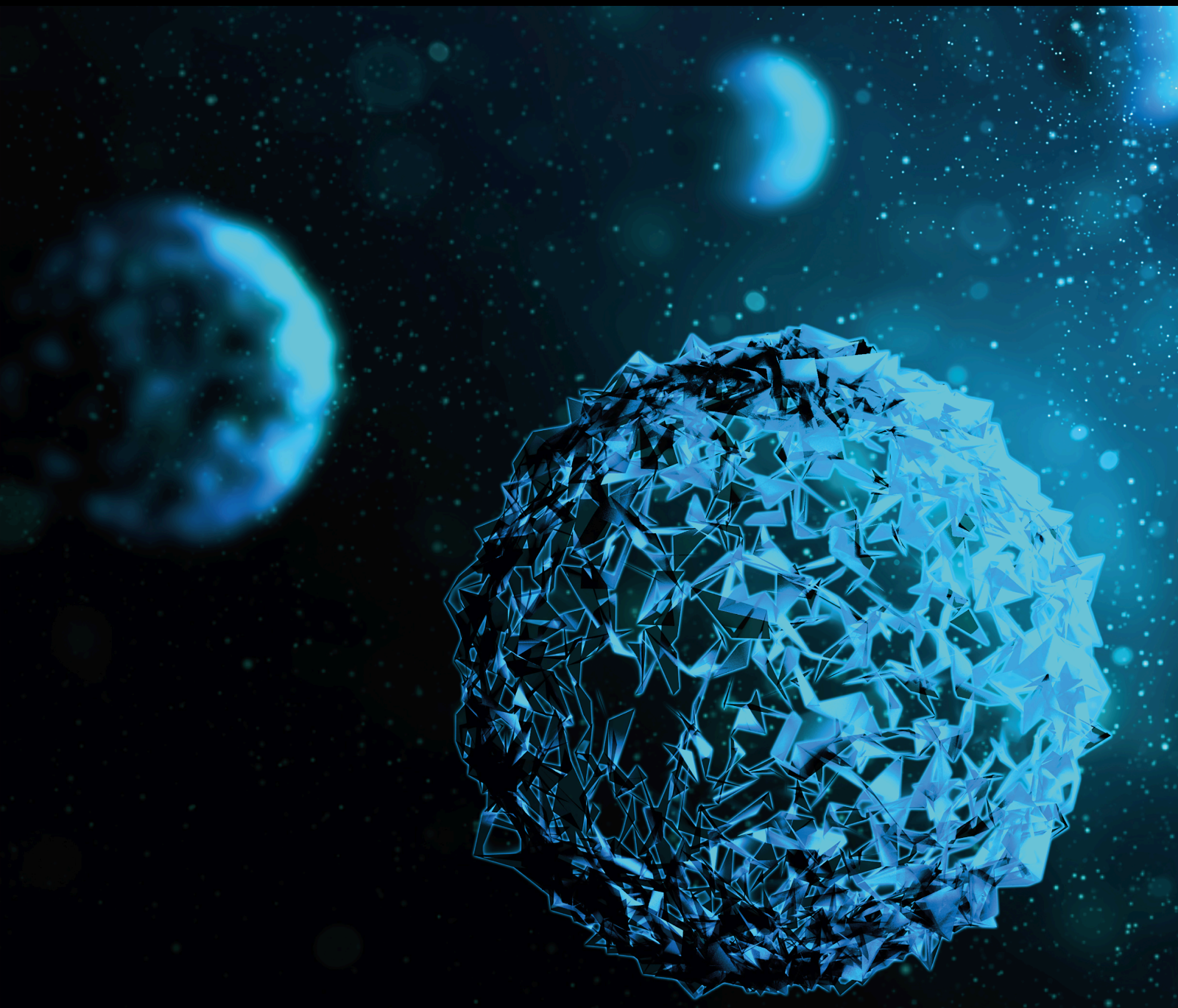# Treatment Strategies for Spinal Diseases in Fragile Patients

Lead Guest Editor: Giorgio Lofrese
Guest Editors: Federico De Iure, Luca Ricciardi, and Luiz Roberto Vialle

Treatment Strategies for Spinal Diseases in Fragile Patients

Treatment Strategies for Spinal Diseases in Fragile Patients

Lead Guest Editor: Giorgio Lofrese
Guest Editors: Federico De Iure, Luca Ricciardi, and Luiz Roberto Vialle

Contents

Hindawi

Review Article

Corrective Mechanism Aftermath Surgical Treatment of Spine Deformity due to Scoliosis: A Systematic Review of Finite Element Studies

Kavita Gunasekaran,[1] **Khairul Salleh Basaruddin** ®,[1,2] **Nor Amalina Muhayudin,**[1] **and Abdul Razak Sulaiman** ®[3]

[1]*Faculty of Mechanical Engineering Technology, Universiti Malaysia Perlis, 02600 Pauh Putra, Perlis, Malaysia*
[2]*Medical Devices and Health Sciences, Sports Engineering Research Center (SERC), Universiti Malaysia Perlis, 02600 Pauh Putra, Perlis, Malaysia*
[3]*Department of Orthopaedics, School of Medical Science, Universiti Sains Malaysia, 16150 Kubang Kerian, Kelantan, Malaysia*

Correspondence should be addressed to Khairul Salleh Basaruddin; khsalleh@unimap.edu.my

This paper presents a systematic study in reviewing the application of finite element method for the analysis of correction mechanism of spine deformity due to scoliosis. The study is aimed at systematically (1) reviewing the use of finite element analysis in spine deformity case, (2) reviewing the modelling of pedicle screw and rod system in scoliosis surgery, and (3) analysing and discussing gap between the studies. Using the restricted key phrases, the review gathered studies from 2001 to 2021 from various electronic databases (Scopus, ScienceDirect, PubMed, Medline, and WorldCAT). Studies were included if they reported a finite element study on spine deformity. Studies that did not fully disclose their methodology and results had significant discrepancies, not published in English or not yet published were all disqualified. Regardless of inconsistencies in the methodological design of the studies, the quality of all papers was above the acceptable level. A total of fifteen manuscripts were considered for inclusion and were given a comprehensive review. This study indicates that analysing the forces acting on the spine, as well as the interrelationship between the force, stress, and degree of correction (which measured as the Cobb angle), could help to improve the corrective mechanism procedure of spine deformity. Pedicle screws and its placement strategies are also important as it influence the corrective forces for scoliosis treatment. Hence, the findings of this study could potentially be used as a guidance to develop a reliable finite element analysis that can predict the biomechanics responses during the corrective spine deformity treatment.

1. Introduction

Scoliosis is a three-dimensional (3D) spinal deformity characterised by axial vertebral rotation. The Cobb angle value is used to determine the severity of a scoliotic deformity. The Cobb angle is the maximum angle made in the frontal plane by two lines drawn parallel to the endplates of scoliotic vertebrae. Surgical treatment with implant fixation is used when the Cobb angle is more than 50° [1]. There are several surgical procedures that have evolved to be more advanced in applying the three-dimensional corrective forces for the cor-

rection of severe scoliotic deformity. Cotrel and Dubousset's (CD) rod derotation technique, ventral derotation spondylodesis (VDS), Halm–Zielke instrumentation (HZI), simultaneous dual rod rotation method (SDRRT), direct incremental segmental translation (DIST), and others are examples of these procedures [1, 2]. These surgical therapies for severe scoliosis need the use of surgical methods to secure implanted devices such as rods, screws, hooks, and wires. For example, the anterior single rod correction procedure in Figure 1 involves removing the malformed intervertebral discs, implanting material to stimulate intervertebral

joint fusion, and attaching metal rods to the spinal vertebrae [3] as spine deformity correction procedure.

The usage of computer simulations of the spine has skyrocketed in the last two decades. Computational techniques, notably finite element method (FEM), have previously been demonstrated to be effective in analysing the mechanics of the scoliotic spine during surgery [3]. For instance, Aubin et al. [4] created a model of the spine that had rigid bodies that represented the thoracic and lumbar vertebrae seen on intraoperative radiographs, as well as flexible parts that represented the intervertebral structures. Developing an optimal system of corrective force for an individual scoliosis patient via trial and error during surgery is actually unrealistic. Hence, FEM has been used to simulate surgical process changes and predicts the three-dimensional outcome in terms of deformity treatment and build flexibility. The FEM used in scoliosis research was divided into four groups based on model complexity: reflective simple variants of beam element-based models, representative complicated versions of beam element-based models, representative segmental volumetric models, and representative extensive volumetric models, according to the previous study [5].

By developing FEM, the relationships between the magnitude of corrective forces, number of screws, screw placement configuration, and degree of correction can be further elucidated [2]. Actually, the well-developed FEM of the spine allows for more complete assessments of internal stress distribution [6]. The studies of internal stress distributions and hypothetical scenarios cannot be properly examined without the help of real patient records, which is a possible drawback of rigid body modelling and patient-based FEM design.

Scoliosis correction aims to distort and restore the scoliotic spine to its original shape without inflicting injury or neurological complications. This could be accomplished by using implant rods and screws to impart appropriate correction forces to the spine. To obtain the optimum correction, the corrective forces required to rectify the deformity must be adequate [6]. Despite the fact that the number of patients was small, there was a growing correlation between the applied force and the degree of correction. Nevertheless, because of the rotating device is only linked to the implant rod, the correction forces acting at every screw were quite hard to be measured.

2. Methods

2.1. Search Strategy.

Database search through the internet performed in November 2021 was restricted to the last twenty years of publication in Scopus (2001-2021), ScienceDirect (2001-2021), WorldCAT (2001-2021), PubMed (2001-2021), and Medline (2001-2021). The key MESH terms included "correction," "spine," and "deformity." A thorough search was also conducted using the additional keyword search query: "finite element." This extra manual search was implemented by manual screening conducted for relevant articles based on the reference lists of the retrieved articles. To rule out the likelihood of those items being overlooked, an additional search was conducted. All
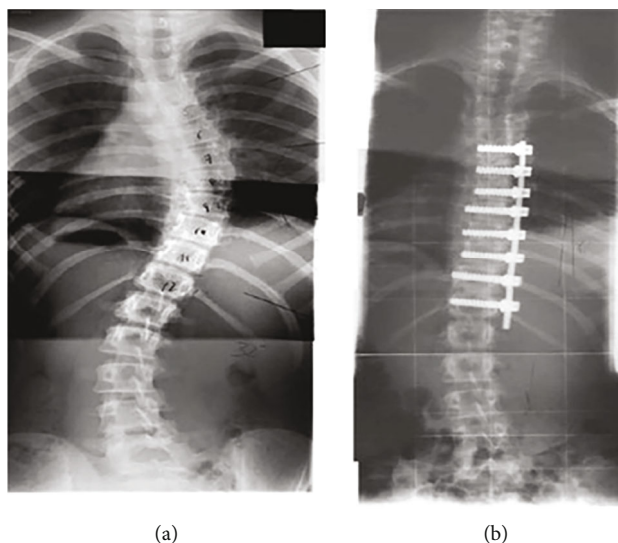
FIGURE 1: Sample of spine radiographs, (a) preoperatively and (b) postoperatively with having a single rod (anterior procedure) [3].

of the articles were retrieved and checked to ensure that the database search results were accurate and related to other articles. The ultimate decision was drawn in order to keep our findings within the scope of the papers.

2.2. Inclusion/Exclusion Criteria.

From the electronic databases, only full-text articles in English were chosen. If there was a disagreement about an article during the screening process, it was debated to reach a consensus. Articles on studies focusing on corrective deformed scoliosis were included in the titles and abstracts screening procedure. The following criteria were used to evaluate articles: (1) rod and pedicle screw system, (2) Cobb angle, and (3) finite element analysis, full nonclinical articles. There were no restrictions on the participants' age, gender, BMI, or medical history. Articles by the same author were double-checked to ensure there were no duplicates.

2.3. Review Process.

Two reviewers (K.G. and K.S.B.) screened the search results according to the inclusion criteria. After the screening procedure, the final articles were extracted and separated from duplicated articles in several databases. Duplicate articles were eliminated from various databases. The eligibility criteria were initially applied to the titles and abstracts of the papers that were chosen. A full-text review was undertaken if the title and abstract did not give enough information in the article screening procedure. To avoid misinterpretation, rejected items were rescreened.

2.4. Assessment of Methodological Quality.

The papers were reviewed and analysed using a systematic quality approach that helped to evaluate the quality of the articles identified, as well as extracting the most relevant information from those publications. There are no standardised methods for evaluating the reliability and credibility of each of the articles

examined aside than the processes provided in this study. To evaluate credibility, 13 questions were adapted from Azizan et al. [7] and Ku et al. [8]. Few questions were had to drop as they are not justifying to spine deformity and its correction mechanism. At the same time, some of the questions were later altered according to FEA. Each question was given a score of "2" if the answer satisfied the standard questions, and a score of "1" if the information was limited. If no information was provided, the questions were marked with "0" or "no," while questions that were not applicable were marked with "NA." The 13 questions are as follows:

(1) Is the study's objective stated in a clear and concise manner?

(2) Is the study design outlined in detail?

(3) Are the patients'/models' characteristics and details clearly provided?

(4) Is the process of geometrical model development clearly explained?

(5) Is the convergence test in the study clearly stated?

(6) Is the boundary condition clearly described?

(7) Are the appropriate mathematical models used to calculate parameters?

(8) Are the mechanical properties of the model distinctly defined?

(9) Are appropriate numerical methods used in data analysis clearly defined?

(10) Is the predicted numerical value appropriately verified or validated?

(11) Is the key outcome measure mentioned clearly?

(12) Are the study's limitations disclosed clearly?

(13) Is the study's conclusion conveyed in a clear and concise manner?

3. Results

3.1. Primary Search Results.
Since the number of findings was limited in terms of quantity of information and the amount of materials available, the authors then conducted full-text reviews of articles. After a thorough screening process, twenty-two retrieved articles were finalised. Figure 2 shows the systematic review process of the present study. A total of 967 items were found after the database screening procedure. 81 of these items, however, were found duplicates and were removed. The relevancy of the studies undertaken was determined by looking at the titles and abstracts, and then, 602 publications were eliminated. Additional screening was carried out by reading the rest of the article's content in order to ascertain the study's goal based on the standard parameters that was assessed. After removing another 42 articles, there were 15 articles that meet all the criteria and were further reviewed.

3.2. Analysed Data Quality.
Table 1 shows the quality ratings of the 15 articles that were assessed. The reviewed papers have a quality score ranging from 80% to 96%. Articles with a score of more than 85% are regarded good because they provide answer for all thirteen questions. These publications offered detailed information about their objectives, study design, key findings, and conclusion [1, 3, 9]. The remaining eleven studies fulfilled at minimum 70% to 90% of the questions [6, 10]–[11]. Other elements that could have aided in the comprehension of the questions were not considered in this review.

3.3. Participant Characteristics.
Table 2 shows a list of physical characteristics and anthropometric factors from 15 articles. The majority of the participants were young people, with only a few adults of average age. Nine studies involved adolescences (aged between 10 and 19) [1, 3, 9, 11, 12, 14, 15, 17], two articles assessed middle-aged individuals (age range from 30–59) [10, 19], and none of the articles involved elderly persons (aged 60 and above). The number of participants in the evaluated publications varied, with the highest number being 20 peoples and seven articles keeping one as patient data for their investigation [6, 9, 11, 12, 16, 18, 19]. Four articles provide no anthropometric data of tested participants as those studies used spine finite element models [6, 16, 18, 20]. The participants were also categorised into presurgical [1, 2] and postsurgical patients [3, 12].

3.4. Finite Element Modelling.
By conducting an exhaustive search for all published papers, a systematic review aims to minimise the incidence of bias. The modelling parameters in FEA, such as loads and boundary conditions, element types and sizes, geometrical model, type of material, and mechanical properties, have a significant influence on prognostic accuracy. These variables have an impact on the simulation's predictive accuracy and should be considered when evaluating the results and conclusions. Table 3 shows finite element modelling variables that were used by the reviewed articles on the corrective mechanism of spine deformity due to scoliosis. These data can provide additional information on the simulations, allowing for replication and comparison.

Ten out of fifteen studies used ANSYS software for FEA studies [1, 2, 6, 9, 15, 18, 19]. Whereas Abolaeha et al., Little et al., and Guan et al. used ABAQUS software [3, 12, 18]. Wang et al. mentioned only radiographic software used for his FEA studies [20]. Special mention to Chen et al. [19] where Solidworks was the primary software for FEA studies where the pedicle screws created based on the imported blueprint then into Hypermesh and assembled into scoliotic spine FE model. Elements are the basic building block of FEA. Several authors used 10 node tetrahedral solid elements [1, 2, 9, 11, 14]. However, Wang et al. [15] and Guan et al. [18] used hexahedron elements. Moreover, beam elements for vertebral and pelvic sections, tension-only cable elements for ligaments, surface contact elements for articular facets, and modified beam elements are all included in FE model by Dumas et al. [10].
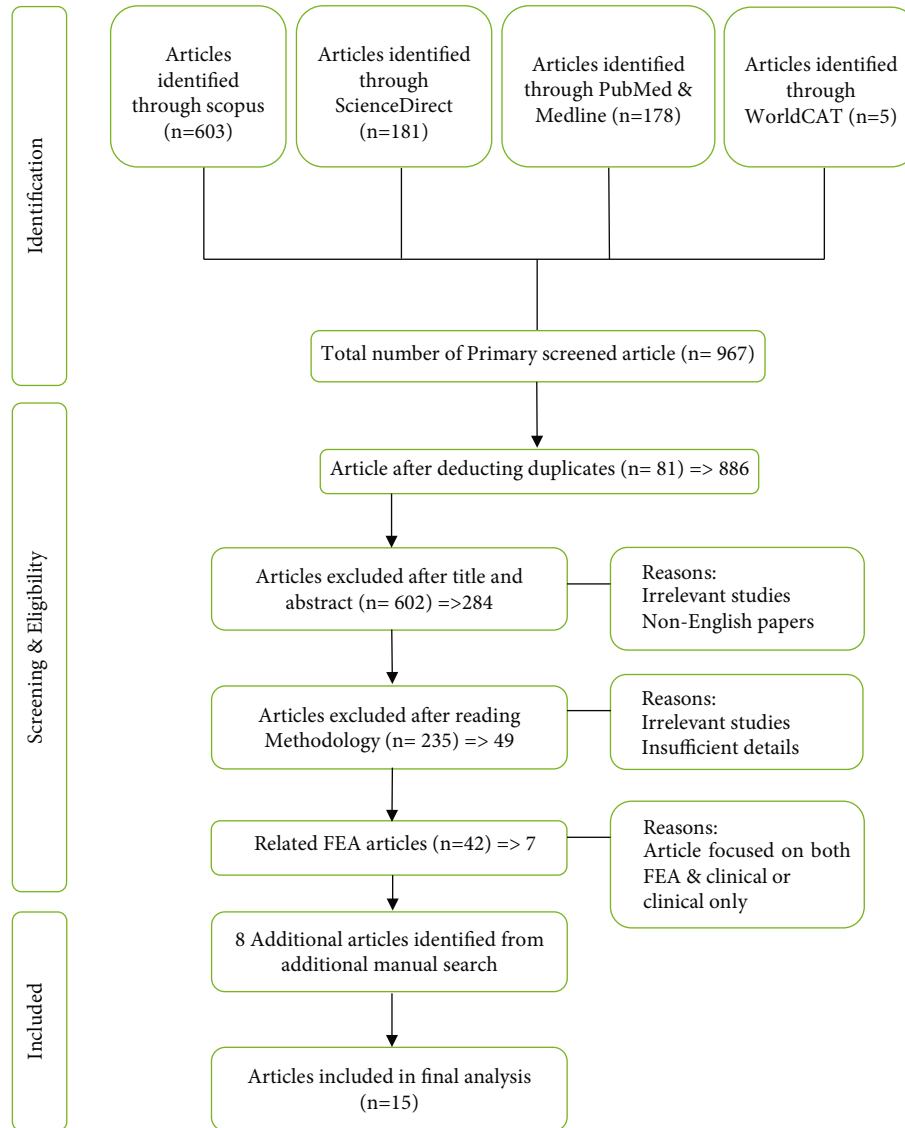
FIGURE 2: The research selection procedure from the reviewed articles.

In order to produce an accurate reconstruction, the image quality is critical. To develop a rebuilt model as accurate as possible, it can be seen that the models in most of the studies were created from computed tomography (CT) scan images that was widely used by the researchers [1, 3, 6, 9–12, 15, 16, 18], either directly or via a previous model's scaling. Meanwhile, only Wang et al. [13] used ADAMS 2005 software (Mechanical Dynamics Inc., Ann Arbor, MI) and the ADAMS Software Development Kit (SDK). Finite analysis has been shown to be useful in understanding the aetiology of scoliosis in these models. To ensure that the model performs realistically, the produced FEM must be tested against existing scientific results on motion and material properties.

As for the material, titanium alloy was widely used for both rod and screws compared to cobalt chromium which also has elastoplastic properties [1, 3, 12, 15, 18, 19]. Abolaeha et al. [12] used stainless steel that also has elastoplastic material behaviour as aluminium alloy. Some authors used both aluminium alloy and cobalt for screws and rod, respectively [3,

17]. As for the mechanical properties, the range of elastic modulus for rod is between 105 GPa to 213 GPa [1, 3, 6, 15, 17, 20].

Modern segmental spinal instrumentation systems are used to execute a variety of deformity correction techniques, including vertebral translation, rod derotation, direct vertebral derotation, and in situ rod contouring, all of which have been thoroughly studied. Dumas et al. [10] introduced situ contouring technique in his studies. Whereas Abolaeha et al. [12] used spinal growth rod instrumentation, an early onset scoliosis management method, and emerging technology that treating scoliosis without fusion hold the exciting prospect of a new paradigm in spinal deformity care. Salmingo et al. in their both studies and Abe et al. [1, 2, 14] used simultaneous double rod rotation technique (SDRRT) surgical technique with rods and polyaxial pedicle screws. Wang et al. [13] studied a posterior instrumentation using monoaxial pedicle screws, whereas Chen et al. [19] presented a procedure that includes rod derotation on the concave side and rod implantation on the convex side for strengthening.

TABLE 1: Overall score based on the articles that were reviewed.

Authors and years	Questions													Overall score	Overall %
	1	2	3	4	5	6	7	8	9	10	11	12	13		
Dumas et al. [10]	2	2	1	1	1	2	0	0	1	2	2	0	2	16/20	80.0
Abolaeha et al. [12]	2	2	NA	1	1	0	1	2	2	2	2	0	2	18/20	90.0
Salmingo et al. [1]	2	2	2	2	1	1	2	2	2	2	2	2	1	23/26	88.5
Wang et al. [13]	2	2	0	0	1	0	0	2	2	2	2	2	2	17/18	94.4
Driscoll et al. [6]	2	1	0	0	NA	0	1	2	2	2	2	0	2	14/16	87.5
Salmingo et al. [2]	2	2	1	1	1	2	2	2	2	2	2	2	2	23/26	88.5
Little et al. [3]	2	2	1	1	2	2	2	1	2	2	2	2	2	23/26	88.5
Abe et al. [14]	2	2	2	2	NA	0	2	1	2	2	2	1	2	20/22	91.0
Wang et al. [15]	2	2	2	2	1	0	1	2	2	2	2	2	1	21/24	87.5
Clin et al. [16]	2	2	2	2	NA	0	2	1	2	2	2	2	2	21/22	95.5
Balamurugan et al. [17]	2	2	0	0	NA	0	2	2	2	1	2	0	2	14/16	87.5
Guan et al. [18]	2	2	2	2	2	2	2	2	2	2	2	1	0	23/24	95.8
Zhang et al. [9]	2	2	2	2	1	2	2	2	2	2	2	2	2	25/26	96.0
He et al. [11]	2	2	2	2	0	1	2	2	2	2	2	1	1	21/24	87.5
Chen et al. [19]	2	2	2	2	0	0	2	2	2	2	2	1	1	20/22	90.1

*Note: significance evaluation: 2—yes; 1—limited detail; 0—no; NA: not applicable.

TABLE 2: Participants' or models' characteristic.

Authors	Condition/category	Number of participants/models	Gender		Anthropometric data
			Male	Female	
Dumas et al. [10]	Postsurgical patients	2	NM	NM	Age: 30 and 35
Abolaeha et al. [12]	Postsurgical patients	NM	NM	NM	NM
Salmingo et al. [1]	Postsurgical patients	3	3	0	Age: 16, 15 and 14
Wang et al. [13]	Postsurgical patients	10	10	0	Age: adolescent Height: 162 cm-172 cm Weight: 47 kg-64 kg
Driscoll et al. [6]	Spine finite element model	1	NM	NM	NM
Salmingo et al. [2]	Pre- and postsurgical patients	6	NM	NM	Age: adolescent
Little et al. [3]	Postsurgical patients	8	NM	NM	Age: adolescent
Abe et al. [14]	Postsurgical patients	20	1	19	Age: adolescent
Wang et al. [15]	Presurgical patient	1	1	0	Age: NM Height: 168 cm Weight: 65 kg
Clin et al. [16]	Postsurgical patients	5	0	5	Age: adolescent
Balamurugan et al. [17]	Spine finite element model	1	NM	NM	NM
Guan et al. [18]	Postsurgical patients	1	NM	NM	Age: 11
Zhang et al. [9]	Presurgical patients	1	0	1	Age: 14 Weight: 45 kg
He et al. [11]	Normal spine	1	1	0	Age: 40 Height: 170 cm Weight: 60 kg
Chen et al. [19]	Postsurgical patients	1	0	1	Age:15

Note: NM-not mentioned.

Setting boundary condition is an important procedure that has to be done while set up simulation process of the finite element analysis. Dumas et al. [10] set displacement to the model as one of the boundary conditions. Displacement by means, the 3D motion of T1 with regards to the pelvis was computed between the bending test measurements and the standing position measurements. Force that could be directly applied was also set as the boundary conditions of the surgical manoeuvre.

There are several studies that have set the boundary conditions as constraining motions of particular vertebra.

TABLE 3: Variables of FEA studies on the corrective mechanism of spine deformity.

Authors	Software(s)	Element type	Geometrical model	Loading and boundary conditions	Type of material	Mechanical properties
Dumas et al. [10]	Ansys 6.0.	(i) Vertebra: beam element (ii) pelvic: beam element (iii) ligament: tension-only cable elements (iv) articular facets: surface contact element	A patient-specific FE model of interverbal disc constructed from CT image.	Displacement: between the bending test measurements and the standing position measurements, 3D motion of T1 in relation to the pelvis was estimated.	Screws and rod: elastoplastic materials	(i) Augmented bending stiffness (about $K_f \times 60$) from T5 to T9; (ii) augmented torsion stiffness (about $K_t \times 80$) from T6 to L5
Abolaeha et al. [12]	Abaqus 6.11-1	(v) Vertebral and intervertebral disc: linear hexahedral (vi) Hooks and screw: quadratic tetrahedral element	A previous patient-specific FE model of vertebral and interverbal disc constructed from X-ray image and CT scan	During the loading and spine growth simulation processes, the inferior extremity of L5 was constrained in all degrees of freedom. Each vertebra is subjected to a dispersed load.	Rod: stainless steel	$E = 190\,GPa\,\nu = 0.4$
Salmingo et al. [1]	Computed tomography (CT), Solidworks 2010, ANSYS 11.0	10 node tetrahedral solid elements	A patient-specific FE model of spine constructed from CT image.	Forces, Fi set with initial values. The coordinates of the screws were rearranged so that the most superior screw is parallel to the z-axis.	Rod: titanium alloy (JIS T 7401-3)	E = 105 GPa yield stress (σY) = 900 MPa yield strain (εY) = 8.57×10^{-3} hardening coefficient (H) = 2.41 GPa
Wang et al. [13]	Radiographic software, ADAMS 2005 software (Mechanical Dynamics)	NM	Previously developed FE model of thoracic spine.	NM	Pedicle screw: titanium rod: titanium	E is 15 to 20 times higher than that of spinal cortical bone.
Driscoll et al. [6]	ANSYS 130.0 APDL	NM	A patient-specific FE model of vertebral and interverbal disc constructed from CT image.	To regulate and measure movement, all bodies assigned multiple coordinate systems centred on their geometric centre of mass.	Screw: titanium (Ti 6Al-4 V, grade 5) rod: cobalt chrome	Pedicle screw: $E = 11\,GPa$ Rod: $E = 213\,GPa$
Salmingo et al. [2]	Solidworks 2010, ANSYS 11.0	10 node tetrahedral solid elements	Three-dimensional FE model of rod geometries before surgery.	Before surgery. Zero force Fi (i = no. of screws) was applied to the corresponding location of each screw on the rod geometry.	Polyaxially pedicle screws and implant rods: titanium	$E = 105\,GPa$ Yield stress (σY) = 900 MPa Yield strain (εY) = $8.57 \times 10 - 3$ Hardening coefficient (H) = 2.41 GPa
Little et al. [3]	Computed tomography	(i) Screw: 8 node brick	A patient-specific FE	A "no separation" normal contact	Screw: titanium	Screw: $E = 108\,GPa$ Rod: $E = 108\,GPa$

TABLE 3: Continued.

Authors	Software(s)	Element type	Geometrical model	Loading and boundary conditions	Type of material	Mechanical properties
	(CT), ABAQUS 6.9-1, Python 2.5	(ii) Rod: 8 node brick and 2 node rigid beam	model with ribcage and Osseo ligamentous spine	and frictionless tangential contact definition were defined between the both surface of the rod and the screw head.	alloy Rod: titanium alloy	Coulomb friction, $\nu = 0.3$ Yield stress = 390 MPa
Abe et al. [14]	Solidworks 2010, Aquilion 64 CT scanner, ANSYS 11.0	10 node tetrahedral solid elements	A patient-specific model of rod geometry constructed from CT image.	NM	Rod: titanium rod (Ti6Al7Nb)	$E = 105$ GPa Yield stress $(sY) = 900$ MPa Yield strain $(\varepsilon Y) = 8.57 \times 10 - 3$ Hardening coefficient $(H) = 2.41$ GPa
Wang et al. [15]	Computed tomography (CT), ANSYS ICEM-CFD	Hexahedron element	A patient-specific FE model of the spine constructed from CT image. -Thoracic spine, the lumbar spine and sacrum.	The upper lamina terminals of T1 were subjected to a fixed loading force of 300 N, which simulated upper body gravity.	Pedicle screw and rod elastoplastic materials	Ligaments elasticity coefficient Anterior longitudinal, $E = 21.34$ N/mm Posterior longitudinal, $E = 36.42$ N/mm, interspinous, $E = 19.96$ N/mm, ligamentum flava, $E = 26.78$ N/mm Supraspinal. $E = 0.04$ N/mm
Clin et al. [16]	ANSYS 14.5	NM	A patient-specific FE model of the spine to pelvis	NM	Screw: titanium alloy Rod: cobalt chrome	$E = 213$ GPa $E = 113$ GPa
Balamurugan et al. [17]	MIMICS 14.0 software, ANSYS 18.0	NM	A patient-specific FE model of thoracolumbar constructed from CT image	All degrees of freedom were limited in the L5 vertebra. Assuming the patient's weight is 800 N (80 kg), apply a compressive force of 50 N all along z-axis to T1. Vertebra.	Rod: titanium	Cortical bone: $E = 1200$ MPa $\nu = 0.26$ Bone posterior: $E = 3500$ MPa $\nu = 0.25$
Guan et al. [18]	Materialise mimics 19.0, Leuven, Abaqus,	Hexahedral elastic elements	A patient-specific FE model of the thoracic spine lumbar vertebrae constructed from CT image	T1 was limited to transverse plan movements.	Elastoplastic spine model	Posterior structure: $E = 3500$ MPa $\nu = 0.25 = 1000$ kg/m³
Zhang et al. [9]	Solidworks 2020, Ansys Workbench 19.0	Tetrahedral elements	A patient-specific FE model of the lumbar spine constructed from CT image	Apply a moment of 10 nm in the planes on the upper surface of the L1 vertebral body to simulate flexion, extension, left and right	Elastoplastic spine model	Cortical bone: $E = 12$ GPa $\nu = 0.3$ Cancellous bone: $E = 100$ MPa $\nu = 0.3$ Annulus fibrosis: $E = 4.2$ MPa $\nu = 0.453$ Nucleus pulposus: $E = 1$ MPa

TABLE 3: Continued.

Authors	Software(s)	Element type	Geometrical model	Loading and boundary conditions	Type of material	Mechanical properties
				bending, left and right rotation.		$\nu = 0.499$
He et al. [11]	Mimics 19.0, ANSYS 15.0	Solid 187 tetrahedral elements	Three-dimensional finite element (FE) model of intervertebral disc and pedicle screw & rod system (PSRS).	500 N applied to the models for directions of flexion, extension, lateral bending, and axial rotation	Screw and rod: titanium alloy	Cortical bone: $E = 12$ GPa Poisson's ratio = 0.3 Cancellous bone: $E = 100$ MPa Poisson's ratio = 0.2 Annulus fibrosis: $E = 4.2$ MPa Poisson's ratio = 0.450 Titanium alloy: $E = 110$ GPa Poisson's ratio = 0.25
Chen et al. [19]	CT scan, Solidworks	NM	Three-dimensional finite element (FE) model of the spine from CT, pedicle screw, and rod system.	NM	Rod: titanium alloy	Cortical bone $E = 14$ Pa Poisson's ratio = 0.3 Cancellous bone $E = 500$ MPa Poisson's ratio = 0.3

*Note: E: Young modulus; ν: Poisson ratio; K: the strength coefficient; NM: Not mentioned.

Balamurugan et al. [16] set the L5 vertebra as constrained from all degrees of freedom, and a compressive force of 50 N along the Z-axis was applied on T1 vertebra for the analysis. On the other hand, in the Salmingo et al. works [1, 2], the boundary condition was set considering the manner of rod fixation during the surgical treatment. The screws' coordinates were reoriented such that the most superior screw coincides with the z-axis (located on top of the most inferior screw) because each patient has different implant rod orientation and fixation levels. The most inferior screw at the end of the rod was fixed in all translations but free to rotate. The most superior screw was also fixed except that it was free to move along the superior direction only. The same practice was applied by Guan et al. [17] in their research where the boundary conditions were included as a fixed pelvis in rotation translation, and $T1$ was limited to transverse plan movements. Zhang et al. [9] also set constraint on the displacement and rotation of all nodes on the base of the L5 vertebral body in all directions. However, there is no thoracic regions vertebra was included to set as boundary conditions.

Apart from abovementioned boundary conditions, the contact between rod and screw surface was also introduced by Little et al. [3] in their research. A "no separation" normal contact and frictionless tangential contact definition were defined between the screw head and the surface along the rod during surgery.

Researchers, on the other hand, have developed a variety of approaches to model the loading circumstances and limitations that are relevant to the corrective spine deformity process. Commonly, to achieve the desired correction, the force required to rectify the deformity must be significant. After a set of iterations with the force optimization method, the corrective forces acting on the implant rod were obtained

[1]. Salmingo et al. [1, 2] analysed forces of screws set with initial values of zero before surgery on each screw's matching point on the rod geometry. According to Wang et al. [15], Balamurugan et al. [17], Abolaeha et al. [12], and He et al. [11] studies, load was applied to the upper region of the vertebrae for observation of stress distribution. This was applied as boundary condition.

3.5. Variability in Measured Parameters. The output and findings of the parameters are summarised in Table 4. The focus of this data analysis is to look at the relevant biomechanical criteria that are often used to identify FEA and/or have clinical value.

Most of the articles focused on the influence of Cobb angles which is to indicate magnitude of spine deformity except for two articles which are Balamurugan et al. [17] and He et al. [11] that concentrated on the effect of surgery on deformity treatment in a scoliotic spine. Preoperative and postoperative main curves were described in four different investigations after follow-up period, and the degree of correction varies from 14° to 70° [1, 3, 12].

In this review, scoliosis in several planes' views such as lateral, sagittal, axial, frontal, transverse, and coronal can be observed. Most of the authors studied scoliosis deformity in both sagittal [2, 9, 12, 13, 18] and coronal plane [3, 9, 11, 15, 16, 18]. However, Salmingo et al. and Zhang et al. focused on frontal plane [1, 9]. Figure 3 shows an example of a lateral displacement of the spine from the midline in the coronal (frontal) plane, decreased curvature in the thoracic region in the sagittal (side) plane and rotation in the axial plane.

Most of the authors carried out force analysis during the treatment of the spinal deformity and growth periods, on the rods and the spine for their studies [1, 3, 6, 12, 14, 16, 19].

TABLE 4: Data extraction on the effect of Cobb angles from the reviewed articles.

Authors	Category	Plane	Situation/ Zone	Cobb Angle	Outcome Measures	Parameter Output	Findings
Dumas et al. [10]	Simulation of clinical data and post-operative measurements comparison & rod rotation analysis	Lateral, Sagittal, Axial	Scheuermann hyper kyphosis / Idiopathic scoliosis	50° / 58°	Rod rotation (°)	Lateral rotation= - Sagittal rotation= Mean :4° = Max: 9° Axial rotation= - Lateral rotation= Mean :3° = Max : 7° Sagittal rotation = Mean :4° = Max: 9° Axial rotation = Mean :5° = Max: 11°	The surgeon's experience was consistent with models of two clinical situations of hypokyphosis and scoliosis. Follow-up: NM.
Abolaeha et al. [12] The rod length was changed until the desired Cobb angle was achieved, which was decreased from an initial value of 37° to 28°. This necessitated a 5 mm lengthening of the rod, resulting in a correction force of 362 N. Follow-up: 2 years	Spinal growing rod analysis	Sagittal & Axial	Cycle of Adjustment period — Initial; 1st growth; 2nd growth; 3rd growth; 4th growth	Before / After 37° / 28° 42° / 34° 40° / 33° 39° / 37° 49° / 40°	Magnitude of force	Compressive force (N) 362N 669N 942N 1215N 1454N Rod	Displacement(mm) 5 10 17 20 30
Salmingo et al. [1]	The three-dimensional corrective force analysis	Frontal (x-z plane)	Patient 1 Patient 2 Patient 3	Before / After 57° / 13° 59° / 28° 68° / 18°	3D Forces(N), Stress, Strain Distribution	Only the rod geometry before and after the surgical treatment was used to analyse the distributions of forces that distorted the implant rod.	The highest force acting on each patient's screw ranged from 198 to 439 N. The force magnitude was clinically acceptable. The maximal forces were generated at each patient's lowest fixation level of vertebra. Follow-up: NM
Wang et al. [13]	The corrective forces & bone-screw forces analysis	Sagittal & Axial	NA	Sagittal curve: 5.3° Vertebral axial: 4°- 8°	Resultant Screw force(N)	TCF magnitudes vs resultant screw force magnitudes associated with monoaxial, dorsoaxial and polyaxial pedicle screw. T3 0 T4 1000N T5 ≈350N T6 300N - 349N	True corrective forces were 50±30N on average. For monoaxial, dorsoaxial and polyaxial screws, the average bone-screw forces were 229±140N, 141±99N, and 103±42N, respectively; the average EF magnitudes were 205±136N, 125 ±93N, & 65±39N respectively. Follow-up: NM.
Driscoll et al. [6]	The three-dimensional corrective force analysis	Transverse, Axial, & Sagittal	NA	Right thoracic 73° Proximal thoracic: 42°	Screw pull-out force	T7 0 T8 0 T9 300N - T10 349N T11 <200N T12 ≈350N L1 >800N 0	Over the course of the surgical process simulation, stress in intervertebral discs discovered between instrumented vertebrae averaged 3.95MPa. Follow-up: NM
Salmingo et al. [2]	The three-dimensional corrective forces analysis	Sagittal	Patient 1 Patient 2	Before / After 76° / 27°	Pull-out and push-in force	The screw density and implant implantation	

TABLE 4: Continued.

Authors	Category	Plane	Situation/Zone	Cobb Angle	Outcome Measures	Parameter Output	Findings
			Patient 3 Patient 4 Patient 5 Patient 6	75° 26° 57° 13° 68° 18° 83° 14° 59° 28°		arrangement all contributed to a higher degree of correction. This shows that if more implants are put closer together, vertebrae can be easily altered.	Forces of correction are unrelated. Although increasing the number of implant screws reduced the magnitude of corrective forces, it did not result in a higher degree of correction. Follow-up: NM
Little et al. [3]	The three-dimensional corrective forces analysis	Coronal	Patient 1 Patient 2 Patient 3 Patient 4 Patient 5 Patient 6 Patient 7 Patient 8	Before After 52° 23° 51° 18° 44° 14° 53° 25° 40° 10° 42° 7° 42° 13° 53° 34°	Degree of deformity correction, Compressive force profile	Convex: F1 113N, F2 31N, F3 48N, F4 55N, F5 52N, F6 34N, F7 123N Concave: F1 424N, F2 105N, F3 169N, F4 218N, F5 214N, F6 142N, F7 466N	Endplate-to-endplate contact was seen on adjacent endplates of one or more intervertebral disc spaces in the instrumented curve after the surgical loading procedures, according to patient model predictions. Follow-up: NM The concave side corrective force is four times greater than in convex side. Follow-up: NM
Abe et al. [14]	The corrective force estimation	NM	NA	Thoracic 53°-74°	Push out or push in forces	Flexion: L2- 3.28°, L3- .4°, L3- 3.06°, L4- 1°, L4- 3.58°, L5- 1° Extension: L2- 2.3°, L3- 3.3°, L3- 1.18°, L4- 2.3°, L4- 2.56°, L5- 4°	Axial compression- The rod was the part that was subjected to the most stress Flexion- the stress was centred on proximal pedicle screws. Extension and lateral bending- an osteotomized L1 vertebra bore the greatest stress on the model. Follow-up: NM
Wang et al. [15] ranges of motion (ROM) Lateral Bending	The stress-strain analysis	Coronal L2-L3 L3-L4 L4-L5	NA 3.31°-5.0° 3.33°-4.3° 2.08°-4.01°	Thoracolumbar: 53°		The	
Clin et al. [16]	Pedicle screw design & Load-Sharing Capacity analysis	Transverse & coronal	NA	Thoracic 53°-85°	Derotation force, axial torque	The average post-instrumentation force sustained by high and low-density pedicle screw design configurations was recorded, as well as the peak force experienced during surgery simulation.	Increased degrees of freedom in the screw head limit the screws ability to cure coronal deformity while lowering bone-screw forces. Follow-up: 10 years
Balamurugan et al. [17]	Effect on spine deformity correction	NM	NA	NM	Stress distribution	T5 <0.5MPa T6 <0.5MPa T7 <0.5MPa T8 300 – L1 349MPa L2 0-0.5MPa L3 0.5-1MPa L4 >1.5MPa L5 >1.5MPa	After surgery, the stress concentration is highest near the end of the lumber area. Follow-up: NM
Guan et al. [18]	The three-dimensional corrective forces analysis		(i) Forward bend (ii) Stretch	Thoracic 14°-36°	Stress	As the 3D corrective forces increased, the cobb angle of	

TABLE 4: Continued.

Authors	Category	Plane	Situation/Zone	Cobb Angle	Outcome Measures	Parameter Output	Findings
		Coronal, sagittal and horizontal	(iii) Side bender (iv) Twists	Lumbar: 10°-17°		the thoracolumbar section reduced, as did the rotation angle of the vertebra. The combined force correction effects were higher.	The objective functions were each lowered by 58%, 52%, and 63 percent. On the convex side of the highest displacement of the vertebral body, the optimal corrective forces point was found. Follow-up: NM
Zhang et al.[9]	Stress distribution	Coronal, sagittal and frontal	NA	Frontal: 43° Lumbar: 45°	Stress distribution	Stress is concentrated on the lumbar vertebral body during flexion loading, with an unequal stress distribution on the left anterior side of the vertebral body (concave side). Stress in the lumbar spine is localised primarily at the pedicle of the vertebral arch and the lamina of the vertebral arch during extension load.	Under all loads, the range of motion (ROM) is reduced. Flexion loads cause a greater distribution of vertebral concave stress. The stress is concentrated in the L3 vertebral arch. Follow-up: NM
He at al. [11]	The three-dimensional corrective forces analysis	Coronal, sagittal and horizontal	NA	NM	Stress shielding rate	FEA analysis of the new improved spinal correction system ISCS to determine its stability and biomechanical features, as well as a comparison of the ISCS to the pedicle screw and rod system (PSRS).	Maximum stress L2 vertebral body & L1/2 and L2/3 discs in PSRS were smaller than in ISCS. PSRS and ISCS have identical maximum stress in lateral bending and axial rotation directions. Follow-up: NM
Chen at al [19]	The pedicle screw placement strategies	Sagittal	(a) All segments have pedicle screws placed. (b) Pedicle screws were implanted in all of the concave side's segments, with interval screws inserted in the convex side. (c) Both side alternate screws (d) instruments on both sides of the interval screws (e) interval and alternate screws instrumentation in each side	Thoracic: 43°	Interaction force	113N 113N 289N 172N 172N	Densities of pedicle screws and screw-placement techniques have little influences in the curve correction. Strategy E has better biomechanics properties for surgery. Follow-up: NM

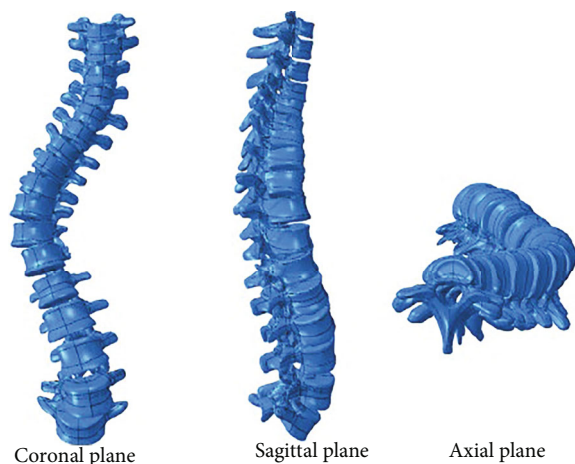Coronal plane   Sagittal plane   Axial plane

Figure 3: A spine with scoliosis with coronal, sagittal, and axial plane views [5].

Few of them created stress profile to understand the stress concentration profile on the vertebra and disc under different loads [1, 9, 11, 17]. Meanwhile, Dumas et al. [10] focused on rod rotation analysis on lateral, sagittal, and axial plane, and Wang et al. [15] demonstrated ranges of motion for L2 to L5 under various loading scenarios.

4. Discussion

4.1. Quality of Search. The aim of this systematic review was to analyse the biomechanical characteristics and parameters that are typically used in finite element analysis to investigate the corrective mechanism of scoliosis-related spine deformity. Understanding the corrective mechanism requires a comprehensive analysis on the parameters used in each investigation. In the present study, fifteen articles were included for the extensive review. In the reviewed studies, participants' characteristics, Cobb angle, pedicle screw systems, and biomechanical responses can be further discussed.

4.2. Effect of Deformity Angles on Spine Corrective Forces and Stresses. The simulated corrected Cobb angle is usually attributed to the clinically established postoperative Cobb angle in the immediate postoperative period. This could provide the models' accuracy in forecasting the change in coronal deformity following surgery. The Cobb angle which is used for comparison of deformity level is the maximum angle that can be projected between the upper and lower endplates of the scoliotic curve. To treat and prevent worsening deformity in severe cases of scoliosis (Cobb angle more than 45°-50°), surgical instrumentation or, in some cases, spinal fusion is sometimes utilised. Developing an optimum method of corrective force and predicting surgically imposed contact stresses between adjacent vertebral endplates for scoliosis patient during surgery through practical experiment is quite difficult. Hence, FEA can be used to model different surgical procedures and anticipate the three-dimensional results in the form of deformity correc-

tion and construct flexibility. Table 3 covers the variables involved in FEA studies.

Understanding and analysing the forces acting on the spine, as well as the interrelationship between both the force and the Cobb angle, will enable us to advance with improved systems [12]. According to Abolaeha et al., the resultant Cobb angles are inversely proportional to the progression of growth, rod lengths, and distraction force during a two-year period. To assess the forces required to treat scoliosis, Salmingo et al. [1] created an elastoplastic FEM. Based on differences in implanted geometry before and after surgery, the three-dimensional forces required to deform a rod were calculated. The instrumented spine's at the lowest level experienced the highest forces.

Using the same FE model, Salmingo et al. continued to study the relationship between the magnitude of corrective forces and the degree of correction, which they measured changes of Cobb angle [2]. Actually, these values can be obtained by calculating the difference between preoperative and postoperative Cobb angle. They claimed that the degree of correction and the corrective forces operating on the rod were unrelated too. They also suggested that other factors, such as screw implantation arrangement and spine rigidity, may be linked to scoliosis repair.

However, from the study carried out by Little et al. [3] revealed that increasing the simulated intraoperative forces caused the anticipated corrected Cobb angle to decrease. Force, geometry (human anatomical), and tissue stress are involved in coronal plane deformity treatment. These are the most significant considerations in getting the best possible correction for a patient with the least amount of risk of high stresses on the spinal tissues, which could lead to implant-related problems.

After adding a growing rod, Abolaeha et al. [12] created a scoliotic spine FEM to model the spine growth over a two-year period. Based on the analysis, the pressures required to induce the correct Cobb angle changes are identical to those seen in patients. To distribute the load, the rod was linked to both vertebrae in the pair, which is identical to the present surgical insertion process. At the time of the original operation, it was expected that the deformity angle would be rectified by 50%. Following the initial operation, invasive lengthening treatments (similarly referred as distractions) were conducted every six months over a year to keep up with the growth of the spine.

Meanwhile, Guan et al. [18] concluded that whenever 3D correction forces rose, the thoracolumbar segment's Cobb angle steadily reduced, and the vertebral body's rotation angle lowered as well. The combined force correction effects were even higher. When correction forces were applied, stress at intervertebral discs in the distorted region changed drastically. Essentially, during scoliosis surgery, corrective force cannot be applied to the spinal implant beyond the anchor holding strength limit. If the corrective force exceeds the anchor's strength, the implant may break or the bone may fracture, resulting in "screw ploughing." Destabilization of the spinal segment by releasing soft tissue or the facet joint could be more critical than using an excessive correction manoeuvre with rigid implant to avoid

implant fracture or pedicle rupture during a more severe curve correction procedure [14].

4.3. Analysis of Pedicle Screws and Implant Rod System due to Spine Deformity. For the treatment of spinal malformations, pedicle screw fixation has become a common surgical instrumentation approach. The better bone-implant connection allows surgeons to diagnose more corrective movements and employ larger correction pressures when translating and derotating the deformed spine. Hence, pedicle screws and its placement strategies are important as it has a minor influence on the curve correction scoliosis treatment [14]. In recent years, fewer screws have been used in scoliosis surgery for cost considerations, and correction rates have been reported as being similar between the less density group and the high-density group. For instance, Salmingo et al. [2] carried out a study by increase in absolute number of implant screws which resulted in reduction of the magnitude of corrective forces and did not give a greater degree of correction, and it was hypothesised that additional screws might prolong the surgery and result in more blood loss for the patients.

On the contrary, Clin et al. [16] discovered that reducing the number of screws raised the postoperative stresses that each screw could withstand, but that the influence on potential problems has to be investigated further. In their investigation, they found that independent of screw type, both high-density and low-density implant designs achieved comparable coronal correction and shared corrective forces equally well. Increased degrees of freedom of the screw head were also discovered to decrease the potential to cure coronal deformity while generating reduced bone-screw forces.

Theoretically, a greater number of implantations might give higher correction forces, resulting in better coronal and sagittal plane correction rates. A screw–rod connection which provides degrees of freedom, on the other hand, may make it difficult to perform the desired manoeuvres [21]. In addition, other variables such as curve flexibility, surgeon-specific objectives, and procedures may also play a role in the contradictory findings [19]. Wang et al. [20] used three forms of screws namely monoaxial, polyaxial, and dorsoaxial pedicle screws for their study. At each step, external forces must be raised until the rods can easily lock into the screw head saddles, which is linked to minimum "true corrective forces" (TCF) and little to no "Extra Forces" (EF) available to deliver the desired correction. The results showed that the dorsoaxial screws allowed for the least amount of EF to be created while forcing in order to make it certain appropriate rod seating and locking at all pedicle screws for corrective deformity correction. Clin et al. [16] claimed that lowering implant density by 30% permitted almost same degree of coronal correction as a fully instrumented construct irrespective of pedicle screw type, but that the influence on potential complications has to be investigated further.

He et al. [11] also claimed as pedicle-screw-rod system (PSRS) has always been regarded as the gold standard for the scoliosis treatment even though it has its own limitations. PSRS has several advantages, including rigorous fixation of deformities, increased osseous fusion, and a lower rate of pseudarthrosis. Front and mid columns are protected by rigid fixing, which counteracts eccentric stress. In addition, the fusion rate of stiff fixing is higher than that of semi-rigid fixing or no fixing. High stiffness, on the other hand, promotes fast scoliosis stability and minimises the physiological stress on the deformed vertebra.

Despite the fact that in recent years, the quality of studies in this field has improved, this review underlines the present literatures lack of regular use of standardised measures of end results and methodologies for preoperative and postoperative assessment. This standard should be broadened to include procedures for classifying and reporting complications. For example, past research has shown that excessive correction forces might could result in implant or bone fractures, which could result in screw extraction from the vertebra. As a result, gaining a better knowledge of scoliosis correction biomechanics necessitates an examination of corrective forces acting on the deformed rod [1].

Once the implant has been installed, the stress is centred on the two ends of the vertebral body, the rod, and the pedicle screw, resulting in a stress shielding effect. The stress shielding reduces the pressure on the intermediate vertebral body, and it just may result in bone loss and osteoporosis. Another limitation is that the cephalic and posterior sides of fixed segments have their rotation centres shifted. Because of these disadvantages, some orthopaedics professionals and researchers recommend using biodegradable or internal fixing materials with a low Young's modulus [11].

Another notable highlight is lack of studies by previous researchers which focus only one specific region either it is lumbar or thoracolumbar region. Most of the researchers either involves whole spine region or mostly thoracolumbar region for their studies ([1, 2, 9, 11, 12, 15, 17, 20]. Actually, between thoracic and lumbar vertebrae, there are changes in transverse process bone mass and anatomical structure [11]. As a result, more research involving patients' thoracic regions is required. The search method was confined to English-language articles, which is a limitation of the study. To discover articles, only five databases were used, and it is possible that some articles were overlooked. For the missing relevant articles, a manual search was conducted.

5. Conclusions

The present review highlights fifteen articles related to corrective mechanism of spine deformity that is published from 2001 until 2021. The correction mechanism, pedicle screw, rod system, Cobb angle, and other variable characteristics related to scoliosis surgery on patients' bodies were the subject of this review. The collected data were able to furnish basic details about the simulations as well as some variables that may affect the predictive accuracy of the simulation. However, insufficient information in certain aspects prevents the analysis of related measured variables. There are various aspects that associated to scoliotic patients such as muscular activation, spine rigidity, deformity severity, the amount of stress that an internal fixation could withstand, and inter-individual differences have yet to be investigated.

Insufficient information prevents the analysis of related measured variables. Hence, to improve and provide a better knowledge of the finite element approach for the analysis of correction mechanisms of spine deformity due to scoliosis, further research is needed in the areas stated above.

Data Availability

The data used to support the findings of this study are available from the corresponding author upon request.

Conflicts of Interest

The authors declare that they do have no conflicting interests which might affect the results of the study.

Acknowledgments

References

[1] R. Salmingo, S. Tadano, K. Fujisaki, Y. Abe, and M. Ito, "Corrective force analysis for scoliosis from implant rod deformation," *Clinical biomechanics*, vol. 27, no. 6, pp. 545–550, 2012.

[2] R. A. Salmingo, S. Tadano, K. Fujisaki, Y. Abe, and M. Ito, "Relationship of forces acting on implant rods and degree of scoliosis correction," *Clinical biomechanics*, vol. 28, no. 2, pp. 122–128, 2013.

[3] J. P. Little, M. T. Izatt, R. D. Labrom, G. N. Askin, and C. J. Adam, "An FE investigation simulating intra-operative corrective forces applied to correct scoliosis deformity," *Scoliosis*, vol. 8, no. 1, 2013.

[4] C. É. Aubin, Y. Petit, I. A. F. Stokes, F. Poulin, M. Gardner-Morse, and H. Labelle, "Biomechanical modeling of posterior instrumentation of the scoliotic spine," *Computer Methods in Biomechanics and Biomedical Engineering*, vol. 6, no. 1, pp. 27–32, 2003.

[5] W. Wang, G. R. Baran, R. R. Betz, A. F. Samdani, J. M. Pahys, and P. J. Cahill, "The use of finite element models to assist understanding and treatment for scoliosis: a review paper," *Spine Deformity*, vol. 2, no. 1, pp. 10–27, 2014.

[6] M. Driscoll, J. M. Mac-Thiong, H. Labelle, and S. Parent, "Development of a detailed volumetric finite element model of the spine to simulate surgical correction of spinal deformities," *BioMed research international*, vol. 2013, Article ID 931741, 2013.

[7] N. A. Azizan, K. S. Basaruddin, and A. F. Salleh, "The effects of leg length discrepancy on stability and kinematics-kinetics deviations: a systematic review," *Applied bionics and biomechanics*, vol. 2018, 2018.

[8] P. X. Ku, N. A. Abu Osman, and W. A. B. Wan Abas, "Balance control in lower extremity amputees during quiet standing: a systematic review," *Gait & Posture*, vol. 39, no. 2, pp. 672–682, 2014.

[9] Q. Zhang, T. E. Chon, Y. Zhang, J. S. Baker, and Y. Gu, "Finite element analysis of the lumbar spine in adolescent idiopathic scoliosis subjected to different loads," *Computers in Biology and Medicine*, vol. 136, article 104745, 2021.

[10] R. Dumas, V. Lafage, Y. Lafon, J. P. Steib, D. Mitton, and W. Skalli, "Finite element simulation of spinal deformities correction by in situ contouring technique," *Computer Methods in Biomechanics and Biomedical Engineering*, vol. 8, no. 5, pp. 331–337, 2005.

[11] Z. He, M. Zhang, W. Li et al., "Finite element analysis of an improved correction system for spinal deformity," *In Vivo*, vol. 35, no. 4, pp. 2197–2205, 2021.

[12] O. A. Abolaeha, J. Weber, and L. T. Ross, "Finite element simulation of a scoliotic spine with periodic adjustments of an attached growing rod," in *2012 Annual International Conference of the IEEE Engineering in Medicine and Biology Society*, vol. 2012, pp. 5781–5785, 2012.

[13] X. Wang, C. E. Aubin, H. Labelle, S. Parent, and D. Crandall, "Biomechanical analysis of corrective forces in spinal instrumentation for scoliosis treatment," *Spine (Phila Pa 1976)*, vol. 37, no. 24, pp. E1479–E1487, 2012.

[14] Y. Abe, M. Ito, K. Abumi, H. Sudo, R. Salmingo, and S. Tadano, "Scoliosis corrective force estimation from the implanted rod deformation using 3D-FEM analysis," *Scoliosis*, vol. 10, Supplement 2, pp. 1–6, 2015.

[15] T. Wang, Z. Cai, Y. Zhao et al., "Development of a three-dimensional finite element model of thoracolumbar kyphotic deformity following vertebral column decancellation," *Applied Bionics and Biomechanics*, vol. 2019, Article ID 5109285, 9 pages, 2019.

[16] J. Clin, F. le Navéaux, M. Driscoll et al., "Biomechanical comparison of the load-sharing capacity of high and low implant density constructs with three types of pedicle screws for the instrumentation of adolescent idiopathic scoliosis," *Spine Deformity*, vol. 7, no. 1, pp. 2–10, 2019.

[17] S. Balamurugan, K. Pandey, S. R. Iyer, A. Krishnan, and S. Patil, "A biomechanical study on post-scoliotic deformity correction," in *IOP Conference Series: Materials Science and Engineering*, vol. 912, 2020.

[18] T. Guan, Y. Zhang, A. Anwar, Y. Zhang, and L. Wang, "Determination of three-dimensional corrective force in adolescent idiopathic scoliosis and biomechanical finite element analysis," *Frontiers in Bioengineering and Biotechnology*, vol. 8, pp. 1–13, 2020.

[19] K. Chen, J. Zhao, Y. Zhao, C. Yang, and M. Li, "A finite element analysis of different pedicle screw placement strategies for treatment of Lenke 1 adolescent idiopathic scoliosis: which is better?," *Computer Methods in Biomechanics and Biomedical Engineering*, vol. 24, no. 3, pp. 270–277, 2021.

[20] X. Wang, C. E. Aubin, D. Crandall, and H. Labelle, "Biomechanical modeling and analysis of a direct incremental segmental translation system for the instrumentation of scoliotic deformities," *Clinical biomechanics*, vol. 26, no. 6, pp. 548–555, 2011.

Review Article

The Influence of Reducing Disease Activity Score on Cervical Spine Deformity in Rheumatoid Arthritis: A Systematic Review

Anna B. Veldman ⓘ,[1] Cornelia F. Allaart,[2] and Carmen L. A. Vleggeert-Lankamp ⓘ[1,3,4]

[1]*Department of Neurosurgery, Leiden University Medical Centre, Leiden, Netherlands*
[2]*Department of Rheumatology, Leiden University Medical Centre, Leiden, Netherlands*
[3]*Department of Neurosurgery, The Hague Medical Centre and HAGA Teaching Hospital, The Hague, Netherlands*
[4]*Department of Neurosurgery, Spaarne Hospital Haarlem/Hoofddorp, Netherlands*

Correspondence should be addressed to Anna B. Veldman; a.b.veldman@lumc.nl

Background. Rheumatoid arthritis (RA) can cause deformity in particularly the craniocervical but also in the lower cervical region. *Objectives*. The aim of this study is to give an overview of current literature on the association of disease activity score (DAS) and the prevalence and progression of rheumatoid arthritis-associated cervical spine deformities. *Methods*. A literature search was done in PubMed, Embase, and Web of Science using a sensitive search string combination (Supplemental File). Studies describing the association between DAS and the incidence and progression of atlantoaxial subluxation, vertical subluxation, and subaxial subluxation were selected by predefined selection criteria, and risk of bias was assessed using a Cochrane checklist adjusted for this purpose. *Results*. Twelve articles were retrieved, and risk of bias on study level was low to moderate. In the eight longitudinal studies, patients demonstrated high DAS at baseline, which decreased upon treatment with medication: cervical deformity at the end of follow-up was associated with higher DAS values. The four cross-sectional studies did not demonstrate a straightforward correlation between DAS and cervical deformity. Deformity progression was evaluated in three studies, but no convincing association with DAS was established. *Conclusion*. A positive association between prevalence of cervical spine deformities and high disease activity was demonstrated, but quality of evidence was low. Progression of cervical deformity in association with DAS control over time is only scarcely studied, and future investigations should focus on halting of deformity progression.

1. Introduction

Rheumatoid arthritis (RA) is known for its destructive influence on the cervical spine anatomy [1]. Inflammation of synovial tissue and release of inflammatory cytokines can result in laxity of the ligaments, progressive joint destruction, and erosion of the bone [2]. As a result, abnormal mobility can develop into atlantoaxial subluxation (AAS) and/or vertical subluxation (VS) in the upper cervical spine and to subaxial subluxation (SAS) at the lower cervical levels [3]. This may cause medullary compression, which can lead to sensory and motor dysfunction, disability of arms and legs, spasms, and pain.

In current rheumatology care, a decrease in rheumatoid arthritis-related peripheral joint deformities is observed. This is ascribed to improvements in treatment aimed at achieving low disease activity, in particular with the biological disease-modifying antirheumatic drugs (bDMARDs), which enable the control of systemic inflammatory processes in RA patients more effectively [3]. In the current treatment policies, DMARDs are not only prescribed to more patients, but also in an earlier stage of the disease, which leads to a more effective decrease in systemic inflammation, represented by disease activity scores (DAS) [4].

In evaluating radiographic structural lesions at the hands and feet of RA patients during the course of the disease, a

clear association between a decrease in systemic disease activity parameters and stabilization of joint erosions has been established [5–9]. It is likely that efforts to suppress inflammation in RA in an earlier stage, and more effectively than in previous decades, result not only in less damage to peripheral joints, but also in less damage to the cervical spine. Clinical practice seems to reflect this hypothesis: in contemporary orthopedic and neurosurgical clinics, a decrease in incidence of rheumatoid arthritis-related cervical deformities is observed. Several papers have demonstrated an association of a (decrease in) disease activity, usually being influenced by synthetic or biological DMARDs, and the incidence of cervical spine deformity [6, 10].

However, it remains unclear whether deformity can stabilize, or even reverse, if DAS values are lowered to satisfactory levels. The aim of this study is to systematically review current literature on the association of the course of disease activity scores (DAS) and the prevalence and progression of rheumatoid arthritis-associated cervical spine deformities.

2. Material and Methods

The systematic review was conducted in accordance with the Preferred reporting items for systematic reviews and meta-analyses: the PRISMA statement [11].

2.1. Search Strategy and Study Selection. In December 2020, the databases PubMed, Cochrane, Embase, Web of Science, and Central were searched for peer-reviewed articles, excluding meeting abstract references, using the search strategy in appendix A based on the following PICO: P, patients suffering from rheumatoid arthritis; I, patients with an increased DAS or DAS28 or DAS44 score; C, patients with a low DAS or DAS28 or DAS44 score or being in remission; and O, cervical deformity, represented by AAS (or AAI), SAS, or VT. Two of the authors (AV and CVL) separately screened the articles by title and abstract, to select studies that met the predefined selection criteria.

Any discrepancy in selection between the two reviewers was resolved in open discussion. The obtained articles were checked for citations of articles missed in the search, so no relevant articles were missed.

Inclusion criteria:

  (i) The article was published in English or Dutch

  (ii) The study included patients diagnosed with rheumatoid arthritis (ANCA, TNF, or rheumatoid factor positive)

  (iii) The study included the measuring of disease activity in all of the patients

  (iv) The study concerned cervical anatomy/deformity diagnosed on cervical fluoroscopy or MRI

  (v) The study was a case control study, cohort study, or randomized controlled trial

Exclusion criteria:

  (i) The study included less than 10 patients

  (ii) Meta-analysis or systematic review

  (iii) The study had a follow-up period of less than 6 months

2.2. Assessment of Quality. The methodological quality of these studies was assessed by two independent reviewers (AV and CVL), using a modified version of the checklist for cohort studies of the Dutch Cochrane Center.

The items reviewed in the assessment, focusing on study level, were definition of patient group (containing information on age, gender, and diagnosis of rheumatoid arthritis), selection bias, allocation bias, and attrition bias (loss to follow-up below 20%). For each item, one point could be attributed, and thus, a maximum score of four points could be achieved by each article.

3. Data Extraction

Data from the studies were extracted by two independent reviewers (ABV and CVL) concerning study design, sample size, patient characteristics, disease duration, severity of RA, follow-up, and type of radiological evaluation. Disease activity in a composite score was based on evaluation of 44 or 28 peripheral joints, by evaluating erythrocyte sedimentation rate (ESR) or C-reactive protein (CRP) and by evaluating general health assessment on a visual analogue scale (VAS). Thus, disease activity can be represented as DAS, DAS28-ESR, or DAS28-CRP [12]. The cut-off values differ for DAS and DAS 28; for DAS, activity can be interpreted as low (DAS ≤ 2.4) or high (DAS > 3.7). A DAS < 1.6 corresponds with being in remission. For DAS28, activity can be interpreted as low (DAS28 ≤ 3.2) or high (DAS28 > 5.1). A DAS28 < 2.6 corresponds with being in remission. There is no difference in cut-off values for DAS28 whether it is calculated using ESR or CRP [12].

DAS were evaluated at baseline and during follow up. Radiological scoring (cervical deformity) evaluated the presence and progression of atlantoaxial subluxation (AAS; or sometimes indicated as AAI: atlantoaxial instability), vertical subluxation (VS), and subaxial subluxation (SAS).

Finally, the assessed correlations between DAS and cervical deformity presence and progression, as indicated by the authors, were extracted from the selected articles.

These data were gathered on piloted forms and compared. Any discrepancies were discussed.

4. Level of Evidence

The quality of evidence for all outcome parameters were planned to be evaluated using the GRADE (Grading of Recommendations Assessment, Development and Evaluation) approach (according to Atkins et al. [13] and adapted from Furlan et al. [14].

5. Results

5.1. Search Results. In the search, 221 articles were identified after duplicates were removed. Titles and abstracts were screened resulting in 28 articles eligible for inclusion. Full-text reading excluded another 14 articles, resulting in the inclusion of 14 articles (Figure 1). In one of these articles, the authors referred to an article that fulfilled the inclusion criteria but was not identified in the search ("snowballing"). This article was added, leading to 15 articles being included. However, amongst these, 4 articles were produced by the same author group [10, 15–17], describing the same correlations in a growing group of patients over the years (2012: 38 patients; 2013: 91 patients; and 2017 and 2019: 151 patients, same population). Therefore, only the 2019 paper is considered in this review.

Consequently, 12 articles are considered in the current review: (a) 7 articles longitudinally describing the correlation between cervical deformity on cervical spine radiographs and disease activity [6, 16, 18–22], including 2 articles describing the same population at 2-year [18] and 5-year follow-up [19], with focus on different aspects of the DAS-cervical deformity association; (b) 2 articles cross-sectionally describing the correlation between cervical deformity on cervical spine radiographs and DAS28 [7, 23] and 1 article describing the correlation of DAS28 measured at baseline and cervical deformity on cervical spine radiographs after years of follow up [24]; and (c) 2 articles describing the correlation between presence of atlantoaxial synovitis on MRI and DAS either longitudinally [25] or in a cross-sectional manner [26].

The number of patients studied varied from 20 to 220, the mean disease duration at baseline varied from 6 months to 11 years, RA severity at baseline varied from "early onset" to an advanced Steinbrocker stage, and the follow-up period varied from 1 to 12 years (Table 1). Most studies evaluated the DAS28 either with ESR or CRP data, and only two studies used the DAS [25, 26].

5.2. Risk of Bias. In all studies, the patient group was defined properly, reporting age, gender, duration of disease at baseline, and reporting that the diagnosis RA was according to the American College of Rheumatology criteria [27]. Selection bias was absent in the study of Neva and Kauppi since the patients were randomized [18, 19]. The two studies describing MRI results indicated that they included "consecutive" patients with strict criteria [25, 26].

Allocation bias was absent in the study of Neva et al. [18, 19] and in the studies of Kanayama, Sandstrom, Zoli, and Carotti [6, 22, 25, 26] since the patients were subjected to a strict medication regimen for all included patients. Attrition bias was consequentially not present in retrospective and cross-sectional studies (Table 2). In some studies, evaluation of radiographic images was done by an independent reviewer [18–20, 24].

5.3. Definitions of Cervical Deformity. Cervical spine deformity is described with a variety of parameters throughout the articles, but all articles used the parameter atlantoaxial subluxation (AAS). The parameters vertical subluxation (VS) (or atlantoaxial impaction, AAI) and subaxial subluxation (SAS) were also frequently reported and evaluated in this article. Definitions of abnormality differ slightly between studies (Table 3). AAS, measured as the distance from the middle of the posterior border of the anterior part of the C1 arch until the anterior cortex of the odontoid peg (ADI), was considered abnormal if the difference in neutral position exceeded 3 mm [16, 21, 23, 26] or exceeded 3 mm difference in flexion radiographs [6, 7, 18, 19, 22, 24].

VS was considered to be present if the odontoid peg entered more than 0 [20, 23] or 4-5 mm through the foramen magnum [26]; if the Sakaguchi-Kauppi value was grades II, III, or IV [6, 18, 19, 22, 24]; or if the Ranawat value was under 13 mm [7, 16, 21]. SAS was defined as the dislocation of two vertebra in the neutral position of the cervical spine exceeding 2 [7, 16] or 3 mm [18, 19, 22, 24].

Progression of AAS was defined as an increase of the ADI of more than 1 [6] or 2 mm [16, 21], progression of VS was defined as an increase of the Ranawat of more than 0 [6] or 2mm [16, 21], and the progression of SAS was defined as an increase of more than 2 mm [16].

5.4. Longitudinal Evaluation of Cervical Deformity and DAS Values. In order to evaluate whether active inflammation, represented by the DAS or DAS28, had an influence on cervical deformity, the seven articles describing the longitudinal correlation between cervical deformity and disease activity are the most informative. In four of those studies, patient groups with recent onset RA are described of which can be assumed that cervical deformity is absent at baseline. No radiographic detectable cervical deformity was evaluated and described by Blom et al. [20] and Sandstrom et al. [22] and assumed in the patient groups described by Neva et al. [18, 19]. With a varying follow up from 2 to 12 years, AAS developed in 2.4 to 8.1% of patients with the DAS ranging between 2.0 and 3.6 (Table 4).

5.4.1. Longitudinal Correlations between Cervical Deformity and DAS in Recent Onset RA. The patient groups with the highest percentages of AAS, VS, and SAS at the end of follow up had the highest DAS (Figure 2). Neva executed a treatment strategy aiming at lowering systemic inflammation but failed to achieve DAS28-remission in the group of patients that developed cervical deformity during the two-year follow-up period, in contrast to the group without cervical deformity [18]. Kauppi demonstrated that the area under the curve for DAS was significantly higher in the groups that developed AAS, VS, or SAS [19]. Blom reasoned that there were so many missing values in their database that longitudinal follow-up was not valuable; they could only conclude that in patients without AAS or VS at the nine-year follow-up timepoint, the mean DAS28 at the three-year follow-up timepoint was lower [20]. They however failed to demonstrate this at the twelve-year follow-up timepoint. Sandstrom concluded that AAS, VS, and SAS occurrence was so low in their patient group, even after 10-year follow-up, that no meaningful correlations to DAS28 could be made [22].
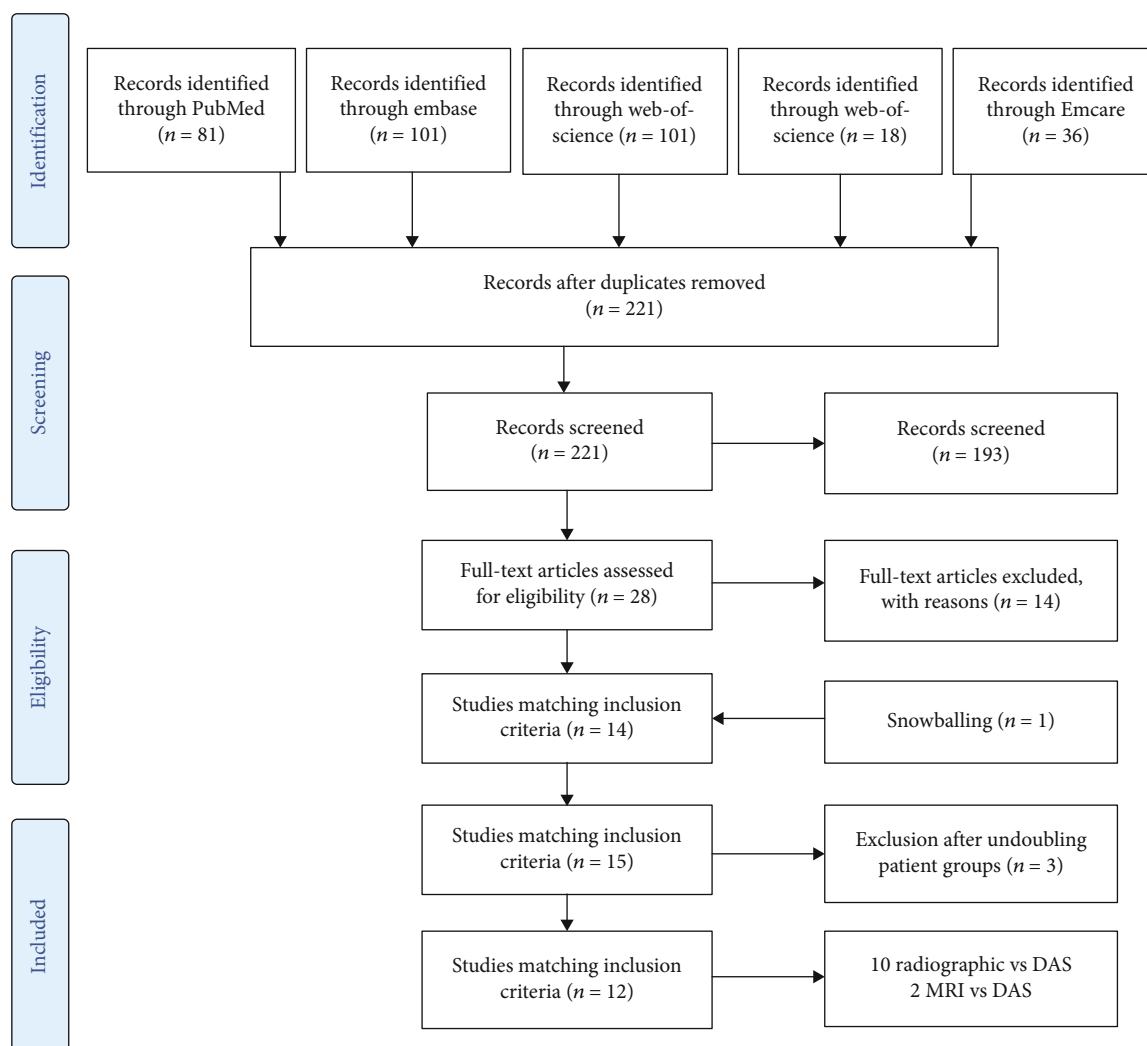
FIGURE 1: Flow chart applying PRISMA criteria to inclusion of articles.

5.4.2. Longitudinal Correlations between Cervical Deformity and DAS Values in Advanced Stage of RA. The other three articles longitudinally describing cervical deformity and DAS over time demonstrate the same pattern. They reported on patient groups that had been suffering from RA for 10 [16], 11 [6], and 17 [21] years. In these populations, 33 to 50% of patients did not demonstrate any deformity at that timepoint, and 6-8% of these patients developed AAS during 3- to 4.5-year follow-up. Horita described that 24% of the patients that already had cervical deformity demonstrated progression of deformity during the 3-year follow-up and that the DAS of those patients was significantly higher (3.2, range 1.1–4.0) than the DAS of patients who did not demonstrate progression of deformity (2.1, range 1.1–3.8; $p < 0.001$) [21]. Kaito described that in the 50% of patients with cervical deformity, 81-86% of patients demonstrated progression although the mean DAS28 at final follow up was 2.6 (representing clinical remission). It was not reported whether the values differed in patients with or without progression [16]. Kanayama reported that 34% of patients with AAS on baseline progressed in AAS and that 21% of patients

with VS progressed in Ranawat score and that the DAS28 was higher in patients who demonstrated progression of cervical deformity (mean 4.2 ± 1.1 vs 3.1 ± 1.3), though seemingly not significant [6].

5.5. Cross-Sectional Evaluation of Cervical Deformity and DAS Values. The cross-sectional papers report on populations suffering from RA for 10 [23], 11 [7], and 13 [24] years. They demonstrate a prevalence of AAS of 10 to 36%, of VS of 5 to 10%, and of SAS of 5 to 13%. The correlation with DAS is not straightforward: Takahashi reports low DAS values [7] and Neva reports moderate DAS values [24] without a difference between patients with and without deformity. Takahashi concluded that suffering from RA for over ten years was a risk factor for developing cervical deformity, while Neva denies that duration of RA correlates to the development of AAS.

Younes evaluated deformity on cervical radiographs and on MRI and reported the presence of synovitis in the upper cervical segments, while the radiographs did not demonstrate deformity (yet). Adding the numbers of patients with

TABLE 1: Prevalence of cervical spine deformity.

	n	% F	Age (yr) ± SD [range]	Disease duration (yr) [range]	Disease activity score	RA severity (Steinbrocker I: II:III:IV) at baseline	Radiological evaluation	Follow-up (mos) [range]
Correlation between cervical deformity on cervical spine radiographs and disease activity from baseline to follow-up								
Neva (2000) [18]	176	63	46 ± 10	0.6 [0.2-1.8]	DAS28-ESR #	Early onset	X cerv (at FU)	24
Kauppi (2009) [19]	149	66	48	0.5 [0.3-0.8]	DAS28-ESR #	Early onset	X cerv	60
Kanayama (2010) [6]	47	77	53 ± 13.4	11 ± 10	DAS28-ESR	2:9:22:14	X cerv	12
Blom (2013) [20]	196	64	51.6 ± 13.7	Max 12 Mos	DAS28-ESR	Early onset	X cerv	144
Kaito (2019) [16]	101	83	57 ± 10 [31-75]	10,7 [0.3–42]	DAS28-CRP	5:20:41:35	X cerv	53 [24-96]
Horita 2019 [21]	49	90	59 [30-81]	17.5 [1-46]	DAS28-CRP	0:0:13:36	X cerv	39 [12-69]
Sandstrom (2020) [22]	85	67	48 ± 10	4	DAS28-ESR		X cerv	120
Correlation between cervical deformity on cervical spine radiographs and DAS-28 in a cross-sectional manner								
Neva (2003) [24]	103	67	45-54	0.5	DAS28-ESR	Early onset	X cerv	96-156 (##)
Younes (2009) [23]	40	78	55.2 ± 11.9	10 ± 7.9	DAS28-CRP		X cerv/MRI cerv	Cross sectional
Takahashi 2014 [7]	220	83	64 [25-84]	11.1 [0.1-57.2]	DAS28-CRP	21:26:35:18	X cerv	Cross sectional
Correlation between presence of atlantoaxial synovitis on MRI and DAS-28								
Zoli (2011) [25]	20	85	54	0.5	DAS	Early onset	MRI cerv	18
Rotti (2019) [26]	50	74	58.2 [36-79]	0.8 [0.41-1]	DAS	Early onset	MRI cerv	Cross sectional

Overview of patient demographics in the studies. MRI was performed with a 1.5 Tesla machine producing fast spin-echo T1-weighted images with fat suppression, with [25] or without [26] intravenous contrast. The MRI scan allowed assessment of the presence of synovitis and erosive joint damage in the upper cervical region. (#) Calculated with DAS28 calculator using the number of swollen joints, number of tender joints, and ESR, (##) recruited in the database 8 to 13 years before; at that time, they were diagnosed with RA 5.6 to 6.4 months before. na: not applicable.

TABLE 2: Risk of bias in the studies.

Study	Score on risk of bias scale	Well-defined patient group	Absence of selection bias	Absence of allocation bias	Absence of attrition bias
Neva (2000) [18]	++++	+	+	+	+
Kauppi (2009) [19]	+++	+	+	+	-
Kanayama (2010) [6]	++	+	-	+	-
Blom (2013) [20]	++	+	+	-	-
Kaito (2019) [16]	++	+	-	-	+
Horita (2019) [21]	++	+	-	-	+
Sandstrom (2020) [22]	+++	+	-	+	+
Neva (2003) [24]	++	+	-	-	+
Younes (2009) [23]	++	+	-	-	+
Takahashi (2014) [7]	++	+	-	-	+
Zoli (2011) [25]	++++	+	+	+	+
Carotti (2019) [26]	++++	+	+	+	+

TABLE 3: Definitions of cervical deformity.

	Definitions of pathology	Definitions of progression of pathology
AAS	(i) Distance from the middle of the posterior border of the anterior part of the C1 arch until the anterior cortex of the odontoid peg (ADI) exceeding 3 mm in *neutral* position [16, 21, 23, 26] (ii) Distance from the middle of the posterior border of the anterior part of the C1 arch until the anterior cortex of the odontoid peg (ADI) exceeding 3 mm in *flexed* position [6, 7, 18, 19, 22, 24]	(i) Increase of the ADI of more than 1 mm [6] (ii) Increase of the ADI of more than 2 mm [16, 21]
VS	(i) Odontoid peg entering more than 0 [20, 23] mm through the foramen magnum [20, 23] (ii) Odontoid peg entering more than 4-5 mm through the foramen magnum [26] (iii) Sakaguchi-Kauppi value being grades II, III, or IV [6, 18, 19, 22, 24] (iv) Ranawat value being less than 13 mm [7, 16, 21]	(i) Increase of the Ranawat of more than 0 mm [6] (ii) Increase of the Ranawat of more than 2mm [16, 21]
SAS	(i) Dislocation of two vertebra in the neutral position of the cervical spine exceeding 3 mm [7, 16] (ii) Dislocation of two vertebra in the neutral position of the cervical spine exceeding 3 mm [18, 19, 22, 24]	(i) Increase the SAS of more than 2 mm [16]

synovitis and patients with cervical deformity on radiograph, they state that 36% of patients have AAS. The mean DAS28 in this study population was 4.79 ± 1.62, without a significant difference in the percentage of patients with a DAS higher than 3.2 in the patients with AAS (78%) compared to the patients without AAS (86%) [23].

5.6. Correlations between Atlantoaxial Synovitis on MRI and DAS Values.

Finally, in the articles that evaluated MRI of the cervical spine of RA patients, active synovitis was reported in 25% of patients with recent onset RA [25, 26]; additionally, performed radiography of the cervical spine did not demonstrate cervical deformity [26] (Table 4). The mean DAS was high in all patients, although it was reported that in patients with deformity, the DAS was significantly higher than in patients without deformity. Zoli reported additionally that after starting medication, aiming at lowering systemic inflammation, one patient demonstrated complete and one patient partial regression of synovial involvement [25].

5.7. Correlation of Cervical Deformity and Peripheral Joint Deformity.

Four of the ten articles that studied RA deformity on radiographs of the cervical spine demonstrate a positive correlation between cervical and peripheral joint deformity [7, 18, 20, 24]. Only Younes fails to demonstrate such a correlation in a patient group suffering from RA for circa ten years [23]. Neva states that in the patient group that has been suffering from RA for five years, the Larsen score is predictive for the development of AAS [24].

In the two articles that compared cervical deformity on MRI with DAS, it was demonstrated that cervical synovitis correlated to erosions in the joints of the hands and feet [25, 26].

6. Discussion

Careful evaluation of literature does not provide us with a satisfactory answer to the question whether control of systemic disease activity in rheumatoid arthritis can prevent progression of RA associated cervical spine deformity. The overall picture however suggests that disease activity, represented by DAS or DAS28, in RA patients with cervical deformity was higher than in those without deformities, although the reported differences were small.

A limitation to the conclusions that could be drawn from this systematic review is that the baseline cervical deformity was not consequently described. Only two studies evaluated the association of DAS in the early stage of disease and cervical deformity after 10-12 years follow-up [20, 24], but due to the abundance of missing values, these studies failed to demonstrate a convincing positive correlation. In future studies, it is advisable to correlate disease activity over time with deformity at the end of follow up. This can be done by using the AUC of DAS values over time. Two studies reported on an AUC value of DAS [19, 24], but again, conflicting results were reported. Kauppi showed a higher DAS-AUC in patients with deformity [19], while Neva could not appoint a positive correlation between the DAS-AUC in the first years of RA with cervical deformity at the end of follow up. Again, a study is set up in which data in individual patients between DAS and deformity can strengthen conclusions.

Another limitation is the scarcity of literature on this topic and the variance in set-up of the available studies. Two studies evaluated patients that already developed deformity; Kanayama reported a higher DAS in patients in which deformity progressed (at least 1 mm increase in ADI or Ranawat after one-year follow-up) in comparison to patients in which AAS and VS remained the same (less than 1 mm increase) [6]. Kaito reports the opposite: halting of progression of deformity could not be achieved; almost 80% of patients with deformity demonstrated progression in deformity though systemic inflammation was tempered [16]. A firm conclusion cannot be drawn, particularly because follow-up was short, and both the differences in AAS and VS and those between DAS in the progressive and nonprogressive group were very small.

The question that remains is whether deformity, once it has developed, can be halted by suppressing disease activity, possibly even to remission of disease. A barrier in studying

TABLE 4: Cervical spine deformity and DAS overview.

Study	n	Deformity none Baseline	Deformity none Progression	AAS Baseline	AAS Progression	AAS + VS/AAI Baseline	AAS + VS/AAI Progression	VS/AAI Baseline	VS/AAI Progression	DAS baseline	DAS final
					Correlation between cervical deformity on cervical spine radiographs and DAS28 from baseline to follow-up						
Neva (2000) [18]	176	100% #	AAS 3.4% AAI 1.1% SAS 2.8%							5.97^	2.01^
Kauppi (2009) [19]	149	100% #	AAS 9% AAI 4% SAS 6%							5.53–5.65	In pts - deformity AUC 3.1 In pts + deformity AUC 3.6*
Kanayama (2010) [6]	47			Mean ADI 4.1 ± 2.2	Mean ADI 4.5 ± 2.3 **, 34% of patients progression of ADI	Mean Ranawat 13.6 ± 2.6	Mean Ranawat 13.4 ± 2.7 **, 21% of patients progression of Ranawat			5.71	Nonprogressive 3.11 ± 1.27, progressive 4.18 ± 1.06
Blom (2013) [20]	196	100% (R1)	3 yrs: AAS 4.8%, AAI 0% 6 yrs: AAS 5.9%, AAI <1% 9 yrs: AAS 7.3%, AAI <1% 12 yrs: AAS 8.1%, AAI <1%							5.45 ± 1.38	Non progressive at 9yrs: 3.69, progressive at 9 yrs: 3.51
Kaito (2019) [16]	101	50%	None: 92% AAS 8%	32%	None 19% AAS 34% VS 63% SAS 9%	12%	None 17% AAS 8% VS 58% SAS 25%	7%	None 14% AAS 14% VS 71% SAS 14%	4.4 ± 0.8	2.6 ± 0.8
Horita (2019) [21]	49	33%	6% (R2)			67%	24% **			In pts – progression in deformity 3.1 In pts + progression in deformity 4.1*	In pts – progression in deformity 2.1 In pts + progression in deformity 3.2*
Sandstrom (2020) [22]	85	100%	None: AAS 2.4% AAI 1.2% SAS 1.2%							5.5 ± 0.9 and 5.6 ± 1.4	< 2.6 (R3)

TABLE 4: Continued.

	n	Deformity none		AAS		AAS + VS/AAI		VS/AAI		DAS baseline	DAS final
		Baseline	Progression	Baseline	Progression	Baseline	Progression	Baseline	Progression		
			Correlation between cervical deformity on cervical spine radiographs and DAS28 in a cross-sectional manner								
Neva (2003) [24]	85	100% #	None: 83% AAS 10% AAI 5% SAS 5%							In pts - deformity 3.3 In pts + deformity 3.5	In pts - deformity 3.5 In pts + deformity 4.5
Younes (2009) [23], Xcerv	50	22.5%			Na	SAS: 10%	Na	10%	Na	MRI and Xcerv findings together: 36% AAS In pts with AAS 78% of pts had DAS> 3.2 and in pts without AAS 86% of pts had DAS> 3.2	Na
Younes (2009) [23], MRI				17.5% active synovitis on MRI, 15% fibrous pannus, 30% hypervascular pannus, 20% of patients demonstrated AAS on MRI							
Takahashi (2014) [7]	220	36%			Na	SAS: 13%	Na	10%	Na	2.66 [1.02 – 6.96]	Na
				Correlation between presence of atlantoaxial synovitis on MRI and DAS							
Zoli (2011) [25]	20	75% no active synovitis				Baseline: 25% active synovitis on MRI				In pts – deformity 3.9 ± 0.2, in pts + deformity 5.0 ± 0.8 *	
Carotti (2019) [26]	50					24% active synovitis on MRI (R4)				In pts – Deformity 4.5 ± 0.5, in pts + deformity 5.7 ± 0.4 *	

Cervical deformity and DAS at baseline and at the end of follow up. The number of patients in the different studies is indicated as well. (#) presumed percentage, regarding the early onset of RA, (^) calculated from data in the article, (∗) significant difference between patients with and without deformity, (∗∗) significant difference compared to baseline value; (R1) remark 1: CWK radiograph available: baseline n = 60; 3 years: n = 66; 6 years: n = 180; 9 years: n = 134; 12 years: n = 78; (R2) remark 2: Calculated from data in discussion "In the present study, the percentage of patients with any cervical instability at baseline (65.3% of 49 patients) increased to 69.4% at final follow up"; (R3) remark 3: derived from the results section: "the four patients with cervical spine deformity were in sustained remission during the whole follow-up time"; (R4) remark 4: contradictory details are given in the article varying from "no obvious radiological lesions were evident" to "AAS was observed in two of the 12 patients with synovitis on MRI," na: not applicable.
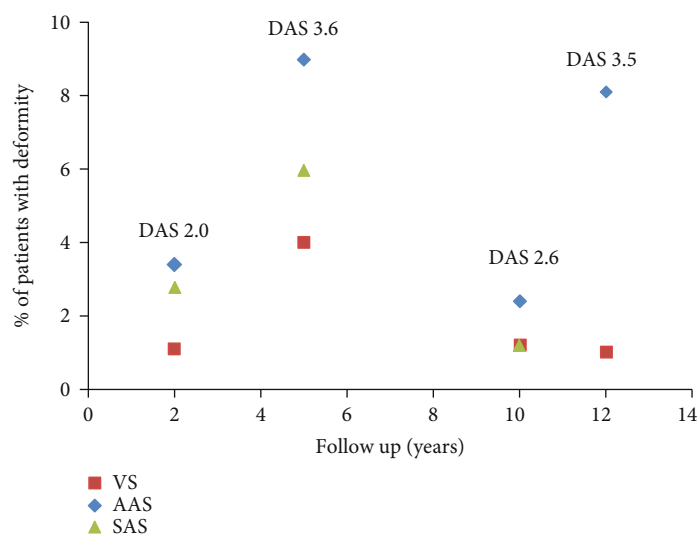
FIGURE 2: Overview of the correlation between duration of follow up, DAS and % of patients with cervical deformity at the end of follow up in the four articles describing longitudinal follow-up in patient groups with recent onset RA. Red squares represent VS, blue diamonds represent AAS, and green triangles represent SAS.

this hypothesis is that with the current successful treatment-to-target regimes [28], the percentage of patients that develop deformity is low, as demonstrated in this review [18–20, 22]. Therefore, in future studies on this topic, large groups of patients have to be included, in order to include enough patients in which treatment-to-target therapy fails and in which patients consequently have high DAS. Moreover, future studies should monitor DAS over many time-points in order to get a good overview of the decrease in DAS, remission, and flares. This should be combined with radiographs at baseline, at intervals, and at the end of sufficiently long follow-up periods.

The paucity of available studies prevented us from performing a meaningful meta-analysis of the included studies. This is caused by the low quality of evidence, as well as the different approaches of diagnosing cervical spine deformity and measuring systemic disease activity in current literature on this topic.

The DAS is not the only parameter that is an indicator for systemic inflammation. MMP3 has also been evaluated in several of the articles studied in this review. Kanayama even demonstrated that the decline in MMP3 was more impressive than the decline in DAS and that it demonstrated a clearer difference between patients with and without progression of cervical deformity [6]. Kauppi performed a multiple regression in a group with recent onset RA and evaluated the correlation of cervical deformity to other parameters and reported that a worse score on HAQ at baseline was predictive for deformity after 5 years follow-up with an OR of 5.81 (1.64-20.52) [19]. The limitation of this study was, however, that no radiographs of the cervical spine were obtained at baseline. It might thus be that the HAQ was worse in those patients that already suffered from cervical synovitis, or even deformity, at baseline. This indicates that in future studies, cervical deformity should not only be correlated to DAS as systemic parameter, but it would be valu-

able to also study correlations with MMP3, self-reported disability, treatment strategy, and/or hand-and-foot erosions.

The goal of finding correlations between certain parameters and cervical deformity after follow up in RA patients is that patients in which progression of deformity is very likely can be appointed and that they can be treated more adequately. Medication treatment can be more aggressive, systemic inflammation more intensely monitored, and, in absence of accomplishing a satisfactory low systemic inflammation status, surgery can be offered in a stage in which deformity is still mild. Once the upper cervical spinal elements are fused by instrumentation, RA pannus diminishes, atlantoaxial deformity stops, and possible compression of the neural structures is prevented [29, 30].

Introduction of biologicals in the treatment of RA has achieved impressive improvement in lowering systemic disease. This is being held responsible for the decrease in prevalence of cervical deformity. This is at least partially true: there is a clear correlation between low DAS values and less cervical deformity. The current overview of literature can however not confirm the hypothesis that progression of deformity can be halted by lowering systemic inflammation. Drawing a conclusion is hindered by the poor quality of data to confirm of reject of the hypothesis. Another hypothesis that may (partially) explain the decrease in cervical deformity in RA patients is that the treatment with biologicals has abandoned the intense treatment with glucocorticosteroids, which have been demonstrated to coincide with cervical spine deformity [31].

7. Conclusion

Lowering disease activity in patients with rheumatoid arthritis has demonstrated to prevent cervical spine deformity with low-quality evidence, but lowering DAS values could

not be demonstrated to halt progression with very low-quality evidence. It is important that the role of DAS in predicting cervical spine deformity development and progression is controversial, and other predictors should be identified in further research. In order to manage expectations on cervical deformity in RA patients optimally, it is crucial that the role of disease activity in cervical spine deformity is further evaluated.

Data Availability

The data used to support the findings of this study are included within the article.

Conflicts of Interest

The authors declare that they have no conflicts of interest with respect to the current study.

Acknowledgments

Supplementary Materials

The search strategy used for this systematic review has been added as a supplemental file. *(Supplementary Materials)*

References

[1] B. R. Wasserman, R. Moskovich, and A. E. Razi, "Rheumatoid arthritis of the cervical spine–clinical considerations," *Bulletin of the Hospital for Joint Diseases*, vol. 69, pp. 136–148, 2011.

[2] H. Nguyen, S. C. Ludwig, J. Silber et al., "Rheumatoid arthritis of the cervical spine," *The Spine Journal*, vol. 4, no. 3, pp. 329–334, 2004.

[3] A. Joaquim and S. Appenzeller, "Cervical spine involvement in rheumatoid arthritis – a systematic review," *Autoimmunity Reviews*, vol. 13, no. 12, pp. 1195–1202, 2014.

[4] G. W. Mallory, S. R. Halasz, and M. J. Clarke, "Advances in the treatment of cervical rheumatoid: less surgery and less morbidity," *World Journal of Orthopedics*, vol. 5, no. 3, pp. 292–303, 2014.

[5] T. Yurube, M. Sumi, K. Nishida, M. Takabatake, K. Kohymama, and O. T. Matsubara, "Progression of cervical spine instabilities in rheumatoid arthritis," *Spine*, vol. 36, no. 8, pp. 647–653, 2011.

[6] Y. Kanayama, T. Kojima, Y. S. T. Hirano, M. Hayashi, K. Funahashi, and N. Ishiguro, "Radiographic progression of cervical lesions in patients with rheumatoid arthritis receiving infliximab treatment," *Modern Rheumatology*, vol. 20, no. 3, pp. 273–279, 2010.

[7] S. Takahashi, A. Suzuki, T. Koike et al., "Current prevalence and characteristics of cervical spine instability in patients with rheumatoid arthritis in the era of biologics," *Modern Rheumatology*, vol. 24, no. 6, pp. 904–909, 2014.

[8] T. Yurube, M. Sumi, K. Nishida, H. Miyamoto, K. M. T. Kohyama, and Y. Miura, "Incidence and aggravation of cervical spine instabilities in rheumatoid arthritis," *Spine*, vol. 37, no. 26, pp. 2136–2144, 2012.

[9] J. Legrand, T. S. Kirchgesner, and P. Durez, "Early clinical response and long-term radiographic progression in recent-onset rheumatoid arthritis: clinical remission within six months remains the treatment target," *Joint, Bone, Spine*, vol. 86, no. 5, pp. 594–599, 2019.

[10] T. Kaito, S. Ohshima, H. Fujiwara, T. Makino, K. Yonenobu, and H. Yoshikawa, "Incidence and risk factors for cervical lesions in patients with rheumatoid arthritis under the current pharmacologic treatment paradigm," *Modern Rheumatology*, vol. 27, no. 4, pp. 593–597, 2017.

[11] D. Moher, A. Liberati, J. Tetzlaff, and D. G. Altman, "Preferred reporting items of systematic review and meta-analyses: the PRISMA statement," *International Journal of Surgery*, vol. 8, no. 5, pp. 336–341, 2010.

[12] J. Fransen, G. Stucki, and P. van Riel, "Rheumatoid arthritis measures: disease activity score (DAS), disease activity score-28 (DAS28), rapid assessment of disease activity in rheumatology (RADAR), and rheumatoid arthritis disease activity index (RADAI)," *Arthritis and Rheumatism*, vol. 49, no. S5, pp. S214–S224, 2003.

[13] D. Atkins, D. Best, and P. Briss, "Grading quality of evidence and strength of recommendations," *BMJ*, vol. 328, no. 7454, pp. 1490–1494, 2004.

[14] A. Furlan, V. Pennick, C. Bombardier, M. van Tulder, and Editorial Board, Cochrane Back Review Group, "2009 updated method guidelines for systematic reviews in the Cochrane Back Review Group," *Spine*, vol. 34, no. 18, pp. 1929–1941, 2009.

[15] T. Kaito, N. Hosono, S. Ohshima et al., "Effect of biological agents on cervical spine lesions in rheumatoid arthritis," *Spine*, vol. 37, no. 20, pp. 1742–1746, 2012.

[16] T. Kaito, S. Ohshima, H. Fujiwara et al., "Predictors for progression of two different types of cervical lesions in rheumatoid arthritis treated with biologic agents," *Journal of Orthopaedic Science*, vol. 24, no. 2, pp. 214–218, 2019.

[17] T. Kaito, S. Ohshima, H. Fujiwara, T. Makino, and K. Yonenobu, "Predictors for the progression of cervical lesion in rheumatoid arthritis under the treatment of biological agents," *Spine*, vol. 38, no. 26, pp. 2258–2263, 2013.

[18] M. Neva, M. Kauppi, H. Kautiainen et al., "Combination drug therapy retards the development of rheumatoid atlantoaxial subluxations," *Arthritis and Rheumatism*, vol. 43, no. 11, pp. 2397–2401, 2000.

[19] M. J. Kauppi, M. H. Neva, K. Laiho, H. Kautiainen, R. Luukkainen, and A. Karjalainen, "Rheumatoid atlantoaxial subluxation can be prevented by intensive use of traditional disease modifying antirheumatic drugs," *The Journal of Rheumatology*, vol. 36, no. 2, pp. 273–278, 2009.

[20] M. Blom, M. Creemers, W. Kievit, J. Lemmens, and P. van Riel, "Long-term follow-up of the cervical spine with conventional radiographs in patients with rheumatoid arthritis," *Scandinavian Journal of Rheumatology*, vol. 42, no. 4, pp. 281–288, 2013.

[21] M. Horita, K. Nishida, K. Hashizume et al., "Prevalence of and risk factors for the progression of upper cervical lesions in patients with rheumatoid arthritis," *Acta Medica Okayama*, vol. 73, no. 3, pp. 235–240, 2019.

[22] T. Sandstrom, V. Rantalaiho, T. Yli-Kerttula, H. Kautiainen, T. Malmi, and A. Karjalainen, "Cervical spine involvement

among patients with rheumatoid arthritis treated actively with treat-to-target strategy: 10-year results of the NEO-RACo study," *The Journal of Rheumatology*, vol. 47, no. 8, pp. 1160–1164, 2020.

[23] M. Younes, S. Belghali, S. Kriaa, S. Zrour, I. Bejia, and M. Touzi, "Compared imaging of the rheumatoid cervical spine: prevalence study and associated factors," *Joint, Bone, Spine*, vol. 76, no. 4, pp. 361–368, 2009.

[24] M. Neva, P. Isomaki, P. Hannonen, M. Kauppi, E. Krishnan, and T. Sokka, "Early and extensive erosiveness in peripheral joints predicts atlantoaxial subluxations in patients with rheumatoid arthritis," *Arthritis and Rheumatism*, vol. 48, no. 7, pp. 1808–1813, 2003.

[25] A. Zoli, S. Bosello, N. Magarelli, G. Dantona, R. Amelia, and A. Fedele, "Atlantoepistrophic magnetic resonance imaging involvement in early rheumatoid arthritis: an aggressive tight control therapy not fully arresting the disease," *Arthritis Care & Research*, vol. 63, no. 11, pp. 1629–1633, 2011.

[26] M. Carotti, F. Salaffi, M. Di Carlo, F. Sessa, and A. Giovagnoni, "Magnetic resonance imaging of the craniovertebral junction in early rheumatoid arthritis," *Skeletal Radiology*, vol. 48, no. 4, pp. 553–561, 2019.

[27] F. Arnett, S. Edworthy, D. Bloch, D. McShane, J. Fries, and N. Cooper, "The American Rheumatism Association 1987 revised criteria for the classification of rheumatoid arthritis," *Arthritis and Rheumatism*, vol. 31, no. 3, pp. 315–324, 1988.

[28] Y. P. M. Goekoop-Ruiterman, J. K. De Vries-Bouwstra, C. F. Allaart et al., "Clinical and radiographic outcomes of four different treatment strategies in patients with early rheumatoid arthritis (the BeSt study): a randomized, controlled trial," *Arthritis & Rheumatism*, vol. 52, no. 11, pp. 3381–3390, 2005.

[29] M. Bydon, M. Macki, M. Qadi et al., "Regression of an atlantoaxial rheumatoid pannus following posterior instrumented fusion," *Clinical Neurology and Neurosurgery*, vol. 137, pp. 28–33, 2015.

[30] S. Matsunaga, K. Ijiri, and H. Koga, "Results of a longer than 10-year follow-up of patients with rheumatoid arthritis treated by occipitocervical fusion," *Spine*, vol. 25, no. 14, pp. 1749–1753, 2000.

[31] S. Zhu, W. D. Xu, Y. Luo, Y. Zhao, and Y. Liu, "Cervical spine involvement risk factors in rheumatoid arthritis: a meta-analysis," *International Journal of Rheumatic Diseases*, vol. 20, no. 5, pp. 541–549, 2017.

Research Article

Value of Postoperative Serum Albumin to Predict Postoperative Complication Severity in Spinal Tuberculosis

Guanyin Jiang, Xing Du ⓘ, Yong Zhu, Muzi Zhang, Wanyuan Qin, Tuotuo Xiong, and Yunsheng Ou ⓘ

Department of Orthopedics, First Affiliated Hospital of Chongqing Medical University, Chongqing 400016, China

Correspondence should be addressed to Yunsheng Ou; ouyunsheng2001@163.com

Background. Many complications occur after surgery in patients with spinal tuberculosis (STB); however, the severity varies in different patients. The complications' severity is evaluated from grades I to V by the Clavien–Dindo classification (CDC), and grade V is the most severe. Most complications are mild, and only severe complications are life threatening, and thus, it is important to identify severe complications in patients with STB. The purpose of this study was to identify the risk factors of postoperative complication severity in patients with STB. *Methods.* Between January 2012 and May 2021, a retrospective study included 188 patients that underwent STB debridement surgery. The patients were divided into three groups based on postoperative complication severity. Clinical characteristics measured included age, sex, body mass index (BMI), comorbidities of diabetes mellitus and pulmonary tuberculosis, alcohol use and smoking history, course of disease, preoperative hemoglobin, preoperative serum albumin, preoperative lymphocytes, preoperative erythrocyte sedimentation rate (ESR), preoperative C-reactive protein (CRP), surgical approach, operating time, blood loss during surgery, postoperative hemoglobin, and postoperative serum albumin. The clinical characteristics of patients with STB who developed postoperative complications were evaluated using logistic regression analysis. *Results.* 188 patients suffered at least one postoperative complication; 77, 91, and 20 patients experienced grade I, II, and III-IV complications, respectively. In the univariate analysis, sex, diabetes mellitus, postoperative hemoglobin, and postoperative albumin are statistically significant. In the multivariable analysis, postoperative albumin (adjusted odds ratio (OR) = 0.861, $P < 0.001$) was an independent risk factor of the postoperative complication severity in patients with STB. Receiver operating characteristic (ROC) analysis showed that the optimal cutoff values for postoperative albumin were 32 g/L (sensitivity: 0.571, specificity: 0.714, area under the ROC curve: 0.680) and 30 g/L (sensitivity: 0.649, specificity: 0.800, area under the ROC curve: 0.697) for grade II and grade III-IV complications, respectively. *Conclusions.* Postoperative albumin is an independent risk factor for postoperative complication severity in patients with STB. The improvement of postoperative albumin levels may reduce the risk of severe complications in patients with STB.

1. Introduction

Spinal tuberculosis (STB) is a type of osteoarticular tuberculosis with high morbidity, taking part of 50% in osteoarticular tuberculosis [1]. Standard antituberculosis (TB) drug administration combined with timely surgery is an important and effective treatment for patients with STB [2]. Lesion focus debridement is a significant treatment in STB therapy, which enhances tuberculosis control, promotes bone graft fusion, improves the efficacy of antituberculosis drugs, and

reduces the risk of STB recurrence [3, 4]. However, debridement of the spinal focus is an iatrogenic trauma that usually causes considerable blood loss. In addition, most patients with STB have comorbidities, such as diabetes, anemia, and hypoalbuminemia, and thus, they are susceptible to the development of different postoperative complications compared with those with degenerative diseases [5–7]. Different complications have various adverse impacts on surgery outcomes and patients' postoperative prognosis. According to the Clavien–Dindo classification, postoperative complication

TABLE 1: Details of the Clavien–Dindo classification of complications.

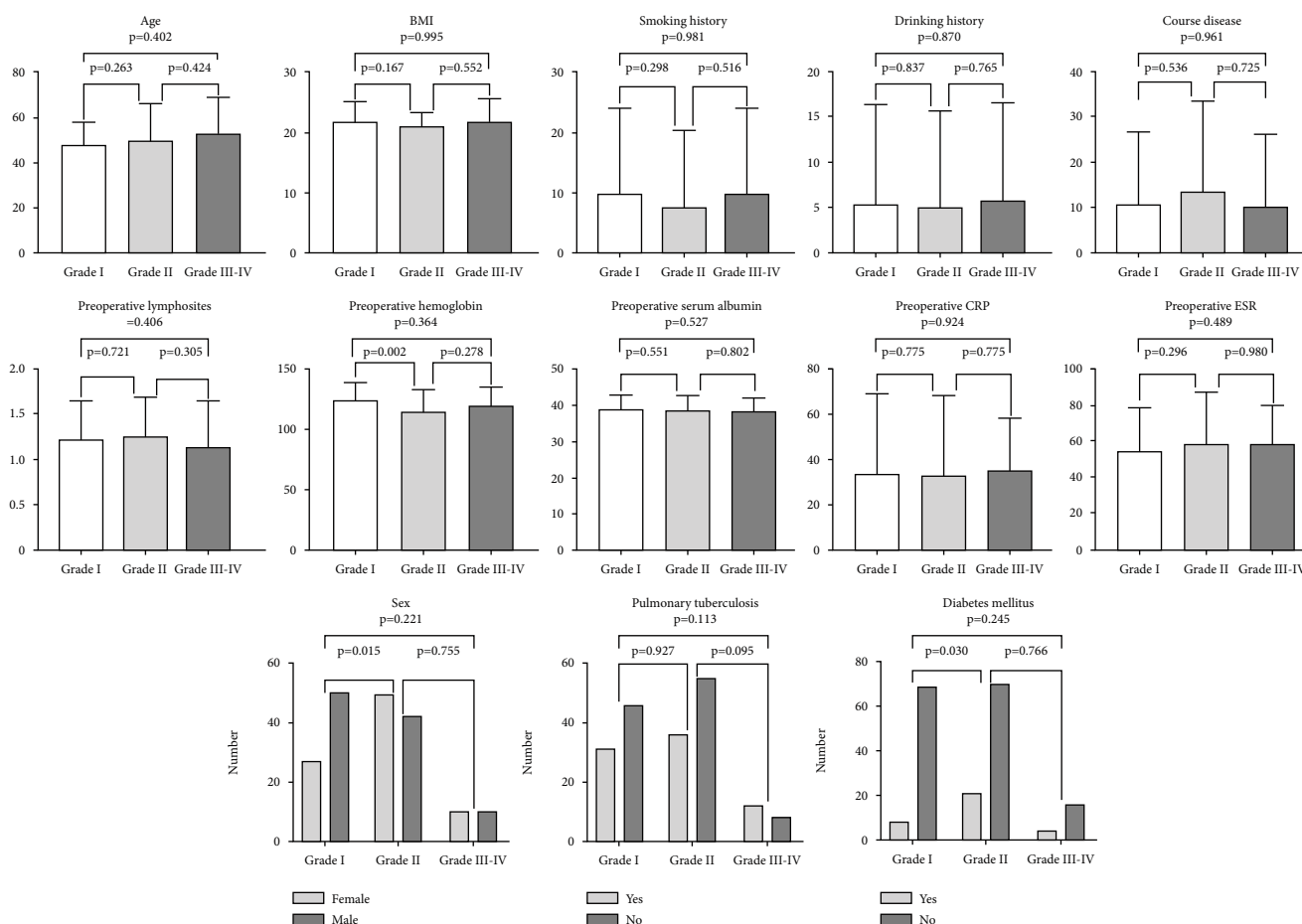| Grade	Definition
I	Any deviation from the normal postoperative course without the need for pharmacological treatment or surgical, endoscopic, and radiological interventions; allowed regimens are antiemetics, antipyretics, analgesics, diuretics, electrolytes, and physiotherapy; includes wound opened at the bedside
II	Requiring pharmacological treatment with drugs other than those allowed for grade I; includes blood transfusions and total parental nutrition
III	Requiring surgical, endoscopic, or radiological intervention
IIIa	Intervention not under general anesthesia
IIIb	Intervention under general anesthesia
IV	Life-threatening complication requiring intensive care unit management
IVa	Single organ dysfunction (including dialysis)
IVb	Multiorgan dysfunction
V	Death

FIGURE 1: Preoperative clinical characteristic comparisons of grade I, grade II, and grade III–IV complication groups using the Clavien–Dindo classification.

severity can be effectively graded for research purposes [8]. Our previous study found that most of the postoperative complications were mild and did not need to be treated and that only severe complications required active treatment. It is of great significance to predict severe postoperative complications in STB patients [9]. To date, research on postoper-ative complications of STB has been confined to specific complications, such as nerve injury and postoperative intes-tinal obstruction [10, 11]. Few reports focus on the severity of different postoperative complications. To reduce the risk of serious postoperative complications and enhance the effects of both debridement surgery and postoperative

recovery in patients with STB, it is necessary to identify the independent risk factors that affect the severity of postoperative complications in STB.

This study retrospectively examined the data of patients with STB who underwent debridement surgery at the First Affiliated Hospital of Chongqing Medical University to identify the risk factors of different degrees of severity that predict postoperative complications.

2. Materials and Methods

All participants provided written informed consent.

2.1. Patient Selection. A total of 188 patients with STB who underwent lesion debridement in our hospital between January 2012 and May 2021 were retrospectively included in this study.

2.1.1. Inclusion Criteria. Patients were selected if they met the following inclusion criteria: (1) medical records were complete, including data on general information, perioperative laboratory examination, imaging results (including magnetic resonance imaging (MRI) and computed tomography (CT)), and clinical data on postoperative complications; (2) patients underwent debridement, bone graft, and instrumented fusion; and (3) lesion tissues were extracted during the surgery, and postoperative pathological diagnosis was confirmed as STB.

2.1.2. Exclusion Criteria. Patients were excluded if they presented with the following: (1) suspected STB not confirmed by pathological examination, (2) preliminary and pathological diagnosis of diseases other than STB, (3) patients without postoperative complication, or (4) a previous history of STB.

2.2. Measures and Statistics

2.2.1. Measures. Based on previous studies and our experience, the following possible items for the analysis of different postoperative CDC complications in patients with STB were assessed: patients' preoperative general conditions, surgery-related indicators, and postoperative laboratory indexes. Measures of preoperative general patient conditions included age, sex, body mass index (BMI), comorbidities of diabetes mellitus and pulmonary tuberculosis, history of alcohol use, history of smoking, course of disease, preoperative hemoglobin, preoperative serum albumin, preoperative lymphocytes, preoperative erythrocyte sedimentation rate (ESR), and preoperative C-reactive protein (CRP). Surgery-related indicators included surgical approach, operating time, and blood loss during surgery. Postoperative laboratory indexes included postoperative hemoglobin and postoperative serum albumin. Postoperative complications were divided into different grades based on the Clavien–Dindo classification (Table 1).

2.2.2. Statistical Analysis. Clinical characteristics were assessed using univariate ordinal logistic regression analysis, and significant factors with $P < 0.1$ were entered into a multivariate ordinal logistic regression. ROC curve analysis determined the threshold values for continuous variables.

TABLE 2: Details of patients with the Clavien–Dindo classification of complications.

	Number
Total	188
Clavien–Dindo I	77 (41.0%)
Low serum albumin	58
Mild and moderate anemia	61
High fever	28
Gastrointestinal symptoms	25
Cerebrospinal fluid leakage	9
Electrolyte disorders	10
Clavien–Dindo II	91 (48.4%)
Hypoalbuminemia	41
Severe anemia	11
Abnormal liver function	18
Abnormal kidney function	4
Delirium	2
Limb nerve symptoms	14
Drug side effect	8
Thrombus	3
Urinary tract infection	2
Clavien–Dindo IIIa	12 (6.4%)
Wound infection and/or poor healing	11
Restricted respiratory function	1
Clavien–Dindo IIIb	7 (3.7%)
Pleural effusion	5
Rupture of iliac vein	1
Internal fixation instability	1
Clavien–Dindo IVa	1 (0.5%)
Respiratory failure	1

$P < 0.05$ was considered as indicating statistical significance. SPSS version 26.0 software was used for statistical analyses.

3. Result

3.1. Patient Population. In total, 188 patients presented with postoperative complications and were enrolled in the study, including 102 males and 86 females (Figure 1). Patients' various complications are shown in Table 2. Mean ages, BMI, smoking and alcohol use history, and disease course of patients in the three groups are shown in Figure 1. Operation time, operation blood loss, surgery approach, postoperative hemoglobin, and postoperative albumin of patients in the three groups are shown in Figures 2 and 3.

3.2. Results of Univariate and Multivariate Ordinal Logistic Regression Analyses. Univariate ordinal logistic regression analysis showed that sex, diabetes mellitus, postoperative hemoglobin, and postoperative serum albumin were all risk factors for the severity of different postoperative Clavien–Dindo complications (Table 3). Multivariate ordinal logistic regression analysis of the above significant risk factors
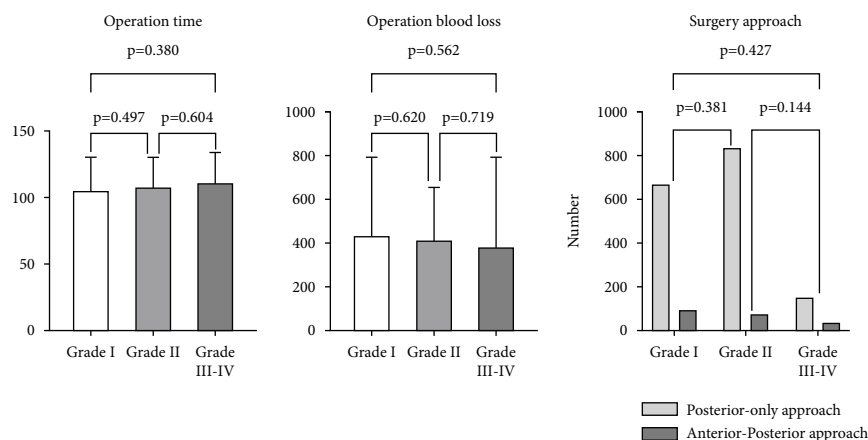
Figure 2: Comparisons of surgery-related clinical characteristics of grade I, grade II, and grade III–IV complication groups using the Clavien–Dindo classification.
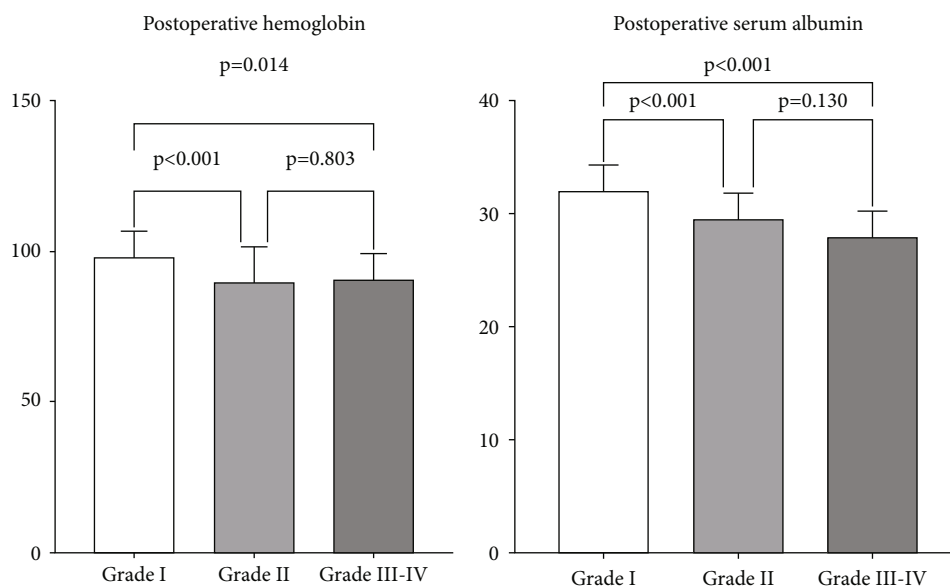

Figure 3: Postoperative clinical characteristic comparisons of grade I, grade II, and grade III–IV complication groups using the Clavien–Dindo classification.

revealed that postoperative serum albumin was an independent risk factor for postoperative complication severity (Table 4).

3.3. ROC Curve Analysis. ROC curves showed that the diagnostic thresholds of postoperative serum albumin in CDC II and CDC III–IV were 32 g/L (sensitivity: 0.571, specificity: 0.714, area under the ROC curve: 0.680) and 30 g/L (sensitivity: 0.649, specificity: 0.800, area under the ROC curve: 0.697), respectively (Figure 4).

4. Discussion

In the present study, ordinal logistic regression analysis revealed that postoperative serum albumin level was an independent risk factor for postoperative complication severity in patients with STB.

Serum albumin is a plasma protein synthesized by the liver, which plays an important role in maintaining blood colloid osmotic pressure and transporting metabolic substances. As an endogenous nutrient, albumin is the most commonly used and most reliable evaluation index for the body's nutritional status [12–14]. Preoperative malnutrition is common in patients with STB, and it has been reported that between 4.8% and 16.8% of patients who underwent spinal surgery develop preoperative hypoalbuminemia as a complication [15, 16]. STB is considered a chronic wasting disease, and patients with STB have a higher risk of preoperative hypoalbuminemia. After STB surgery, patients have significantly reduced levels of postoperative albumin, and in one study, the incidence of postoperative hypoalbuminemia has been found to be 72.8% [17]. Many factors can lead to low albumin levels, including insufficient protein intake or malabsorption, protein synthesis disorder, increased

Table 3: Univariate ordinal logistic regression analysis of risk factors in patients with different grades of complications.

Characteristics	Estimate (SE)	Unadjusted odds ratio (OR)	95% CI	P value
Age	0.012	1.012	-0.005-0.029	0.178
Sex	-0.623	0.536	-1.181-0.065	0.029*
BMI	-0.036	0.965	-0.117-0.046	0.391
Diabetes mellitus	-0.684	0.505	-1.414-0.047	0.066*
Pulmonary tuberculosis	-0.271	0.763	-0.827-0.286	0.340
Smoking history	-0.007	0.993	-0.027-0.013	0.515
Alcohol use history	0.000	1.000	-0.025-0.025	0.984
Course of disease	0.001	1.001	-0.008-0.011	0.754
Preoperative hemoglobin	0.013	1.014	0.983-1.045	0.388
Preoperative serum albumin	-0.025	0.975	-0.092-0.041	0.458
Preoperative lymphocytes	-0.101	0.904	-0.724-0.523	0.751
Preoperative CRP	0.000	1.000	-0.008-0.008	0.910
Preoperative ESR	0.005	1.005	-0.005-0.016	0.323
Surgery approach	0.020	1.020	-0.833-0.872	0.964
Operating time	0.003	1.003	-0.002-0.007	0.319
Blood loss during surgery	0.000	1.000	-0.001-0.001	0.463
Postoperative hemoglobin	-0.034	0.967	-0.055-0.014	0.001*
Postoperative serum albumin	-0.169	0.845	-0.241-0.096	<0.001*

BMI: body mass index; CRP: C-reactive protein; ESR: erythrocyte sedimentation rate.

Table 4: Multivariate ordinal logistic regression analysis of risk factors in patients with different grades of complications.

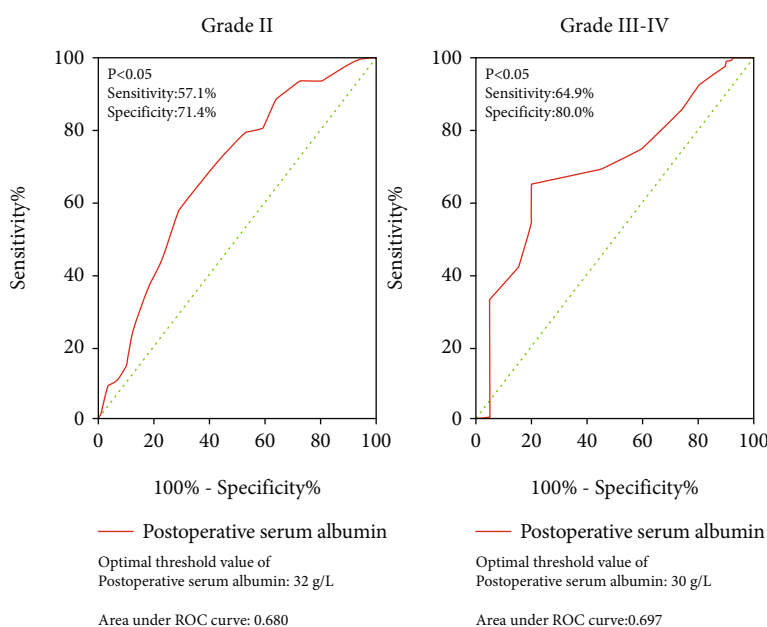| Characteristics	Estimate (SE)	Crude odds ratio (OR)	95% CI	P value
Sex	-0.435	0.647	-1.051-0.180	0.166
Diabetes mellitus	-0.358	0.699	-1.117-0.401	0.355
Postoperative hemoglobin	-0.011	0.989	-0.036-0.014	0.396
Postoperative serum albumin	-0.150	0.861	-0.230-0.069	<0.001*

Figure 4: Receiver operating characteristic curves of postoperative serum albumin for grade II and grade III-IV complications.

albumin catabolism rate, abnormal albumin distribution, and external albumin loss [18–21]. There are two main factors that lead to low albumin levels in patients with STB. First, STB is a chronic wasting disease with 25.7% of patients experiencing pulmonary tuberculosis as a complication. These patients have high nutritional requirements and lower protein intake, and the inflammation caused by the tuberculosis infection increases albumin consumption, which in turn leads to the half-life time of albumin being decreased to 8.2 ± 1.4 days, while the normal value is 12.5 ± 1.7 days [22, 23]. Second, debridement surgery in patients with STB is a critical factor that can lead to low postoperative albumin levels. Compared with surgery for degenerative spinal disease, STB surgery also involves focus debridement as a step, resulting in longer operating time, more bleeding, and more trauma. Surgery has several effects on postoperative albumin levels. (a) First, bleeding following surgery removes some of the albumin from the blood and dilutes the remaining serum albumin concentration [24]. (b) Second, surgery leads to a physiological stress state and inflammatory reaction, which injures the capillary endothelial cells in the whole body and increases capillary permeability. Thus, the albumin in the blood vessel penetrates into the tissue space and reduces serum albumin, a mechanism called transcapillary escape of albumin [25]. (c) Finally, during this stress state, the liver decreases albumin synthesis and prioritizes acute phase protein synthesis including that of C-reactive protein. Several causes contribute to impaired liver function and reduce the liver's ability to synthesize albumin, which in turn decreases serum albumin [26]. Due to the nature of the disease and the surgical methods used, patients with STB experience significant decreases in serum albumin and are at high risk of hypoalbuminemia following surgery.

To date, many studies found that preoperative albumin is associated with postoperative complications. Yi et al. found an increased risk of major perioperative complications after total hip replacement in patients with serum albumin levels < 35 g/L [27, 28]. Patients with preoperative hypoalbuminemia have a significantly increased risk of sepsis, myocardial infarction, and perioperative pneumonia after total hip replacement [29, 30]. Patients who underwent cervical surgery with hypoalbuminemia had a higher rate of any major postoperative complications, particularly pulmonary and cardiac complications, and were more likely to require a reoperation and longer hospital stays [31]. Preoperative hypoalbuminemia is a risk factor for postoperative surgical site infection after spinal surgery and prolongs the hospital stay [16, 32]. One of our previous studies also suggested that preoperative albumin is an independent risk factor for overall postoperative complications of STB [33]. Many studies have confirmed that preoperative albumin is significantly associated with postoperative complications in patients with STB. Our study further revealed that postoperative albumin is an independent risk factor for the severity of postoperative complications in patients with STB, and the lower the postoperative albumin, the greater the risk of more serious complications. In addition, when the postoperative albumin is less than 30 g/L, more attention should be paid to the occurrence of complications above CDC III grade.

Such complications have important implications for perioperative management and enhanced recovery after surgery of patients and indicate that clinicians should pay more attention to postoperative albumin levels in patients with STB.

It remains controversial whether exogenous albumin supplementation should be used to treat postoperative hypoalbuminemia in patients with STB. Exogenous human serum albumin supplementation can effectively improve postoperative albumin levels for patients with hypoalbuminemia after surgery. However, studies have demonstrated that the use of albumin after surgery will not reduce the risk of postoperative incision complications and will increase the risk of postoperative infection [9]. After the infusion of exogenous albumin, about 10% of albumin exudes from the blood vessels within 2 hours, and 75% is distributed outside the blood vessels within 2 days. Also, albumin takes a long time to decompose, and if it cannot decompose, it produces the required amino acids in the short term [18, 34]. In addition, exogenous albumin contains different kinds of amino acids excluding tryptophan and isoleucine and has low nutritional value, and therefore, it is generally not recommended for improving nutritional status and correcting hypoproteinemia [35].

One of our unpublished studies found that albumin in patients with STB decreased every day starting on the first postoperative day, reached the lowest value on the third day, then rose slowly, and returned to a normal level on about the fifth day. The latter may be related to the relief of patients' stress levels following surgery and the release of albumin return from tissues into the blood [24]. Most complications in patients occurred within a week after the application of exogenous albumin. It only took a short time to increase albumin levels to more than 32 g/L. Moreover, the risk of CDC II and higher complications provides guidance for postoperative albumin applications and suggests directions of further research. Most of the complications in patients occur during the first week after surgery. If exogenous albumin is applied for a short time within one week after surgery and the albumin level is increased to more than 32 g/L, the risk of CDC II level complications may be reduced. This in turn may provide further guidance for the application of albumin after surgery and for further research.

5. Conclusion

This investigation identified postoperative albumin as an independent risk factor for the severity of postoperative complications in patients with STB. When postoperative albumin was less than 32 g/L, there is a high risk of occurrence of CDC II complications, and when postoperative albumin is less than 30 g/L, CDC III-IV complications have a high risk of incidence occurrence. The improvement of postoperative albumin levels may reduce the risk of severe complications in patients with STB.

6. Study Limitations

This study has some limitations. First, there may be some risk factors we did not take into inclusion. Second, a better

complication classification method may exist. Third, a larger sample size would increase the statistical power available and hence the ability to detect smaller effect sizes. Fourth, this study is a retrospective study; the role of improvement of postoperative albumin in complication prevention needs to be evaluated. Future studies addressing these limitations will be required to confirm these results.

Data Availability

The data used to support the findings of this study are available from the corresponding author upon request.

Ethical Approval

The authors are accountable for all aspects of the work in ensuring that questions related to the accuracy or integrity of any part of the work are appropriately investigated and resolved. This study was conducted in accordance with the Declaration of Helsinki (as revised in 2013) and was approved by the Institutional Ethics Board of the First Affiliated Hospital of Chongqing Medical University (no. ChiCTR1800019109).

Consent

All participants provided written informed consent to participate in this study.

Conflicts of Interest

The authors declare that there is no conflict of interest regarding the publication of this paper.

References

[1] R. N. Dunn and H. M. Ben, "Spinal tuberculosis," *Bone Joint J*, vol. 100-B, no. 4, pp. 425–431, 2018.

[2] Y. X. Wang, H. Q. Zhang, M. Li et al., "Debridement, interbody graft using titanium mesh cages, posterior instrumentation and fusion in the surgical treatment of multilevel noncontiguous spinal tuberculosis in elderly patients via a posterior-only," *Injury*, vol. 48, no. 2, pp. 378–383, 2017.

[3] O. Boachie-Adjei, E. C. Papadopoulos, F. Pellisé et al., "Late treatment of tuberculosis-associated kyphosis: Late treatment of tuberculosis-associated kyphosis: literature review and experience from a SRS-GOP site," *European Spine Journal*, vol. 22, no. 4, pp. 641–646, 2013.

[4] S. Rajasekaran and S. Soundarapandian, "Progression of kyphosis in tuberculosis of the spine treated by anterior arthrodesis," *The Journal of Bone and Joint Surgery. American Volume*, vol. 71, no. 9, pp. 1314–1323, 1989.

[5] M. C. Swann, K. S. Hoes, S. G. Aoun, and D. L. McDonagh, "Postoperative complications of spine surgery," *Best Practice & Research. Clinical Anaesthesiology*, vol. 30, no. 1, pp. 103–120, 2016.

[6] J. A. Rihn, R. Patel, J. Makda et al., "Complications associated with single-level transforaminal lumbar interbody fusion," *The Spine Journal*, vol. 9, no. 8, pp. 623–629, 2009.

[7] Z. Hongqi, Y. Xinhua, and L. Fen, "Investigation of the complications associated with surgery for treating spinal tuberculo-

sis," *Orthopedic Journal of China*, vol. 22, no. 1, pp. 20–27, 2014.

[8] D. Dindo, N. Demartines, and P. A. Clavien, "Classification of surgical complications: a new proposal with evaluation in a cohort of 6336 patients and results of a survey," *Annals of Surgery*, vol. 240, no. 2, pp. 205–213, 2004.

[9] G. Jiang, Y. Ou, Y. Zhu et al., "Development of a scoring scale for predicting the risk of postoperative complications after spinal tuberculosis debridement: a retrospective cohort study of 233 patients," *Annals of Palliative Medicine*, vol. 10, no. 9, pp. 9372–9382, 2021.

[10] W. Xiyang, Z. Bingyan, and L. Weiwei, "Cause analysis and prevention of the complications after surgical treatment for spinal tuberculosis," *Chinese Journal of Spine and Spinal Cord*, vol. 20, no. 12, pp. 993–997, 2010.

[11] H. Wang, X. Yang, Y. Shi et al., "Early predictive factors for lower-extremity motor or sensory deficits and surgical results of patients with spinal tuberculosis: a retrospective study of 329 patients," *Medicine (Baltimore)*, vol. 95, no. 34, article e4523, 2016.

[12] D. C. McMillan, W. S. Watson, P. O'Gorman, T. Preston, H. R. Scott, and C. S. McArdle, "Albumin concentrations are primarily determined by the body cell mass and the systemic inflammatory response in cancer patients with weight loss," *Nutrition and Cancer*, vol. 39, no. 2, pp. 210–213, 2001, 11759282.

[13] M. B. Cross, P. H. Yi, C. F. Thomas, J. Garcia, and C. J. Della Valle, "Evaluation of malnutrition in orthopaedic surgery," *The Journal of the American Academy of Orthopaedic Surgeons*, vol. 22, no. 3, pp. 193–199, 2014.

[14] M. Bernardi, P. Angeli, J. Claria et al., "Albumin in decompensated cirrhosis: new concepts and perspectives," *Gut*, vol. 69, no. 6, pp. 1127–1138, 2020.

[15] N. J. Lee, P. Kothari, J. S. Kim et al., "Nutritional status as an adjunct risk factor for early postoperative complications following posterior cervical fusion," *Spine (Phila Pa 1976)*, vol. 42, no. 18, pp. 1367–1374, 2017.

[16] D. D. Bohl, M. R. Shen, B. C. Mayo et al., "Malnutrition predicts infectious and wound complications following posterior lumbar spinal fusion," *Spine*, vol. 41, no. 21, pp. 1693–1699, 2016.

[17] F. Zhang, X. Liu, Z. Tan, J. Li, D. Fu, and L. Zhu, "Effect of postoperative hypoalbuminemia and supplement of human serum albumin on the development of surgical site infection following spinal fusion surgery: a retrospective study," *European Spine Journal*, vol. 29, no. 7, pp. 1483–1489, 2020.

[18] J. Boldt, "Use of albumin: an update," *British journal of anaesthesia*, vol. 104, no. 3, pp. 276–284, 2010.

[19] K. M. Druey and P. R. Greipp, "Narrative review: the systemic capillary leak syndrome," *Annals of Internal Medicine*, vol. 153, no. 2, pp. 90–98, 2010.

[20] R. Sion-Sarid, T. Lerman-Sagie, L. Blumkin, D. Ben-Ami, I. Cohen, and S. Houri, "Neurologic involvement in a child with systemic capillary leak syndrome," *Pediatrics*, vol. 125, no. 3, pp. e687–e692, 2010.

[21] A. Gatta, A. Verardo, and M. Bolognesi, "Hypoalbuminemia," *Internal and Emergency Medicine*, vol. 7, Suppl 3, pp. S193–S199, 2012.

[22] H. Wang, C. Li, J. Wang, Z. Zhang, and Y. Zhou, "Characteristics of patients with spinal tuberculosis: seven-year experience of a teaching hospital in Southwest China,"

International Orthopaedics, vol. 36, no. 7, pp. 1429–1434, 2012.

[23] A. Greissman, P. Silver, L. Nimkoff, and M. Sagy, "Albumin bolus administration versus continuous infusion in critically ill hypoalbuminemic pediatric patients," *Intensive Care Medicine*, vol. 22, no. 5, pp. 495–499, 1996.

[24] M. Hübner, S. Mantziari, N. Demartines, F. Pralong, P. Coti-Bertrand, and M. Schäfer, "Postoperative albumin drop is a marker for surgical stress and a predictor for clinical outcome: a pilot study," *Gastroenterology Research and Practice*, vol. 2016, Article ID 8743187, 2016.

[25] P. E. Ballmer, "Causes and mechanisms of hypoalbuminaemia," *Clinical Nutrition*, vol. 20, no. 3, pp. 271–273, 2001.

[26] A. Hülshoff, T. Schricker, H. Elgendy, R. Hatzakorzian, and R. Lattermann, "Albumin synthesis in surgical patients," *Nutrition*, vol. 29, no. 5, pp. 703–707, 2013.

[27] P. H. Yi, R. M. Frank, E. Vann, K. A. Sonn, M. Moric, and C. J. Della Valle, "Is potential malnutrition associated with septic failure and acute infection after revision total joint arthroplasty?," *Clinical Orthopaedics and Related Research*, vol. 473, no. 1, pp. 175–182, 2015.

[28] C. L. Nelson, N. M. Elkassabany, A. F. Kamath, and J. Liu, "Low albumin levels, more than morbid obesity, are associated with complications after TKA," *Clinical Orthopaedics and Related Research*, vol. 473, no. 10, pp. 3163–3172, 2015.

[29] D. Kishawi, G. Schwarzman, A. Mejia, A. K. Hussain, and M. H. Gonzalez, "Low preoperative albumin levels predict adverse outcomes after total joint arthroplasty," *The Journal of Bone and Joint Surgery. American Volume*, vol. 102, no. 10, pp. 889–895, 2020.

[30] X. Wang, L. Dai, Y. Zhang, and Y. Lv, "Gender and low albumin and oxygen levels are risk factors for perioperative pneumonia in geriatric hip fracture patients," *Clinical Interventions in Aging*, vol. 19, no. 15, pp. 419–424, 2020.

[31] M. C. Fu, R. A. Buerba, and J. N. Grauer, "Preoperative nutritional status as an adjunct predictor of major postoperative complications following anterior cervical discectomy and fusion," *Clinical Spine Surgery*, vol. 29, no. 4, pp. 167–172, 2016.

[32] Y. Yamamoto, H. Shigematsu, E. Iwata et al., "Hypoalbuminemia increased the length of stay in the treatment of postoperative acute surgical site infection in spinal surgery," *Spine (Phila Pa 1976)*, vol. 45, no. 23, pp. E1564–E1571, 2020.

[33] G. M. Liumbruno, F. Bennardello, A. Lattanzio, P. Piccoli, and G. Rossettias, "Italian Society of Transfusion Medicine and Immunohaematology (SIMTI). Recommendations for the use of albumin and immunoglobulins," *Blood Transfus*, vol. 7, no. 3, pp. 325–334, 2009.

[34] G. C. Matos, S. Rozenfeld, and M. Martins, "Human albumin use at hospitals in the Metropolitan Region of Rio de Janeiro," *Cadernos de Saude Publica*, vol. 26, no. 5, pp. 981–990, 2010.

[35] G. J. Quinlan, G. S. Martin, and T. W. Evans, "Albumin: biochemical properties and therapeutic potential," *Hepatology*, vol. 41, no. 6, pp. 1211–1219, 2005.

Hindawi

Research Article

Meta-Analysis of the Efficacy and Safety of Alendronate Combined with Atorvastatin in the Treatment of Osteoporosis in Diabetes Mellitus

Zhencheng Xiong [iD],[1] **Ping Yi** [iD],[1] **Xiangsheng Tang,**[1] **Li Shu,**[2] **and Chi Zhang** [iD]2,3

[1]*Department of Spine Surgery, China-Japan Friendship Hospital, Beijing 100029, China*
[2]*Department of Orthopedics, Peking University International Hospital, Beijing 102206, China*
[3]*Biomedical Engineering Department, Peking University, Beijing 100191, China*

Correspondence should be addressed to Chi Zhang; chi.zhang@case.edu

Objective. Diabetes is a chronic disease caused by defective insulin secretion in the body, resulting in metabolic abnormalities with persistent blood glucose elevation. Osteoporosis is the most common diabetes complication. The aim of this study was to perform a meta-analysis of the effects of alendronate combined with atorvastatin compared with alendronate alone in the treatment of osteoporosis in diabetes mellitus. *Methods.* Two researchers independently used PubMed, ScienceDirect, Cochrane Library, Wanfang Data, CNKI, and VIP databases to search for all relevant studies that met the inclusion criteria and used RevMan 5.3 and STATA 16.0 for data analysis. *Results.* Fourteen studies that met the inclusion criteria were selected, including 1456 patients. Among the data extracted in this meta-analysis, bone mineral density (BMD) was the primary outcome measurement, while total effective rate, VAS, osteoprotegerin (OPG), bone Gla protein (BGP), bone alkaline phosphatase (BAP), blood P and Ca, and adverse effects were secondary outcome measurements. Our results showed that alendronate combined with atorvastatin is more effective than alendronate alone, with higher BMD, OPG, BGP, and BAP, more significant pain relief, and fewer adverse events. *Conclusion.* The results of this meta-analysis indicate that alendronate combined with atorvastatin is a better treatment for osteoporosis in diabetes mellitus, showing more effective and higher BMD and fewer adverse events than alendronate alone.

1. Introduction

The prevalence of diabetes mellitus has increased significantly with the aging of populations in recent decades [1]. Diabetes is a chronic disease caused by the defective insulin secretion in the body, resulting in abnormal metabolism with a continuous increase in blood sugar [2]. Diabetes may cause different complications, of which osteoporosis is the most common one [3]. Diabetes causes bone metabolism disorders and reduces bone mineral content, which lead to osteoporosis. If diabetes-caused osteoporosis is left untreated, bone pain will occur, which may lead to disability eventually in severe cases [3]. Alendronate is an aminobisphosphonate that acts as a potent inhibitor of bone resorp-

tion [4]. A clinical study showed that 70 mg of alendronate per week was effective in improving bone mineral density (BMD) and reducing bone loss in patients with proximal femur osteoporosis [4]. Atorvastatin is a statin drug widely used to lower cholesterol levels [5]. Statins have been reported to have multiple effects, such as antioxidant properties, inhibition of inflammatory response, and bone metabolism. A nationwide population-based cohort study showed that atorvastatin had a potential protective effect on osteoporosis [5]. In addition, statins directly affect osteoclasts through a mechanism similar to bisphosphonates. Both statins and bisphosphonates exert their effects through the mevalonate pathway. However, alendronate is not highly bioavailable and easily binds to plasma proteins, resulting in
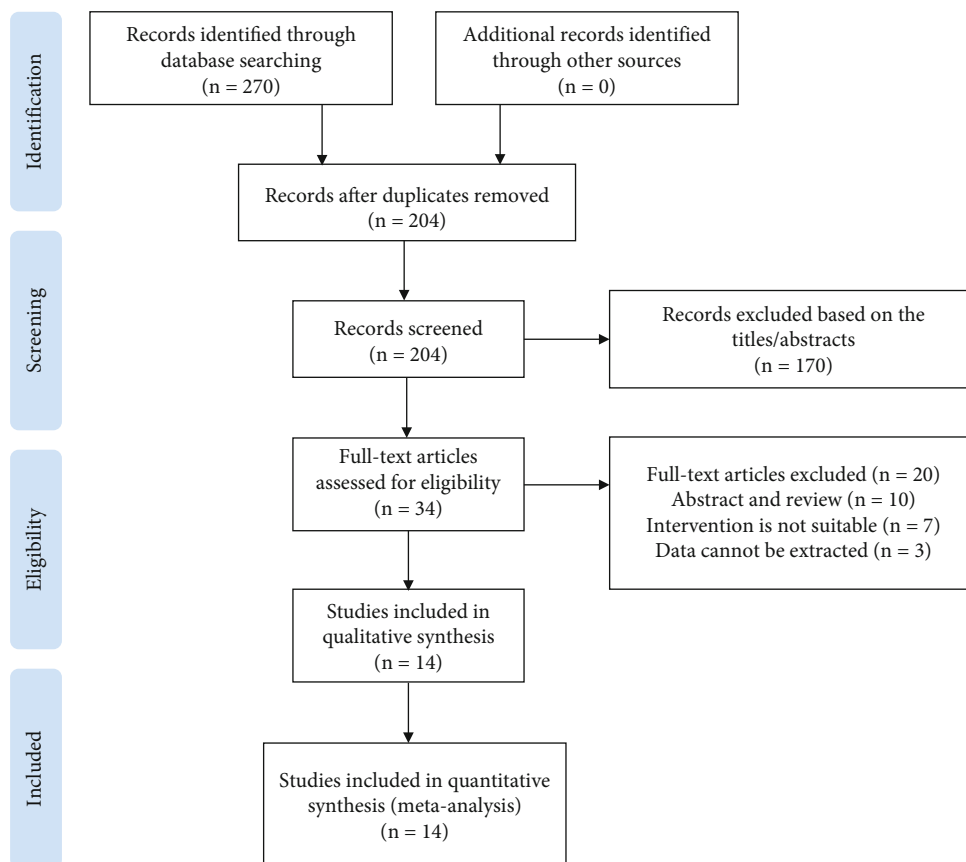
FIGURE 1: Flow chart of literature search and screening for meta-analysis.

a low bone tissue resorption rate and unsatisfactory therapeutic effect [6]. Therefore, combining alendronate with atorvastatin to treat osteoporosis in diabetes mellitus has become a new approach, and it has been addressed in some studies [7–20]. In order to investigate the effect of the alendronate combined with atorvastatin group compared to the alendronate alone group in patients with osteoporosis in diabetes mellitus, we performed this meta-analysis by pooling the relevant studies.

2. Materials and Methods

2.1. Search Method. In order to obtain all relevant studies to the study topic, two researchers independently searched multiple databases according to the Cochrane Collaboration guidelines, including PubMed (1966 to October 1, 2021), ScienceDirect (1990 to October 1, 2021), Cochrane library (1966 to October 1, 2021), Wanfang Data (1990 to October 1, 2021), CNKI (1990 to October 1, 2021), and Chinese Scientific Journal Database (VIP) (1990 to October 1, 2021). The relevant study search was achieved by using Boolean operators (AND or OR) to link MeSH terms to their corresponding keywords, including "alendronate," "atorvastatin," "diabetes mellitus or diabetes," and "osteoporosis." The two researchers independently screened all retrieved articles, first on a title-by-title and abstract-by-abstract basis, followed by a detailed reading of the full text, and also looked through the references of the screened articles for potentially compat-

ible studies. The final obtained studies are discussed and integrated. The Preferred Reporting Items for Systematic Reviews and Meta-Analyses (PRISMA) statement is an important reference for this meta-analysis [21].

2.2. Study Screening. Screening of all retrieved articles was performed according to the inclusion and exclusion criteria developed for the topics of this meta-analysis. Inclusion criteria included the following: (1) all studies involved a comparison of alendronate combined with atorvastatin versus atorvastatin alone for the treatment of osteoporosis in diabetes mellitus, (2) all included studies were randomized controlled trials (RCTs), and (3) data relevant to the outcome measures could be successfully extracted. Exclusion criteria included the following: (1) studies that were lacking a control group; (2) relevant data for the outcome measures could not be extracted; (3) the type of study was a review, conference abstract, commentary, case report, or letter; and (4) all studies that did not meet the inclusion criteria.

2.3. Data Extraction. Two researchers independently complete the extraction of the required data, and then, another researcher summarizes the above data and resolves the divergent data after discussion within the research team. Of the data extracted in this meta-analysis, BMD was the primary outcome measurement, while total effective rate, VAS, osteoprotegerin (OPG), bone Gla protein (BGP), bone alkaline phosphatase (BAP), blood P and Ca, and adverse

TABLE 1: Characteristic of all studies included in the meta-analysis.

Study	Country	Study type	Mean age (years) E:C	No. of patients E:C	Mean BMI (kg/m^2) E:C	Experimental group	Experimental dose	Control group	Control dose	Outcome measures
Ji et al., 2017	China	RCT	64.6/64.2	60/60	25/23	AL+AT	10 mg/d/6 m + 10 mg/d/ 6 m	AL	10 mg/d/ 6 m	A, G
Su et al., 2019	China	RCT	64/64	40/40	NP	AL+AT	10 mg/d/6 m + 10 mg/d/ 6 m	AL	10 mg/d/ 6 m	A, D, F, H
Duan et al., 2019	China	RCT	67.58/68.39	50/50	NP	AL+AT	10 mg/d/6 m + 10 mg/d/ 6 m	AL	10 mg/d/ 6 m	A, G, H
Fu et al., 2020	China	RCT	65.7/65.9	59/59	24.95/25.03	AL+AT	10 mg/d/6 m + 10 mg/d/ 6 m	AL	10 mg/d/ 6 m	A, B, C, D, E, F, G, H
Zou et al., 2021	China	RCT	62.45/62.48	40/40	23.55/23.51	AL+AT	10 mg/d/6 m + 10 mg/d/ 6 m	AL	10 mg/d/ 6 m	B, C, D, E, G, H
Li et al., 2017	China	RCT	65.5/66.5	90/90	24.58/25.5	AL+AT	70 mg/w/6 m + 10 mg/d/ 6 m	AL	70 mg/w/ 6 m	A, G, H
Wang et al., 2017	China	RCT	68.7/67.2	75/75	NP	AL+AT	70 mg/w/6 m + 10 mg/d/ 6 m	AL	70 mg/w/ 6 m	G, H
Wang et al., 2019	China	RCT	64.2/63.3	20/20	NP	AL+AT	70 mg/w/6 m + 10 mg/d/ 6 m	AL	70 mg/w/ 6 m	A, C, D, E, F, H
Yang et al., 2019	China	RCT	66.27/66.43	35/35	23.04/23.25	AL+AT	70 mg/w/6 m + 10 mg/d/ 6 m	AL	70 mg/w/ 6 m	A, C, E, F, H
Hu et al., 2020	China	RCT	58.23/57.89	100/100	NP	AL+AT	70 mg/w/6 m + 10 mg/d/ 6 m	AL	70 mg/w/ 6 m	B, H
Hou et al., 2018	China	RCT	64.5/62.5	40/40	NP	AL+AT	70 mg/w/6 m + 10 mg/d/ 12 m	AL	70 mg/w/ 6 m	A, H
Li X et al., 2019	China	RCT	65.09/65.43	50/50	NP	AL+AT	10 mg/w/6 m + 10 mg/d/ 12 m	AL	10 mg/d/ 6 m	A, B
Li Y et al., 2019	China	RCT	68.4/67.5	29/29	NP	AL+AT	70 mg/w/6 m + 10 mg/d/ 12 m	AL	70 mg/w/ 6 m	A, H
Feng et al., 2019	China	RCT	58.93/61.9	50/50	NP	AL+AT	70 mg/w/6 m + 10 mg/d/ 12 m	AL	70 mg/w/ 6 m	H

E: experimental group; C: control group; RCT: randomized controlled trial; BMI: body mass index; AL: alendronate; AT: atorvastatin; d: day; w: week; m: month; NP: not provided. Outcome measure: A: BMD (femoral neck, femoral trochanter, forearm, lumbar spine); B: VAS; C: OPG; D: BGP; E: BAP; F: blood P and Ca; G: total effective rate; H: adverse events.

FIGURE 2: Risk of bias summary. +: low risk of bias; −: high risk of bias; ?: bias unclear.

effects were secondary outcome measurements. The following data were also extracted: first author, year of publication, country/region, study type, drug dose and month of use (experimental group : control group), body mass index (BMI), and gender.

2.4. Quality Assessment. The Cochrane Handbook of Systematic Reviews is commonly used to assess the quality of RCTs in meta-analyses [22]. Two researchers used a "risk of bias" table with seven main elements to assess the quality of each included RCT. Depending on the actual content of the study, each element could be judged as high risk of bias, low risk of bias, or one of the unclear risks of bias.

2.5. Statistical Analysis. Subgroup analyses were performed according to the period of atorvastatin application, as well as the time of detection of outcome measurements. When included outcome measurements were continuous data, as well as unit differences, we used standardized mean differences (SMD) and 95% confidence intervals (CI) for analysis; risk ratio (RR) and 95% CI were used when dichotomous data were included. Heterogeneity of included studies was assessed by I^2 and was considered low, moderate, and high when I^2 values were 25%, 50%, and 75%, respectively [23]. The magnitude of I^2 determined the choice of the random effects and fixed effects models, with the former executed when $I^2 > 50\%$ and $P < 0.1$; otherwise, the latter was executed. We used STATA software version 16.0 and RevMan 5.3 for Windows for statistical analysis of all data. The results of the meta-analysis were considered statistically significant when $P < 0.05$.

3. Results

3.1. Search Results for Literature. A total of 270 potentially relevant articles were generated based on the search strategy and inclusion and exclusion criteria, including PubMed ($n = 1$), ScienceDirect ($n = 177$), Cochrane Library ($n = 0$), Wanfang Data ($n = 34$), CNKI ($n = 31$), and VIP ($n = 27$). A total of 170 articles were excluded after careful independent screening of titles and abstracts and brief review of the full text by two researchers. The full text of the remaining 34 articles was then evaluated in detail based on the inclusion and exclusion criteria. Finally, the meta-analysis included 14 RCTs (Figure 1) [7–20].

3.2. Study Characteristics. A total of 14 RCTs involving 1456 patients, published between 2017 and 2021, were included in this meta-analysis [7–20]. All included studies investigated the effect of the alendronate combined with atorvastatin group compared to the alendronate alone group in patients with osteoporosis in diabetes mellitus. A total of 10 studies have used BMD as the primary outcome measurement [7, 8, 10, 11, 13–18]. BMD was classified into four types depending on the site of measurement, including femoral neck, femoral rotor, forearm, and lumbar spine. Each type of BMD was further divided into 4 subgroups according to the time of detection and the period of application of the intervention. Five studies were also conducted to assess the difference in efficacy between the two groups by serological examination, including OPG, BGP, BAP, blood P, and Ca [15–18, 20]. However, there were also 12 studies that reported adverse effects associated with the application of both groups of interventions, including headache, abdominal pain, nausea, vomiting, and constipation [8–12, 14–20]. The characteristics of all included studies are listed in Table 1.

3.3. Risk of Bias Assessment for the Included Studies. Figure 2 shows the risk of bias assessment for the included 14 RCTs [7–20]. Random assignment was stated in all 14 studies, but none of them explicitly mentioned blinding and
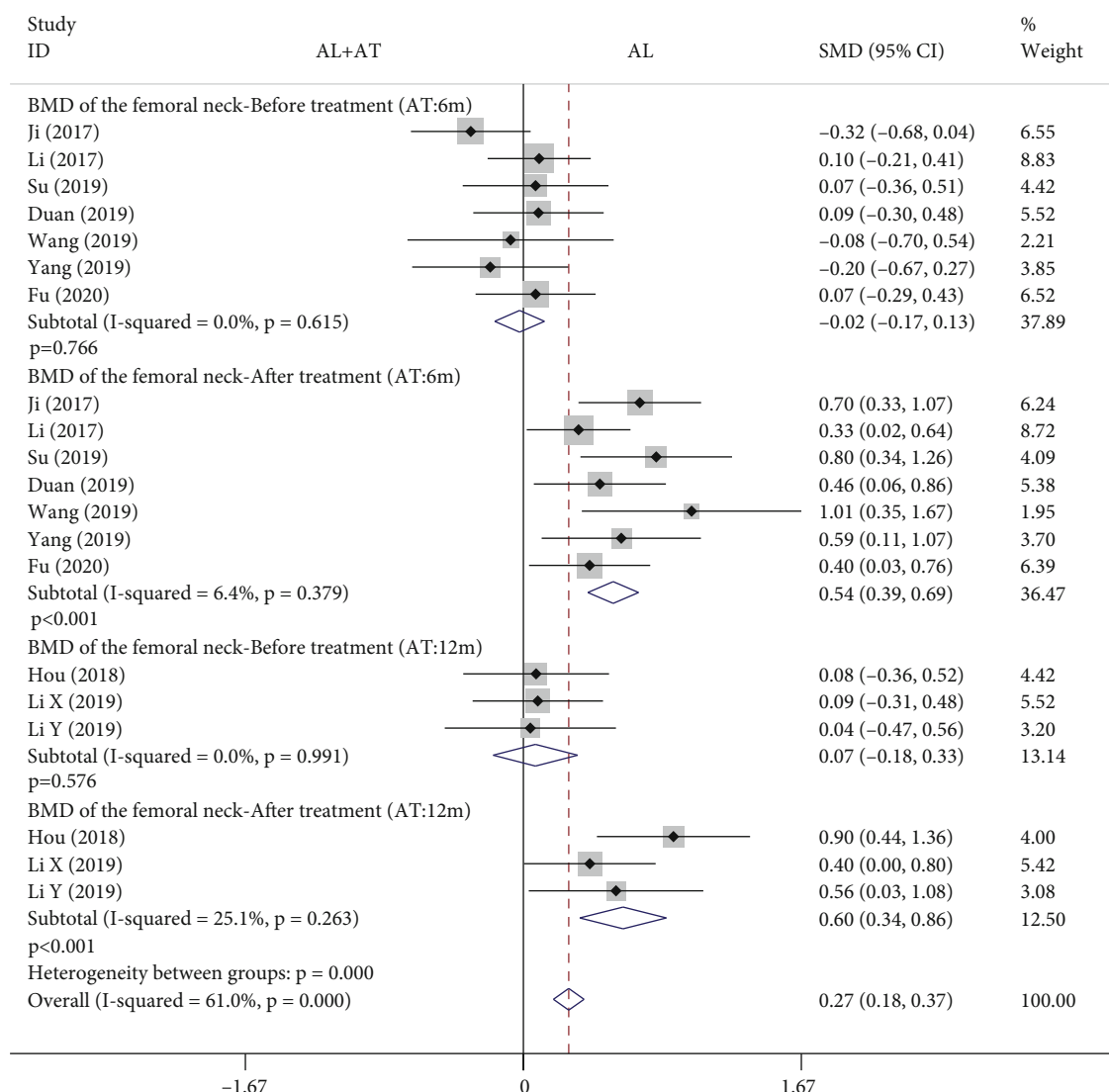
FIGURE 3: Forest plot showing the effect of alendronate combined with atorvastatin group compared to the alendronate alone group in BMD of the femoral neck (BMD: bone mineral density; AL: alendronate; AT: atorvastatin; SMD: standard mean difference).

allocation concealment. Selective reporting or incomplete outcome data were also not found. Other biases could not be identified.

3.4. Results of the Meta-Analysis

3.4.1. BMD. Among the 14 included studies, there are a total of 10 studies with BMD as the primary outcome measurement [7, 8, 10, 11, 13–18]. The BMD is classified into 4 types depending on the measurement site, including femoral neck, femoral trochanter, forearm, and lumbar spine. Each BMD, in turn, was divided into 4 subgroups depending on the time of detection and the period of application of the intervention. The forest plot in Figure 3 shows the effect of alendronate combined with the atorvastatin group compared to the alendronate alone group in BMD of the femoral neck. Given that there are studies in which atorvastatin was given for 6 months and also for 12 months, it is discussed in subgroups. A total

of 7 studies (688 patients) [7, 8, 11, 15–18] provided data for 6-month dosing cycles of atorvastatin and 3 studies (238 patients) [10, 13, 14] provided data for 12-month dosing cycles of atorvastatin. The fixed effects model was applied to this analytical process because I^2 was less than 50%. According to the results of the pooled analysis, there was no statistically significant difference between the two groups before treatment (6-month atorvastatin: SMD = −0.02, 95% CI: [-0.17, 0.13], $P = 0.766$, $I^2 = 0\%$; 12-month atorvastatin: SMD = 0.07, 95% CI: [-0.18, 0.33], $P = 0.576$, $I^2 = 0\%$). However, according to the results of the pooled analysis, there were statistically significant differences between the two groups after treatment (6-month atorvastatin: SMD = 0.54, 95% CI: [0.39, 0.69], $P < 0.001$, $I^2 = 6.4\%$; 12-month atorvastatin: SMD = 0.6, 95% CI: [0.34, 0.86], $P < 0.001$, $I^2 = 25.1\%$).

The forest plot in Figure 4 shows the effect of the alendronate combined with atorvastatin group compared to the alendronate alone group in BMD of the femoral trochanter.
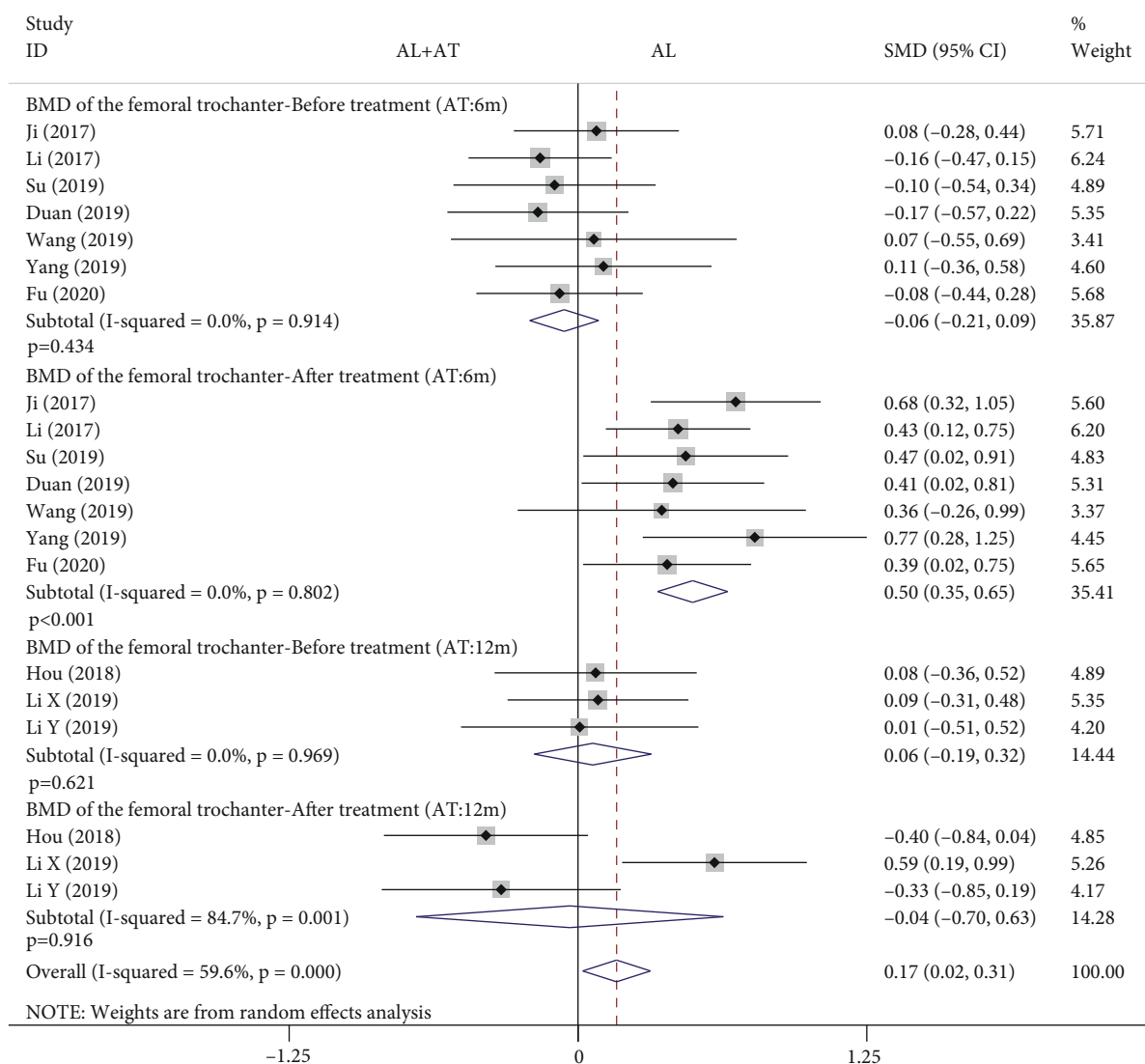
FIGURE 4: Forest plot showing the effect of alendronate combined with atorvastatin group compared to the alendronate alone group in BMD of the femoral trochanter (BMD: bone mineral density; AL: alendronate; AT: atorvastatin).

The random effects model was applied to this analytical process because I^2 was greater than 50%. According to the results of the pooled analysis, there was no statistically significant difference between the two groups before treatment and a statistically significant difference after treatment when the atorvastatin dosing period was 6 months (before treatment: SMD = −0.06, 95% CI: [-0.21, 0.09], $P = 0.434$, $I^2 = 0$ %; after treatment: SMD = 0.5, 95% CI: [0.35, 0.65], $P <$ 0.001, $I^2 = 0$%). However, according to the results of the pooled analysis, there was no statistically significant difference between the two groups before and after treatment when the atorvastatin dosing period was 12 months (before treatment: SMD = 0.06, 95% CI: [-0.19, 0.32], $P = 0.621$, $I^2 = 0$%; after treatment: SMD = −0.04, 95% CI: [-0.7, 0.63], $P = 0.916$, $I^2 = 84.7$%).

The forest plot in Figure 5 shows the effect of the alendronate combined with atorvastatin group compared to the alendronate alone group in BMD of the forearm. The fixed effects model was applied to this analytical process because I^2 was less than 50%. According to the results of the pooled analysis, there was no statistically significant difference between the two groups before treatment (6-month atorvastatin: SMD = 0.01, 95% CI: [-0.14, 0.16], $P = 0.898$, $I^2 = 0$ %; 12-month atorvastatin: SMD = 0.03, 95% CI: [-0.23, 0.28], $P = 0.824$, $I^2 = 0$%). However, according to the results of the pooled analysis, there were statistically significant differences between the two groups after treatment (6-month atorvastatin: SMD = 0.5, 95% CI: [0.35, 0.65], $P < 0.001$, I^2 = 0%; 12-month atorvastatin: SMD = 0.38, 95% CI: [0.12, 0.63], $P = 0.004$, $I^2 = 0$%).

The forest plot in Figure 6 shows the effect of the alendronate combined with atorvastatin group compared to the alendronate alone group in BMD of the lumbar spine. The fixed effects model was applied to this analytical process because I^2 was less than 50%. According to the results of the pooled analysis, there was no statistically significant difference between the two groups before treatment and a statistically significant difference after treatment when the
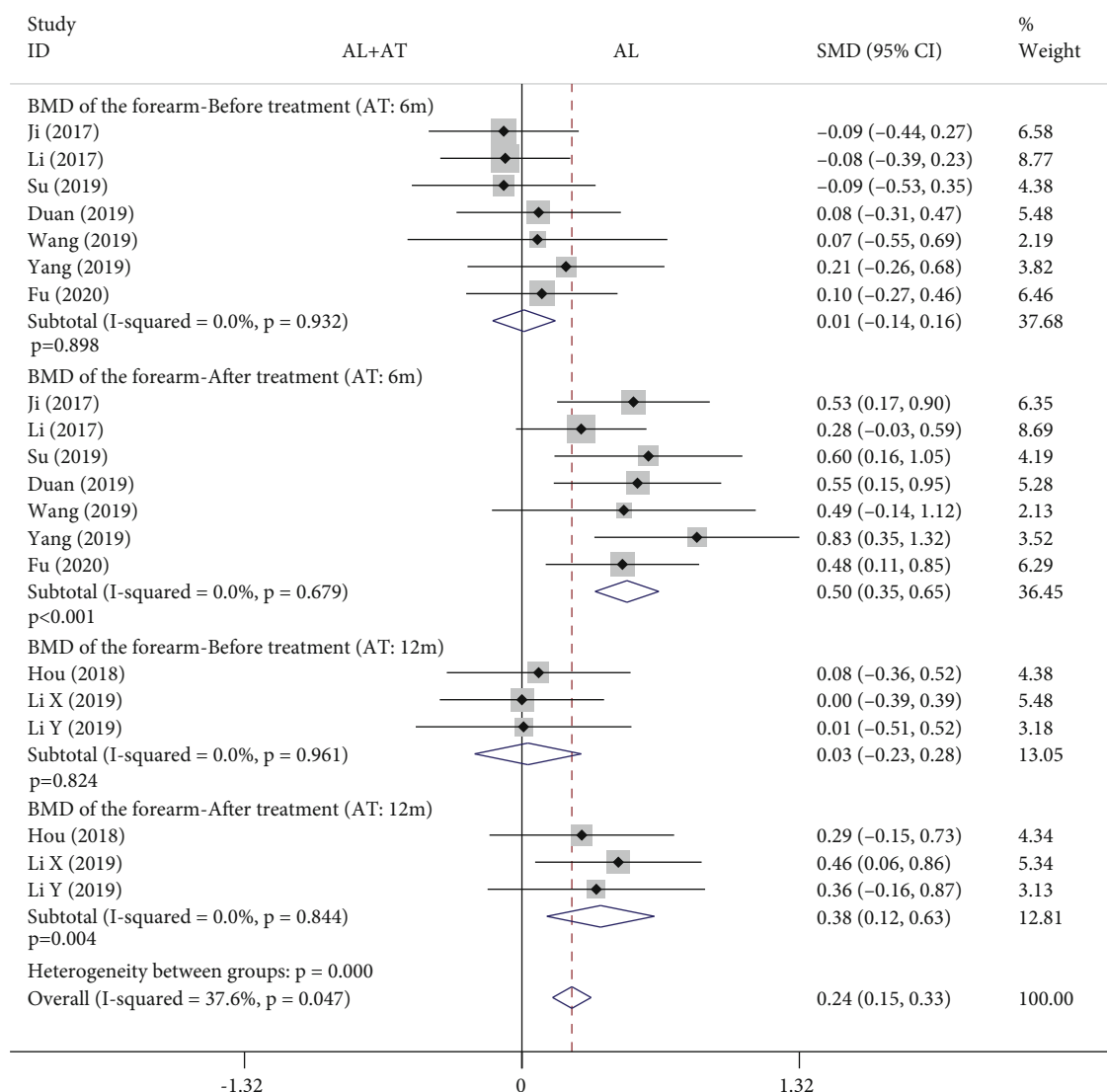
FIGURE 5: Forest plot showing the effect of alendronate combined with atorvastatin group compared to the alendronate alone group in BMD of the forearm (BMD: bone mineral density; AL: alendronate; AT: atorvastatin).

atorvastatin dosing period was 12 months (before treatment: SMD = 0.07, 95% CI: [-0.18, 0.33], $P = 0.573$, $I^2 = 0\%$; after treatment: SMD = 0.45, 95% CI: [0.19, 0.7], $P = 0.001$, $I^2 = 0\%$). However, according to the results of the pooled analysis, there were statistically significant differences between the two groups before and after treatment when the atorvastatin dosing period was 6 months (before treatment: SMD = −0.17, 95% CI: [-0.33, -0.02], $P = 0.022$, $I^2 = 1.4\%$; after treatment: SMD = 0.34, 95% CI: [0.19, 0.49], $P < 0.001$, $I^2 = 35.2\%$).

3.4.2. Total Effective Rate. Among the 14 included studies, there are a total of 6 studies (728 patients) with the total effective rate as the secondary outcome measurement [7–9, 11, 18, 20]. The forest plot shown in Figure 7 shows the effect of the alendronate combined with atorvastatin group compared to the alendronate alone group on total effective rate. The fixed effects model was applied to this analytical process because I^2 was less than 50%. According to the

results of the pooled analysis, there was a statistically significant difference between the two groups (SMD = 1.22, 95% CI: [1.15, 1.3], $P < 0.001$, $I^2 = 46.4\%$).

3.4.3. VAS. Among the 14 included studies, there are a total of 3 studies (398 patients) with VAS as the secondary outcome measurement [18–20]. The analysis was divided into two subgroups according to the time of detection. The forest plot shown in Figure 8 shows the effect of the alendronate combined with atorvastatin group compared to the alendronate alone group on VAS. The random effects model was applied to this analytical process because I^2 was greater than 50%. According to the results of the pooled analysis, there was no statistically significant difference between the two groups before treatment and a statistically significant difference after treatment (before treatment: SMD = 0.14, 95% CI: [-0.08, 0.37], $P = 0.206$, $I^2 = 19.1\%$; after treatment: SMD = −3.82, 95% CI: [-5.07, -2.58], $P < 0.001$, $I^2 = 92.5\%$).
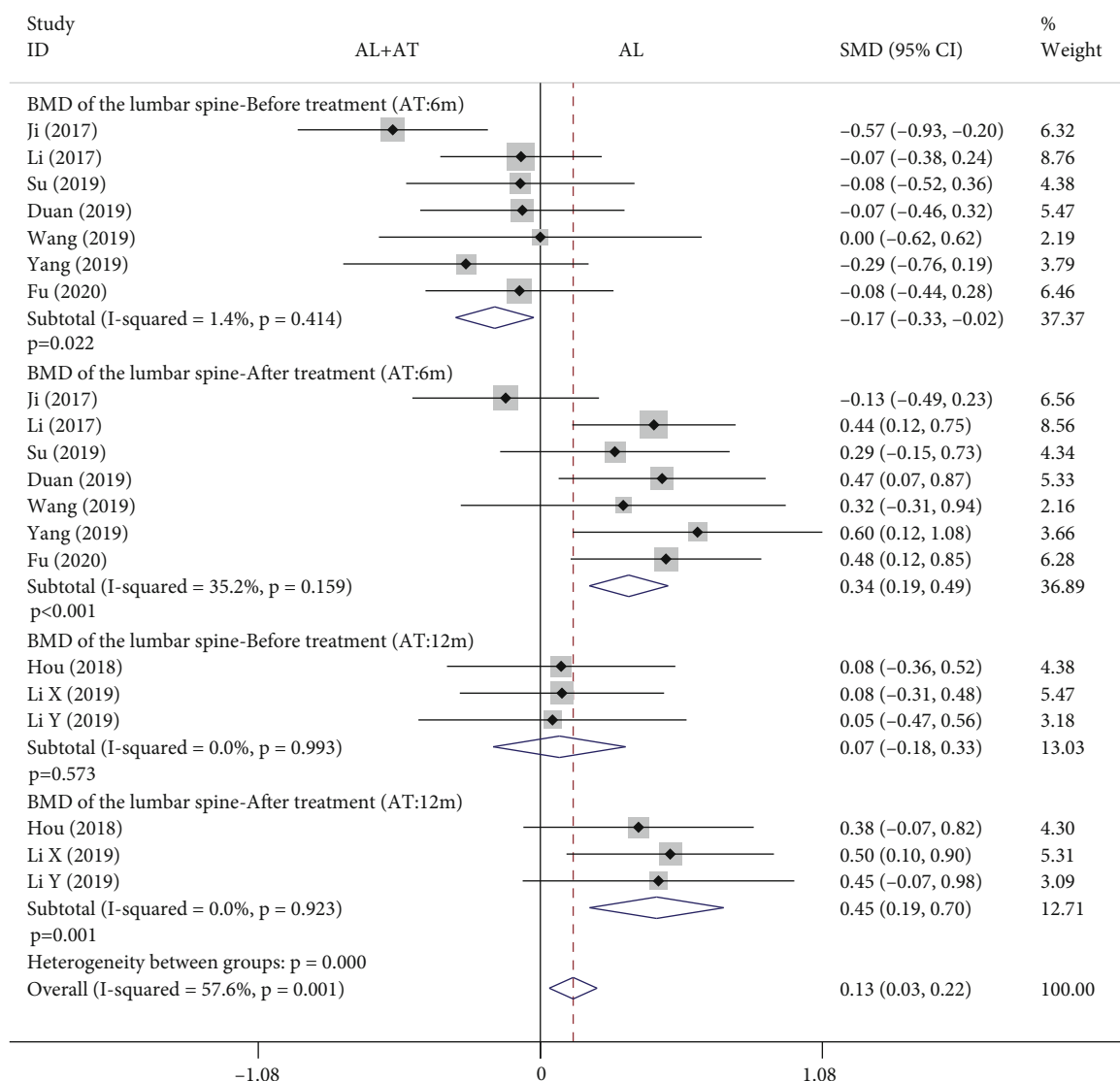
FIGURE 6: Forest plot showing the effect of alendronate combined with atorvastatin group compared to the alendronate alone group in BMD of the lumbar spine (BMD: bone mineral density; AL: alendronate; AT: atorvastatin).

3.4.4. OPG, BGP, and BAP. Among the 14 included studies, there are a total of 5 studies with OPG, BGP, and BAP as the secondary outcome measurements [15–18, 20]. The forest plot shown in Figure 9 shows the effect of the alendronate combined with atorvastatin group compared to the alendronate alone group on OPG, BGP, and BAP. A total of four studies (308 patients) provided OPG and BAP data [16–18, 20]; four studies (318 patients) provided BGP data [15, 16, 18, 20]. The random effects model was applied to this analytical process because I^2 was greater than 50%. According to the results of the pooled analysis, there was no statistically significant difference between the two groups before treatment (OPG: SMD $= -0.04$, 95% CI: [-0.27, 0.18], $P = 0.702$, $I^2 = 0\%$; BGP: SMD $= 0.01$, 95% CI: [-0.21, 0.23], $P = 0.946$, $I^2 = 0\%$; BAP: SMD $= -0.04$, 95% CI: [-0.27, 0.18], $P = 0.703$, $I^2 = 0\%$). However, according to the results of the pooled analysis, there were statistically significant differences between the two groups

after treatment (OPG: SMD $= 1.09$, 95% CI: [0.84, 1.34], $P < 0.001$, $I^2 = 5\%$; BGP: SMD $= 1.76$, 95% CI: [0.3, 3.21], $P = 0.018$, $I^2 = 96.3\%$; BAP: SMD $= 1.24$, 95% CI: [0.77, 1.71], $P < 0.001$, $I^2 = 70.4\%$).

3.4.5. Blood P and Ca. Among the 14 included studies, there are a total of 4 studies (308 patients) with blood P and Ca as the secondary outcome measurements [15–18]. The forest plot shown in Figure 10 shows the effect of the alendronate combined with atorvastatin group compared to the alendronate alone group on blood P and Ca. The fixed effects model was applied to this analytical process because I^2 was less than 50%. According to the results of the pooled analysis, there was no statistically significant difference between the two groups before and after treatment on blood P and Ca (blood P-before treatment: SMD $= -0.01$, 95% CI: [-0.23, 0.22], $P = 0.953$, $I^2 = 0\%$; blood P-after treatment: SMD $= 0.15$, 95% CI: [-0.07,
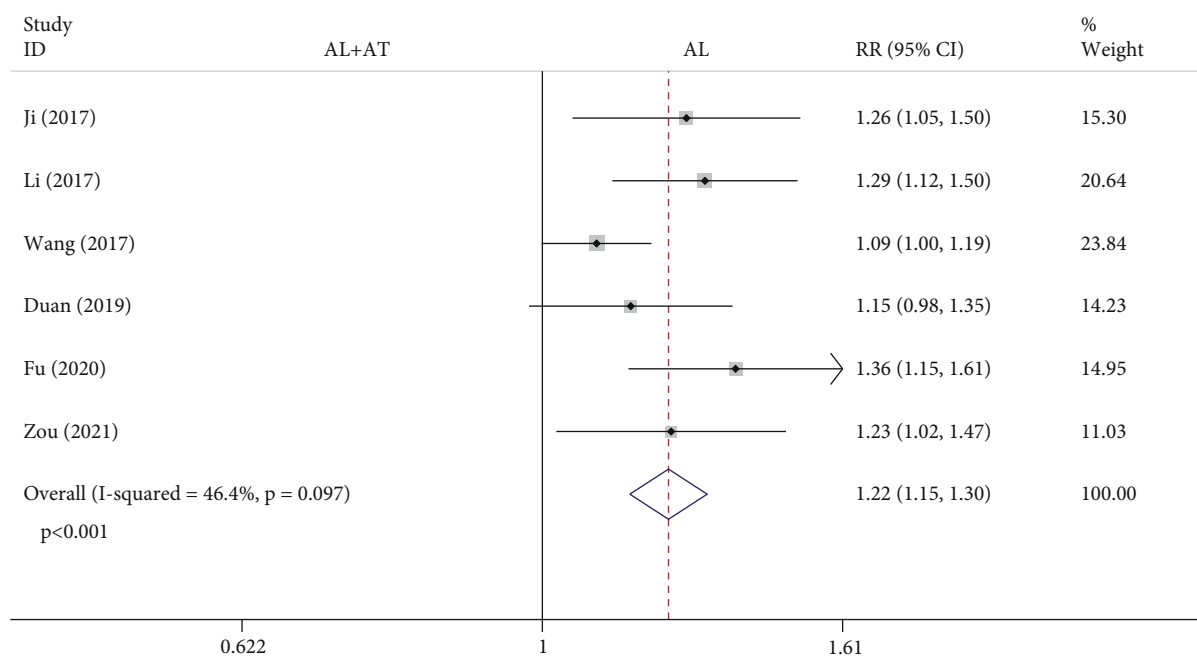
FIGURE 7: Forest plot showing the effect of alendronate combined with atorvastatin group compared to the alendronate alone group on total effective rate (AL: alendronate; AT: atorvastatin).
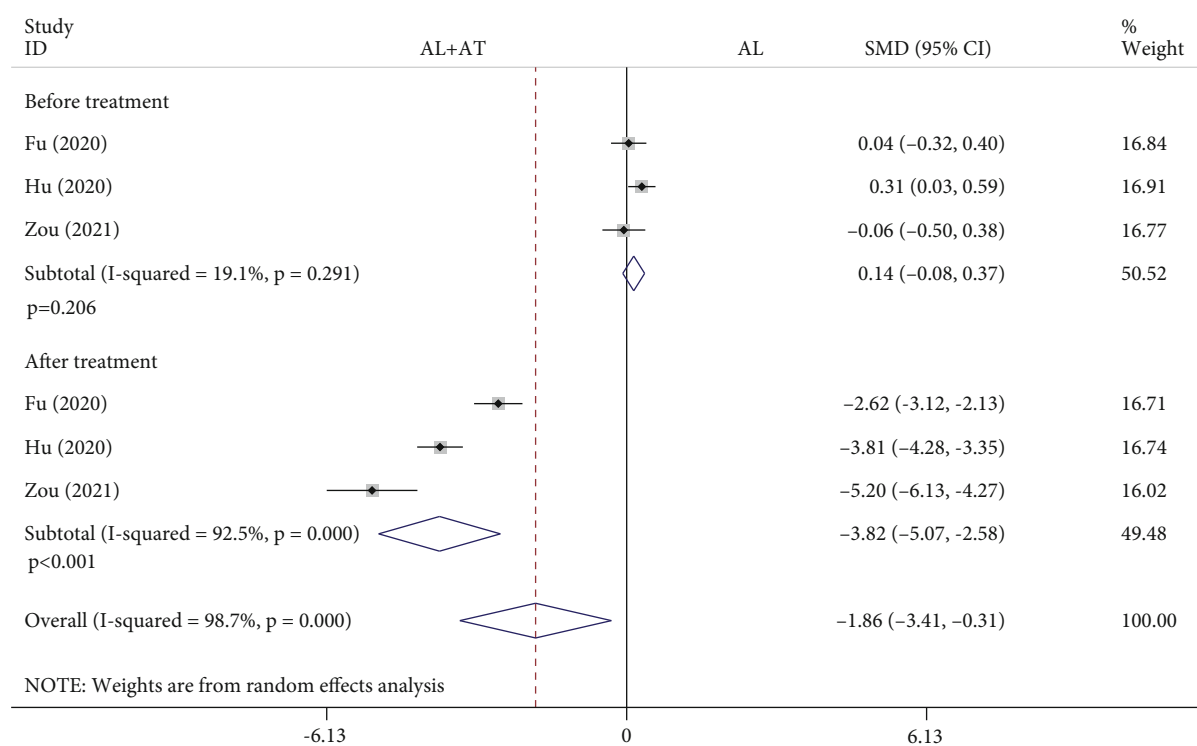

FIGURE 8: Forest plot showing the effect of alendronate combined with atorvastatin group compared to the alendronate alone group on VAS (AL: alendronate; AT: atorvastatin).

0.38], $P = 0.185$, $I^2 = 0\%$; blood Ca-before treatment: SMD = 0.02, 95% CI: [-0.2, 0.24], $P = 0.854$, $I^2 = 0\%$; blood Ca-after treatment: SMD = 0.07, 95% CI: [-0.15, 0.29], $P = 0.541$, $I^2 = 0\%$).

3.4.6. Adverse Events. Twelve studies reported adverse events, including headache, abdominal pain, nausea, vomiting, and constipation [8–12, 14–20]. The forest plot shown in Figure 11 shows the results regarding adverse events of
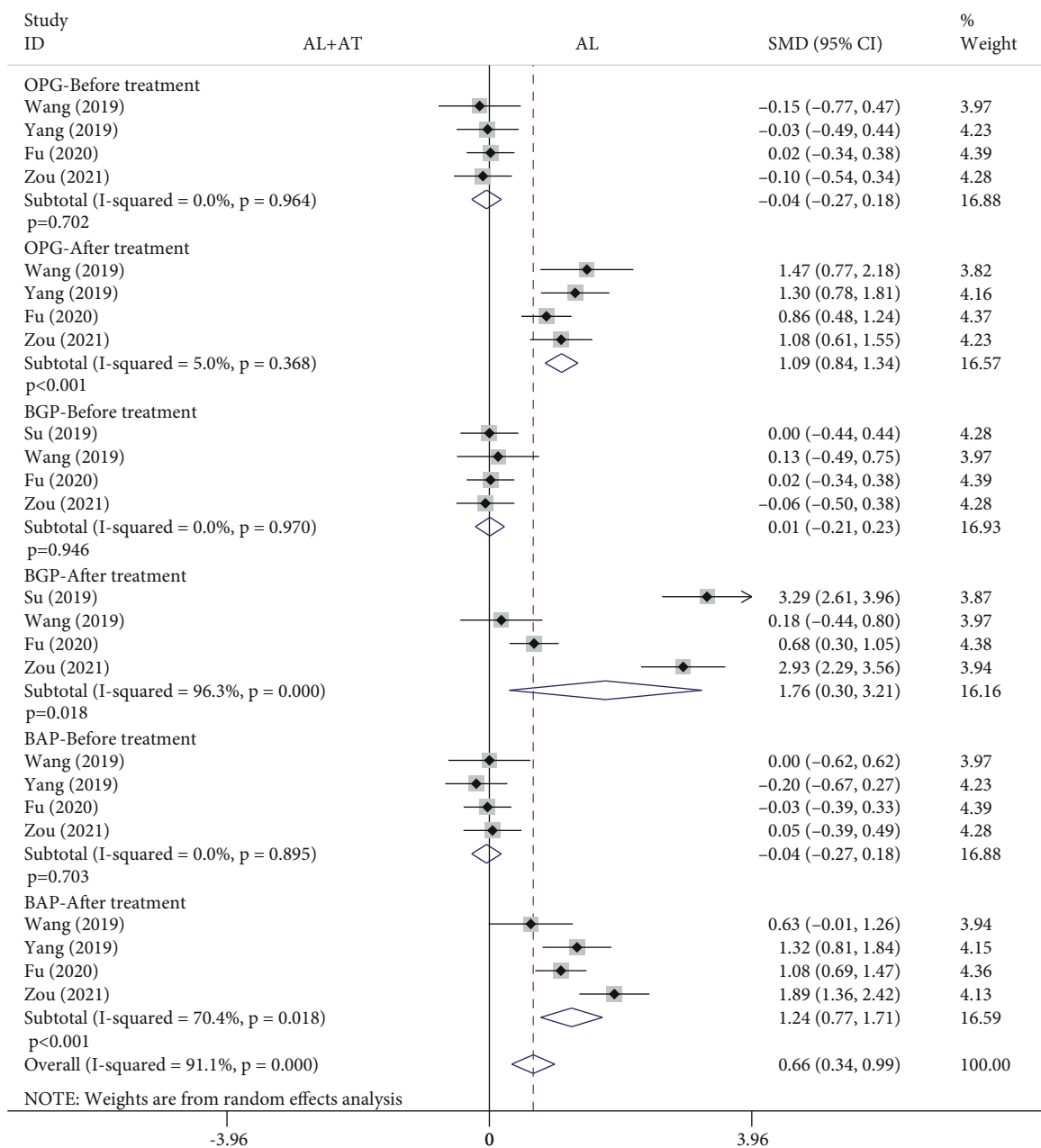
Figure 9: Forest plot showing the effect of alendronate combined with atorvastatin group compared to the alendronate alone group on OPG, BGP, and BAP (OPG: osteoprotegerin; BGP: bone Gla protein; BAP: bone alkaline phosphatase; AL: alendronate; AT: atorvastatin).

the alendronate combined with atorvastatin group compared to the alendronate alone group. The fixed effects model was applied to this analytical process because I^2 was less than 50%. According to the results of the pooled analysis, there was a statistically significant difference between the two groups on adverse events (RR = 0.41, 95% CI: [0.3, 0.56], $P < 0.001$, $I^2 = 45.1\%$).

3.5. Publication Bias. Begg's funnel plot and Egger's test are now commonly used in meta-analyses to assess publication bias, usually for at least 10 studies [23]. Since $P < 0.05$ for Begg's test and Egger's test results, this suggests

a possible publication bias for the included studies of total effective rate (Egger's test: $P = 0.048$), adverse events (Egger's test: $P = 0.043$), and OPG, BGP, and BAP (Begg's test: $P = 0.003$, Egger's test: $P = 0.04$). No bias was published for other outcome measurements as the results of Begg's test and Egger's test $P > 0.05$.

3.6. Sensitivity Analysis. When the results are heterogeneous, sensitivity analysis is usually performed in a meta-analysis to assess the stability of the results of the pooled literature analysis. We used sensitivity analysis to remove all outcome measurements from all included literature one by one, and the above results did not change significantly, which implies the robustness of the results.
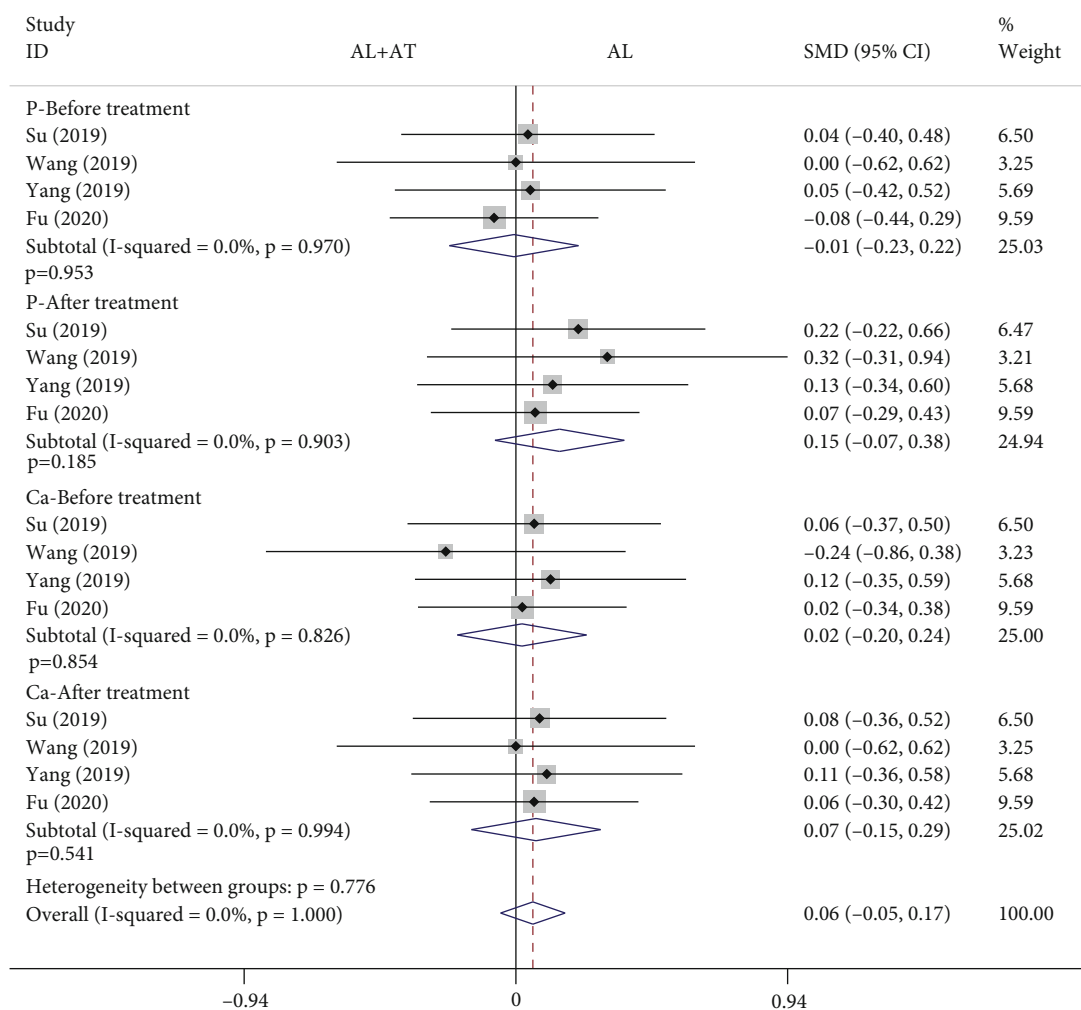
FIGURE 10: Forest plot showing the effect of alendronate combined with atorvastatin group compared to the alendronate alone group on blood P and Ca (AL: alendronate; AT: atorvastatin).

4. Discussion

This meta-analysis explored the effect of the alendronate combined with atorvastatin group compared to the alendronate alone group in patients with osteoporosis in diabetes mellitus. Diabetes is a lifelong endocrine disease, and osteoporosis is a serious complication of diabetes [3]. The high fasting blood glucose level caused by the impairment of insulin metabolism in the body prompts hyperparathyroidism and then hyperalgesia, resulting in the inability to effectively convert vitamin D to active vitamin D. This in turn triggers abnormal bone metabolism in the body, leading to a decrease in bone content and osteoporosis. Clinical symptoms include prolonged pain and dysfunction of the bones, easy to fracture, and not easy to heal, which seriously affect the quality of life and safety of patients [2]. Therefore, more attention should be paid to the treatment and prevention of osteoporosis, and it is crucial to find effective treatment methods. Alendronate is an aminobisphosphonate that acts as a potent inhibitor of bone resorption [4]. A clinical study showed that 70 mg of alendronate per week was effective in improving BMD and reducing bone loss in patients with

proximal femur osteoporosis [4]. As a statin drug, atorvastatin has been widely used to lower cholesterol levels [5]. It has been reported that statins have a variety of effects, such as antioxidant properties, inhibition of inflammation, and bone metabolism. A nationwide population-based cohort study suggests that high-potency statins (atorvastatin and rosuvastatin) and moderate-potency statin (simvastatin) appear to have a potential protective effect against osteoporosis [5]. Some of the available studies have reported that the combination of alendronate and atorvastatin is more effective than alendronate alone in the treatment of osteoporosis in diabetes mellitus [7–20]. Therefore, we performed this meta-analysis to pool related studies and to assess the effectiveness of the combination group and the alendronate alone group.

A total of 14 articles that met the inclusion criteria were included in this meta-analysis [7–20]. The experimental group in all studies was alendronate in combination with atorvastatin, while the control group was alendronate alone, and the patients were diabetic with osteoporosis. BMD measurement was divided into 4 types according to the measurement site, including the femoral neck, femoral trochanter,

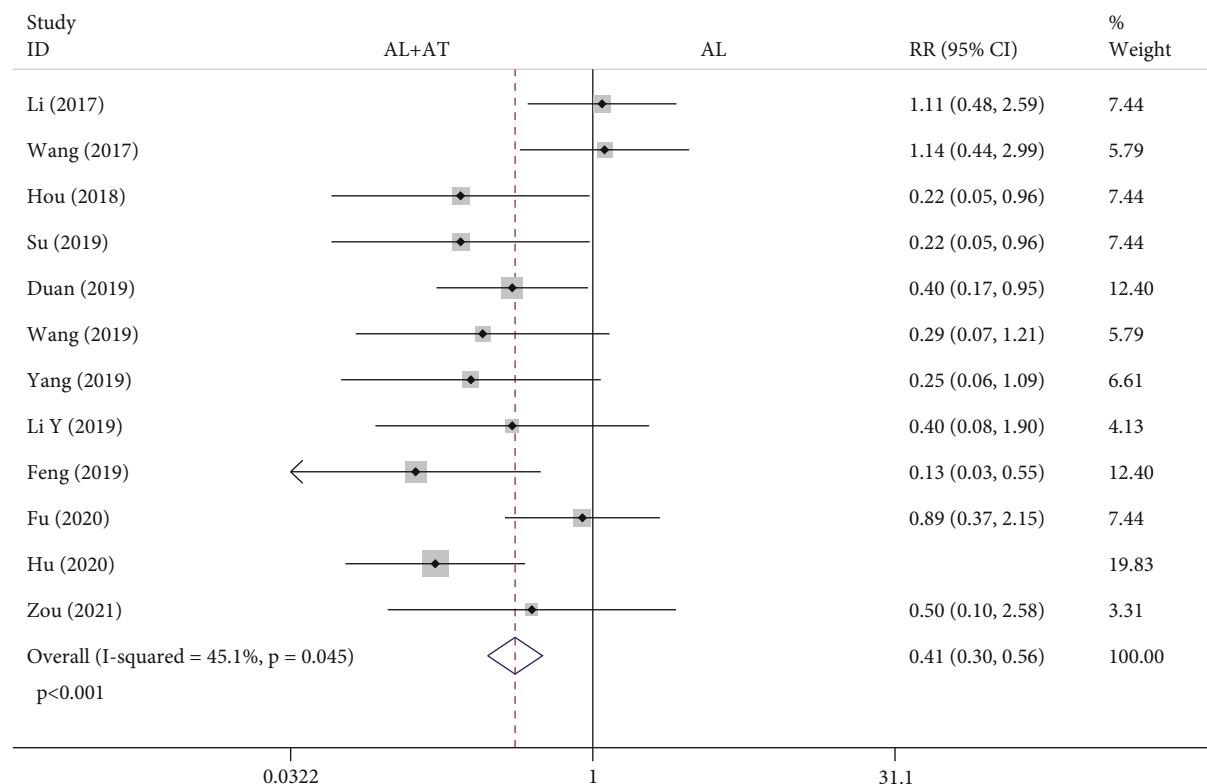| Study ID	AL+AT	AL	RR (95% CI)	% Weight
Li (2017)			1.11 (0.48, 2.59)	7.44
Wang (2017)			1.14 (0.44, 2.99)	5.79
Hou (2018)			0.22 (0.05, 0.96)	7.44
Su (2019)			0.22 (0.05, 0.96)	7.44
Duan (2019)			0.40 (0.17, 0.95)	12.40
Wang (2019)			0.29 (0.07, 1.21)	5.79
Yang (2019)			0.25 (0.06, 1.09)	6.61
Li Y (2019)			0.40 (0.08, 1.90)	4.13
Feng (2019)			0.13 (0.03, 0.55)	12.40
Fu (2020)			0.89 (0.37, 2.15)	7.44
Hu (2020)				19.83
Zou (2021)			0.50 (0.10, 2.58)	3.31
Overall (I-squared = 45.1%, p = 0.045)			0.41 (0.30, 0.56)	100.00
p<0.001				

0.0322   1   31.1

FIGURE 11: Forest plot showing the results regarding adverse events of alendronate combined with atorvastatin group compared to the alendronate alone group (AL: alendronate; AT: atorvastatin).

forearm, and lumbar spine. Based on the results of the pooled analysis, it was concluded that BMD of the femoral neck was higher with alendronate combined with atorvastatin than with alendronate alone, regardless of whether the cycle of atorvastatin application was 6 (before treatment: SMD = −0.02, 95% CI: [-0.17, 0.13], $P = 0.766$, $I^2 = 0\%$; after treatment: SMD = 0.54, 95% CI: [0.39, 0.69], $P < 0.001$, $I^2 = 6.4\%$) or 12 months (before treatment: SMD = 0.07, 95% CI: [-0.18, 0.33], $P = 0.576$, $I^2 = 0\%$; after treatment: SMD = 0.6, 95% CI: [0.34, 0.86], $P < 0.001$, $I^2 = 25.1\%$). When the site of measurement was the femoral trochanter, BMD was higher with alendronate combined with atorvastatin (6 months) than with alendronate alone (before treatment: SMD = −0.06, 95% CI: [-0.21, 0.09], $P = 0.434$, $I^2 = 0\%$; after treatment: SMD = 0.5, 95% CI: [0.35, 0.65], $P < 0.001$, $I^2 = 0\%$), while there was no significant difference between the two groups at 12 months (before treatment: SMD = 0.06, 95% CI: [-0.19, 0.32], $P = 0.621$, $I^2 = 0\%$; after treatment: SMD = −0.04, 95% CI: [-0.7, 0.63], $P = 0.916$, $I^2 = 84.7\%$). The results for the BMD of the forearm and femoral neck are consistent. When the measurement site was the lumbar spine and the period of atorvastatin application was 6 months, there were statistically significant differences in BMD between the two groups before treatment and after treatment, showing that BMD was higher with alendronate combined with atorvastatin than with alendronate alone (before treatment: SMD = −0.17, 95% CI: [-0.33, -0.02], $P = 0.022$, $I^2 = 1.4\%$; after treatment: SMD = 0.34, 95% CI:

[0.19, 0.49], $P < 0.001$, $I^2 = 35.2\%$); it was also higher in the combination group when atorvastatin was applied for 12 months (before treatment: SMD = 0.07, 95% CI: [-0.18, 0.33], $P = 0.573$, $I^2 = 0\%$; after treatment: SMD = 0.45, 95% CI: [0.19, 0.7], $P = 0.001$, $I^2 = 0\%$). A pooled analysis of the total effective rate showed that alendronate combined with atorvastatin was more effective than alendronate alone in the treatment of osteoporosis in diabetes mellitus (SMD = 1.22, 95% CI: [1.15, 1.3], $P < 0.001$, $I^2 = 46.4\%$). The VAS results indicated that alendronate combined with atorvastatin was more effective in relieving pain than alendronate alone (before treatment: SMD = 0.14, 95% CI: [-0.08, 0.37], $P = 0.206$, $I^2 = 19.1\%$; after treatment: SMD = −3.82, 95% CI: [-5.07, -2.58], $P < 0.001$, $I^2 = 92.5\%$). Serological findings showed that alendronate combined with atorvastatin had higher OPG, BGP, and BAP than alendronate alone (before treatment: OPG: SMD = −0.04, 95% CI: [-0.27, 0.18], $P = 0.702$, $I^2 = 0\%$; BGP: SMD = 0.01, 95% CI: [-0.21, 0.23], $P = 0.946$, $I^2 = 0\%$; BAP: SMD = −0.04, 95% CI: [-0.27, 0.18], $P = 0.703$, $I^2 = 0\%$) (after treatment: OPG: SMD = 1.09, 95% CI: [0.84, 1.34], $P < 0.001$, $I^2 = 5\%$; BGP: SMD = 1.76, 95% CI: [0.3, 3.21], $P = 0.018$, $I^2 = 96.3\%$; BAP: SMD = 1.24, 95% CI: [0.77, 1.71], $P < 0.001$, $I^2 = 70.4\%$), while there were no significant differences in serum P and Ca between the two groups (blood P-before treatment: SMD = −0.01, 95% CI: [-0.23, 0.22], $P = 0.953$, $I^2 = 0\%$; blood P-after treatment: SMD = 0.15, 95% CI: [-0.07, 0.38],

$P = 0.185$, $I^2 = 0\%$; blood Ca-before treatment: SMD = 0.02, 95% CI: [-0.2, 0.24], $P = 0.854$, $I^2 = 0\%$; blood Ca-after treatment: SMD = 0.07, 95% CI: [-0.15, 0.29], $P = 0.541$, $I^2 = 0\%$). A pooled analysis of adverse events showed a higher incidence of adverse events in the alendronate alone group (RR = 0.41, 95% CI: [0.3, 0.56], $P < 0.001$, $I^2 = 45.1\%$). These results suggest that alendronate combined with atorvastatin is more effective than alendronate alone in treating osteoporosis in diabetes mellitus, with higher BMD, fewer adverse events, and more significant pain relief.

4.1. Limitations. This meta-analysis has some limitations due to the number and quality of the included studies. First, some studies lacked details such as blinding and allocation concealment. Second, the heterogeneity of some results was high. The heterogeneity may be at least partially due to the difference of BMD measurement. It is known that many methods can be used to measure BMD, such as micro-CT, dual-energy X-ray absorptiometry, and ultrasound. Dual-energy X-ray absorptiometry is much less sensitive in recording changes than a CT scan of the bone. Different methods used in different studies may lead to the possible heterogeneous results. Finally, the included studies generally lacked the timing of testing for outcome measurements.

5. Conclusion

This is a meta-analysis to evaluate the effectiveness of alendronate combined with atorvastatin compared with alendronate alone in the treatment of osteoporosis in diabetes mellitus. Our results showed that alendronate combined with atorvastatin is more effective than alendronate alone, with higher BMD, OPG, BGP, and BAP; more significant pain relief; and fewer adverse events. Due to the limited number and quality of relevant studies, more high-quality RCTs are still needed in the future to complement the existing findings.

Data Availability

The data supporting this meta-analysis is from previously reported studies and datasets, which have been cited.

Conflicts of Interest

The authors declare that there are no conflicts of interest regarding the publication of this article.

Authors' Contributions

Zhencheng Xiong, Ping Yi and Xiangsheng Tang are joint first authors.

Acknowledgments

References

[1] O. Rabe, M. Winther-Jensen, K. Allin, and O. Svendsen, "Fractures and osteoporosis in patients with diabetes with Charcot foot," *Diabetes Care*, vol. 44, no. 9, pp. 2033–2038, 2021.

[2] A. García-Martín, R. Reyes-García, J. García-Castro, and M. Muñoz-Torres, "Diabetes and osteoporosis: action of gastrointestinal hormones on the bone," *Revista clinica espanola*, vol. 213, no. 6, pp. 293–297, 2013.

[3] G. Schacter and W. Leslie, "Diabetes and Osteoporosis," *Endocrinology and Metabolism Clinics of North America*, vol. 50, no. 2, pp. 275–285, 2021.

[4] M. Asadullah, S. Sarfaraz, S. Tanzil, R. Ikram, and N. Kamil, "The effects of alendronate treatment in the diagnosis and management of proximal femur osteoporosis: a real-life scenario," *Pakistan Journal of Pharmaceutical Sciences*, vol. 34, no. 4, pp. 1393–1396, 2021.

[5] T. Lin, P. Chou, C. Lin, Y. Hung, and G. Jong, "Long-term effect of statins on the risk of new-onset osteoporosis: a nationwide population-based cohort study," *PLoS One*, vol. 13, no. 5, article e0196713, 2018.

[6] J. Chen, J. Zheng, M. Chen, S. Lin, and Z. Lin, "The efficacy and safety of Chinese herbal medicine Xianling Gubao capsule combined with alendronate in the treatment of primary osteoporosis: a systematic review and meta-analysis of 20 randomized controlled trials," *Frontiers in Pharmacology*, vol. 12, article 695832, 2021.

[7] W. Ji and L. Xue, "60 cases of alendronate combined with atorvastatin calcium for the treatment of osteoporosis complicated by diabetes mellitus," *Shaanxi Medical Journal*, vol. 46, no. 9, p. 1291, 2017.

[8] W. Li, T. Zi, J. Wu, and S. Zhu, "Clinical evaluation of alendronate joint atorvastatin in the treatment of diabetic patients with osteoporosis," *Northwest Pharmaceutical Journal*, vol. 32, no. 2, p. 214, 2017.

[9] X. Wang, "Clinical investigation on the application of alendronate combined with atorvastatin in patients with diabetes mellitus combined with osteoporosis," *Cardiovascular Disease Journal of Integrated Traditional Chinese and Western Medicine (Electronic)*, vol. 5, no. 18, p. 25, 2017.

[10] G. Hou, "Sodium alendronate combined with atorvastatin in the treatment of diabetes mellitus with osteoporosis," *China Foreign Medical Treatment*, vol. 37, no. 5, p. 126, 2018.

[11] X. Duan and S. Tang, "Clinical effects of alendronate combined with atorvastatin in the treatment of diabetes mellitus combined with osteoporosis," *World Latest Medicine Information*, vol. 19, no. 97, p. 134, 2019.

[12] L. Feng and J. Wang, "Evaluation of alendronate combined with atorvastatin in the treatment of diabetes mellitus combined with osteoporosis," *Diabetes World*, vol. 16, no. 11, p. 69, 2019.

[13] X. Li and X. Li, "Analysis of the clinical value of alendronate combined with atorvastatin in the treatment of diabetes mellitus with osteoporosis," *Heilongjiang Journal of Traditional Chinese Medicine*, vol. 48, no. 4, p. 27, 2019.

[14] Y. Li, C. Guan, and J. Sun, "Evaluation of alendronate combined with atorvastatin in the treatment of diabetes mellitus combined with osteoporosis," *Healthful Friend*, vol. 24, p. 74, 2019.

[15] X. Su, "Effects of alendronate combined with atorvastatin on bone mineral density and bone metabolism levels in patients with diabetes mellitus combined with osteoporosis," *Shanxi Medical Journal*, vol. 48, no. 22, p. 2769, 2019.

[16] S. Wang, "Effects of alendronate combined with atorvastatin on bone density and bone metabolism in diabetic patients with osteoporosis," *Medical Innovation of China*, vol. 16, no. 2, p. 13, 2019.

[17] C. Yang and W. Dong, "Efficacy and safety of alendronate sodium combined with atorvastatin in the treatment of diabetes mellitus complicated with osteoporosis," *Clinical Research and Practice*, vol. 4, no. 36, p. 48, 2019.

[18] X. Fu, G. Xue, S. Zhong, and Q. Tang, "Effect of atorvastatin combined with alendronate on bone density in patients with diabetes mellitus and osteoporosis," *Journal of Clinical and Experimental Medicine*, vol. 19, no. 7, p. 740, 2020.

[19] X. Hu and H. Wang, "Clinical effects of alendronate and atorvastatin in the combined treatment of diabetes mellitus with osteoporosis," *Diabetes World*, vol. 17, no. 9, p. 57, 2020.

[20] L. Zou, N. Yi, and R. Yi, "The effect of alendronate sodium combined with atorvastatin on pain degree and bone metabolism balance in patients with diabetic osteoporosis," *Drug Evaluation*, vol. 18, no. 11, p. 680, 2021.

[21] D. Moher, A. Liberati, J. Tetzlaff, D. G. Altman, and for the PRISMA Group, "Preferred reporting items for systematic reviews and meta-analyses: the PRISMA statement," *PLoS Medicine*, vol. 6, no. 7, article b2535, 2009.

[22] J. P. Higgins, D. G. Altman, P. C. Gotzsche et al., "The Cochrane Collaboration's tool for assessing risk of bias in randomised trials," *BMJ*, vol. 343, article d5928, 2011.